

The Probabilistic Characterization of Severe
Rainstorm Events: Applications of Threshold
Analysis

THE PROBABILISTIC CHARACTERIZATION OF SEVERE
RAINSTORM EVENTS: APPLICATIONS OF THRESHOLD
ANALYSIS

BY
BARRY PALYNCHUK, M.A.Sc.

A THESIS
SUBMITTED TO THE DEPARTMENT OF CIVIL ENGINEERING
AND THE SCHOOL OF GRADUATE STUDIES
OF MCMASTER UNIVERSITY
IN PARTIAL FULFILMENT OF THE REQUIREMENTS
FOR THE DEGREE OF
DOCTOR OF PHILOSOPHY

© Copyright by Barry Palynchuk, February 2012
All Rights Reserved

Doctor of Philosophy (2012)
(Civil Engineering)

McMaster University
Hamilton, Ontario, Canada

TITLE: The Probabilistic Characterization of Severe Rainstorm
Events: Applications of Threshold Analysis

AUTHOR: Barry Palynchuk
M.A.Sc., (Civil Engineering)
McMaster University, Hamilton, Canada

SUPERVISOR: Dr. Y.Guo

NUMBER OF PAGES: x, 123

Dedications

To my wife Roslyn, for her tolerance and patience.

Abstract

Hourly archived rainfall records are separated into individual rainfall events with an Inter-Event Time Definition. Individual storms are characterized by their depth, duration, and peak intensity. Severe events are selected from among the events for a given station. A lower limit, or threshold depth is used to make this selection, and an upper duration limit is established. A small number of events per year are left, which have relatively high depth and average intensity appropriate to small to medium catchment responses. The Generalized Pareto Distributions are fitted to the storm depth data, and a bounded probability distribution is fitted to storm duration. Peak storm intensity is bounded by continuity imposed by storm depth and duration. These physical limits are used to develop an index measure of peak storm intensity, called intensity peak factor, bounded on $(0, 1)$, and fitted to the Beta distribution. The joint probability relationship among storm variables is established, combining increasing storm depth, increasing intensity peak factor, with decreasing storm duration as being the best description of increasing rainstorm severity. The joint probability of all three variables can be modelled with a bivariate copula of the marginal distributions of duration and intensity peak factor, combined simply with the marginal distribution of storm depth. The parameters of the marginal distributions of storm variables, and the frequency of occurrence of threshold-excess events are used to assess possible shifts in their values as a function of time and temperature, in order to evaluate potential climate change effects for several stations. Example applications of the joint probability of storm variables are provided that illustrate the need to apply the methods developed.

The overall contributions of this research combine applications of existing probabilistic tools, with unique characterizations of rainstorm variables. Relationships between these variables are examined to produce a new description of storm severity, and to begin the assessment of the effects of climate change upon severe rainstorm events.

Acknowledgements

I would like to thank Prof. Yiping Guo for his ongoing support over the years. My family has been an inspiration, and without their acceptance of my late return to school, I could never have continued.

Table of Contents

| | |
|--|----|
| Abstract | iv |
| Acknowledgements | v |
| Chapter 1. Introduction | 1 |
| 1. Problem statement | 2 |
| 2. Threshold analysis of rainstorm depth and duration statistics at Toronto, Canada | 3 |
| 3. A probabilistic description of rain storms incorporating their peak intensity | 4 |
| 4. Changes in heavy rain storm characteristics with time and temperature at four locations. | 5 |
| 5. Example Applications | 7 |
| Chapter 2. Threshold analysis of rainstorm depth and duration statistics at Toronto, Canada | 9 |
| 1. Introduction | 9 |
| 2. Definition of Rainstorm Events | 12 |
| 3. Extreme Value Probability Distributions and Parameter Estimation | 14 |
| 4. Example Analysis of Hourly Rainfall Data from Toronto, Canada | 19 |
| 5. Summary and Conclusions | 32 |
| Chapter 3. A probabilistic description of rain storms incorporating their peak intensity | 35 |
| 1. Introduction | 35 |
| 2. Alternative Approaches to Rainstorm Peak Intensity Characterization | 41 |
| 3. Joint Probability of Storm depth, duration and Intensity Peak Factor | 46 |
| 4. Conclusions | 58 |
| 5. Acknowledgements | 60 |
| 6. Appendix Rainfall Data Analysis | 60 |
| Chapter 4. Changes in heavy rainstorm characteristics with time and temperature at four locations. | 65 |
| 1. Introduction | 65 |
| 2. Storm event definition and analysis | 70 |

| | |
|--|-----|
| 3. Review of analysis - rainstorm parameter changes with time and temperature | 85 |
| 4. Time series trend analysis - Background | 90 |
| 5. Conclusions | 93 |
| Chapter 5. Example applications | 95 |
| 1. Introduction | 95 |
| 2. Application of the joint probability distribution to evaluate conventional design storm hyetographs | 96 |
| 3. Application of the joint probability distribution to identify critical combinations and levels of uncertainty | 99 |
| 4. Conclusions | 101 |
| Chapter 6. Conclusions and Recommendations | 103 |
| 1. Approach | 103 |
| 2. Threshold Analysis of Rainstorm Depth and Duration Statistics at Toronto, Canada | 103 |
| 3. A probabilistic description of rain storms incorporating their peak intensity | 104 |
| 4. Changes in heavy rainstorm characteristics with time and temperature at four locations | 105 |
| 5. Overall conclusions | 106 |
| Appendix A. References | 107 |

List of Tables

| | |
|--|----|
| 2.1 Rainstorm depth parameters and test statistics. | 21 |
| 2.2 Rainstorm duration parameters and test statistics. | 25 |
| 2.3 Statistical moments for conventional DDF annual maximum series. | 26 |
| 3.1 Correlation of intensity peak factor with storm depth and duration. | 43 |
| 3.2 Beta distribution parameters for intensity peak factor. | 45 |
| 3.3 Correlation of intensity peak factor with storm depth ($I_{pf} - V$) for three separate ranges of storm duration.. | 47 |
| 3.4 Kendall's τ for intensity peak factor and storm duration ($I_{pf} - T$), Ali-Mikhail-Haq and Frank copula parameters α . | 50 |
| 3.5 Relative Goodness-of-fit, Theoretical models compared to Empirical Plotting Point Distribution. | 57 |
| 3.6 Table A1. Summary of statistical analysis results for two stations in Toronto, Canada. | 62 |
| 4.1 Station Descriptions, Threshold Analysis of Rainstorm Events March-November, ≤ 24 hours | 71 |
| 4.2 Threshold statistics | 73 |
| 4.3 Difference in values, pre- and post-1980, of statistical parameters. | 75 |
| 4.4 J_u , average probability of exceedence of u_v , pre- and post-1980. | 76 |
| 4.5 χ^2 analysis of difference between pre- and post-1980 empirical distributions of storm variables. | 77 |
| 4.6 Correlation analysis between V , T , and I_{pf} , pre-1980 and post-1980. | 79 |
| 4.7 Correlation analysis between the mean monthly temperature (MMT) when storm events occur and V , T , I_{pf} , pre- and post-1980. | 80 |
| 4.8 Average of mean monthly temperature when threshold-excess storm events occurred, pre- and post-1980. | 83 |
| 4.9 Summary of major time-span and temperature changes and trends | 87 |
| 5.1 Intensity peak factor and return periods of different design storm hyetographs. | 98 |

List of Figures

| | |
|---|----|
| 2.1 The plotting point distribution of rainstorm data is compared with the one-parameter exponential distribution. Crosses are used to represent actual measures of storm depth. | 14 |
| 2.2 Comparison of the plotting point distribution with Type I and III distributions, storm threshold depth $u_v = 25$ mm. Solid line shows GPD Type I modeled storm depths, dashed line plots Type III. | 20 |
| 2.3 Figure 3a (left). Storm duration histogram based upon hourly rainfall records, using IETD = 6 hours to define individual events. Figure 3b (right). Storm duration histogram, adjusted for start and finish time uncertainty. | 23 |
| 2.4 100, 25 and 5-year return period storm-event depth-durations are compared with conventional DDF rainfall accumulation. Box symbol indicates conventional DDF GEV I-modeled rainfall accumulation. Cross symbol is used to show SEA GPD Type I-modelled depth. | 27 |
| 2.5 Comparison of event-based and DDF annual maximum rainfall depths, for durations/time intervals of one hour. Actual conventional DDF depths are shown with a box symbol. SEA measures of storm depth are shown with a cross. | 29 |
| 2.6 Comparison of event-based annual maximum storm depths for durations of 6 hours or less and DDF annual maximum depths for the 6-hour time interval. | 30 |
| 2.7 Comparison of event-based annual maximum storm depths for durations of 12 hours or less, and DDF annual maxima rainfall accumulations for the 12-hour time interval. | 31 |
| 3.1 Plot showing actual peak discharge for Mimico Creek (Ontario, Canada) catchment on y-axis, and predicted by regression equation on x-axis. Independent variables for regression equation are runoff depth and peak hour intensity. | 39 |
| 3.2 Plotting point or empirical distribution of intensity peak factor (I_{pf}, i_{pf}) , based upon Eq. (5), together with Beta distribution in solid line, fitted by method of moments. | 45 |

| | |
|--|-----|
| 3.3 Comparisons of plotting position and theoretical joint probability distributions. Plotting position empirical distribution established with Eq. (23) plotted on y-axis. Theoretical distributions based upon Eq. (19) for AMH copula, Eq. (20) for Frank copula, and Eq. (24) for simple joint probability plotted along x-axis. Figure 3(a) for Toronto station, Figure 3(b) for TPIA. Points falling closest to 45-degree line indicate best fit between empirical and theoretical models. | 55 |
| 4.1 Storm duration frequency by 3-hour duration increments, pre- and post-1980 | 78 |
| 4.2 Mean storm depth versus mean monthly temperature | 81 |
| 4.3 Mean storm duration and mean intensity peak factor, versus mean monthly temperature | 81 |
| 4.4 Storm frequency versus temperature ranges. p-value of difference in proportions shown on reverse scale, significance assessed as $p < 0.10$ | 82 |
| 4.5 Mann-Kendall test statistic for Peoria station, on a 20-year moving window basis. | 92 |
| 5.1 Maximization of peak discharge for 100-year joint return period. | 100 |

CHAPTER 1

Introduction

Rainfall-runoff modelling is a necessary component in a variety of water resources management and design tasks. Rainfall inputs are processed through a model that mimics the real-world processes of rainfall infiltration, and runoff of rainfall excess on catchment surfaces, then concentration and routing of flows through stream channels. Assessment of risk and uncertainty, rather than simply modelling responses deterministically is of critical importance. Risk and uncertainty are evaluated by incorporating the probability distributions of variables which influence the ultimate outputs of the modelling processes. Chief among these variables are those describing rainfall inputs.

Rainfall variables are measures such as depth of rainfall as measured over a defined time interval, storm duration, and measures of storm shape such as temporal location of the peak of rainfall intensity, and rainfall peak intensity. By characterizing the probability distributions of these variables, as well as the correlations between them, the likelihood of occurrence of a combination of values, ranges, or limits defined by particular values of the variables may be determined. These probabilistic characterizations are typically the probability of exceedence of given combinations of storm variables, or return period in years.

In this thesis, unique approaches were developed for the measurement of storm variables, focusing upon extreme events (those storms with much greater than average depths, and their associated durations and peak intensities). The probability distributions of these variables, and their dependencies are developed so that the results may be applied by practitioners. Potential shifts in statistical parameters and changes in correlations between rainstorm variables as a result of climate change are also examined.

1. Problem statement

Rainstorms are observed as individual events, but conventional definitions suffer from a number of problems:

- The most commonly used definitions are measures of rainfall accumulation over prescribed time intervals, not related to the start and end of actual rainstorm events (Adams et al., 1986).
- When rainstorms are identified as individual events there are a mixture of definitions (Karl et al., 1998), or a mixture of climatological measures are used (Karl and Trenberth, 2003; Groisman et al., 1999; Groisman, 2010).
- Rainstorms are characterized by their depth, duration, and peak intensity. In the examination of extreme, severe events, conventional approaches effectively ignore actual storm durations, and assume that the peak intensity has no impact upon the frequency of occurrence of rainstorms.
- Where some researchers have begun to examine the joint probabilities of storm depth, duration, and peak intensity for extreme events, they have used annual maximum statistics. However, this requires a priori, arbitrary, pre-selection of annual maximum measures. The result may lead to biased probabilistic models (Kao and Govarindju, 2010).
- There is much discussion about the effects of climate change upon extreme rainstorm events. The same problems of event definition plague the examination of changes in patterns of rainstorms as a function of time and temperature, and those relationships to climate change forcings.

The underlying problems of storm event definition, and appropriate probabilistic modelling of the measures of storms as random variables is addressed in the research described in this thesis.

The balance of this chapter briefly summarizes the subsequent chapters, along with the principal contributions in each.

2. Threshold analysis of rainstorm depth and duration statistics at Toronto, Canada

Chapter 2 in this thesis introduces the initial application of threshold analysis to the definition and characterization of extreme rainstorm events. One of the key contributions is the discovery that, for storms with depths exceeding a high threshold, storm depth and duration are not correlated, a rupture with the conventional paradigm of an assumed coupling between the two variables. This chapter has been reformatted from a paper presented by the author and Dr.Y. Guo in the Journal of Hydrology, vol. 348, published in January 2008. Following is the abstract of this paper, together with the Keywords which precede the body of the paper:

Abstract - Storm-event based probabilistic models characterizing the probability distributions of storm depth and duration are developed. They overcome the primary limitation of conventional rainfall Depth-Duration-Frequency (DDF) analysis. The application of threshold-excess extreme-value analysis techniques to storm-event statistics provides a simple, statistically efficient means of characterizing frequency of extreme storm event depths and durations. The best-fit probability density functions of storm-event depth and duration are used to derive storm-event depth-duration frequency combinations. The resulting models may be used to develop design storms based upon actual storm-event statistics. Comparisons between conventional and Storm Event Analysis (SEA) models highlights the improvements and benefits of using storm-event-based probability distributions, and brings into question the application of conventional DDF techniques for design storm development.

Keywords: Design Storms; Storm Event Analysis; Inter-Event Time Definition; Annual maximum series; Threshold analysis; Generalized Pareto Distribution; Joint Probability.

The mathematical basis of this chapter/paper is the application of threshold statistics, applied through the Generalized Pareto Distributions (GPD). This family of distributions has unique similarities to the Generalized Extreme Value Distributions, typically used with annual maximum statistics.

3. A probabilistic description of rain storms incorporating their peak intensity

In Chapter 3, the techniques developed in the previous chapter are expanded to incorporate a measure of peak intensity into an expression for the joint probability of storm depth, duration, and peak intensity for extreme rainstorms. In the process, a unique measure of peak intensity is developed. This material prepared by the author, under the supervision of Dr. Y. Guo, was published in the Journal of Hydrology, vol. 409, October, 2011. The abstract and key words from the paper are presented in the following two paragraphs.

Design storms with standardized hyetograph shapes and selected combinations of storm depths and durations are widely used in engineering hydrology. The key distinguishing feature between equal-duration design storms is their distinct intensity distributions. Differences in design storm hyetographs do not affect storm frequency, since only the frequency of the combination of storm depth and duration are determined through the use of Depth-Duration-Frequency curves. Probability distributions of peak intensity within rainfall events are not determined in current practice. Some current research applies copulas to joint distributions of rainstorm variables, but most of these are limited to bivariate distributions, and those that are developed for trivariate distributions do not address key variables important to everyday practice, or are limited by complexity of analysis. An alternative approach to characterizing peak storm intensity, intensity peak factor, together with its probability distribution is developed in this paper. An Archimedean copula is applied to describe the joint probability distribution of storm duration with intensity peak factor. That joint distribution is combined with the probability distribution of storm depth, to produce a joint probability distribution for storm depth, duration, and peak intensity. The result is a simple approach to fully characterizing the storm variables of direct interest to practitioners, thereby providing a complete probabilistic description of the return period or frequency of a selected design storm.

Keywords: Design Storms; Storm Event Analysis; Peak Intensity; Beta Distribution; Joint Probability; Copula.

Rainfall data from two meteorological stations in Toronto were evaluated and compared, providing a level of validation to the techniques developed in Chapter two. The key contributions in Chapter 3 include:

- the identification of an index measure of relative rainstorm intensity that is independent of storm depth
- the application of bivariate copulae to the joint probability of storm duration and intensity peak factor
- identification of the combination of storm variables that lead to increasing storm severity
- combining these primary contributions, the joint probability of all major variables quantifying a rainstorm event was developed.

4. Changes in heavy rain storm characteristics with time and temperature at four locations.

The popular scientific literature provides projections of increasing rainstorm severity, manifested in increasing rainfall depth, and increasing storm intensities (Flannery, 2005). The explanations tend towards high-level descriptions of basic causal linkages between increasing atmospheric temperature and available precipitable atmospheric water vapour. The objective is public education, so explanations of the effects of increasing concentrations of greenhouse gases must be clear. When the detailed references from within the popular literature are examined, the evaluations of rainfall data tend towards the assessment of accumulations of rainfall, and the analysis of conventional rainfall accumulation over fixed time spans. The definition and analysis of rainstorms as measured individual events is performed by smaller numbers of researchers, with a wide variety of storm-event definitions. An opportunity exists to define and analyze rainstorms with models and definitions that are a close match to their actual manifestation.

The techniques developed in prior chapters were applied to three US stations in the state of Illinois, and one Canadian station. Marginal distributions, based upon

estimation of statistical parameters of storm depth, duration, and intensity peak factor were established, applying techniques developed in Chapters 2 and 3. However, the fitting techniques are not reviewed in detail. The objective of the research described in Chapter 4 was the evaluation of changes in statistical parameters of rain-storm variables, and shifts in dependencies between them, as a function of time and temperature. The available data was split into two groups; events occurring prior to 1980, and events occurring since 1979. The split in data is at 00:01, 1980-01-01. In order to avoid confusion, the data spans will be referred to pre-1980, and post-1980, even though the correct description would be pre-1980, and post-1979.

In general, mean values of storm variables and frequency estimators did not change significantly over the time ranges of available data, pre-1980 and post-1980. Comparison of empirical distributions of storm variables between the two data sets showed some significant differences, but differences in distributions between the two time spans did not follow patterns across the stations. Because the sizes of the data sets are reduced due to the division of the population of the whole set, and the time spans for each set are therefore shorter, there is a risk that the effects of decadal and multi-decadal climactic trends resulting in changes in distribution of storm variables may either cause an apparent trend that does not exist, or alternatively, hide a trend within long-period cycles.

Evaluation of rainfall variables in relation to mean monthly temperature provided the clearest indications of direct linkages between temperature, storm variables, and storm frequencies. Storm duration is inversely correlated with temperature, while intensity peak factor is directly correlated with mean monthly temperature. Those relationships did not change between the two time spans into which the storm events were divided. Storm depth correlation with temperature generally decreased in the post-1980 time span, compared to the pre-1980 time span.

The most remarkable difference between the two time spans was a significant increase in frequency of storms occurring in the highest temperature range for each station examined. Average of mean monthly temperature for storm events did not change significantly; an indication of the complexity of factors contributing to provision of precipitable water in the lower atmosphere.

The primary contribution of this chapter is in the application of clear rainstorm event definition to the analysis of the effects of temperature upon mean values of storm variables. Previous analysis of the influence of climate change provided indications of increases in extreme storm depth and intensity. Unfortunately, those conclusions were often inferred from analysis of data that does not clearly identify individual storm events. Research in this thesis establishes clearly the relationships between temperature and mean values of storm variables, as well as an increasing frequency of occurrence of storm events during warmer temperatures.

A brief review of conventional trend analysis techniques is carried out. Limitations in conventional time-series trend analysis are demonstrated, as explanation for use of more basic techniques of trend analysis developed in this chapter.

5. Example Applications

From the theory developed into methods in Chapters 2 and 3, two applications are shown. The first illustrates the difference in storm frequency when the full joint probability of storm depth, duration and intensity peak factor is applied. The second demonstrates maximization of output discharge from a catchment, when storms with identical return periods, but different combinations of input storm variables are used as inputs to the hydrologic system.

In the following chapters, equation, table, and figure numbering will incorporate chapter and sequence number within the chapter. References within the text will refer to numbering within the chapter, rather than using the chapter prefix. This is done primarily to avoid modifying text references within those chapters that have been published already. For a similar reason, references are organized by chapter, in order to respect the form and format of those chapters that have already been published.

CHAPTER 2

Threshold analysis of rainstorm depth and duration statistics at Toronto, Canada

1. Introduction

Rainfall, as the input to a hydrologic system, has been characterized in a few basic ways:

- Continuous series records of distribution of rainfall depths on a temporal basis may be used as input to a continuous simulation model. The outputs of the model may then be calibrated against actual output measurements.
- Actual storm events, such as the Hurricane Hazel rainstorm which occurred in Ontario, Canada in 1954, are analyzed. The distribution of rainfall depth with time is determined from measurements, and used in rainfall-runoff models to determine outputs from a single extreme event.
- Design Storms constructed from Intensity Duration Frequency (IDF) curves. A design storm is a standardized distribution of rainfall intensity with time, for a selected total storm duration. Records of rainfall accumulation occurring over defined time intervals are fitted to an appropriate extreme value distribution. Depth-Duration-Frequency (DDF) relationships result. IDF curves are produced by dividing depth by the corresponding time interval. Rainfall depth or intensity for a given time interval and return period may then be determined. These values are applied to the prescribed temporal distribution of rainfall intensity to create design storm hyetographs.
- Storm-Event Analysis (SEA) external measures of actual rainstorm events are analyzed and fitted to appropriate probability density functions (PDFs).

Typically, exponential distributions are used to characterize event duration, depth, and inter-event time (Adams et al., 1986; Adams and Papa, 2000).

Each technique has its appropriate use. Continuous simulation, if carried out with a sufficiently long series of rainfall records, could be used to characterize the return period of hydrologic outputs such as peak discharge. However, the computational burden would be heavy, and the precision of the simulated outputs will necessarily be a function of the runoff model parameters, and the calibration of the model against measured outputs. The technique does not, in itself, provide any characterization of frequency of occurrence of rainfall input events.

Extreme actual storm events provide an ultimate test of a hydrologic system, but the return period of the event is not possible to determine, since this type of event occurs so infrequently as compared to existing periods of rainfall record.

Extensive research has been conducted on the frequency characteristics of rainfall depth accumulation during prescribed time intervals, usually on the basis of analysis of annual maximums (Wenzel, 1982; U.S.NWS, 2002; Boni et al., 2006). The result of this effort has been the development of conventional DDF curves. These may take the form of plots of depth or intensity versus duration for various return periods (Carr, 1987), or isohyetal maps of rainfall accumulation for prescribed time intervals and return period (Hershfield, 1961). Rainfall depth accumulations are the subject of analysis; appropriate extreme value distributions, typically GEV I (Gumbel distribution) (Chow, 1988; Stedinger et al., 1993), are fitted to rainfall depth accumulations for each selected time interval. Recent work has made use of Two-component extreme value distributions to characterize the probability distributions of extreme rainfall depth accumulations, and developed techniques for regional characterization (Boni et al., 2006). It is important to point out that storm duration is not measured and considered in these conventional DDF development procedures, nevertheless, there is an underlying assumption that the time intervals correspond to storm durations when DDF curves are used to develop design storms. It has been recognized for some time that these conventional techniques do not provide an appropriate characterization of individual storm events, but includes portions of events

(Wenzel, 1982). The application of DDF curves in the development of design storms has been criticized in many respects:

- The return period of rainfall depth is equated to that of all characteristics of a given design storm hyetograph, when each measure of a rainstorm (depth, duration, intensity measures) will have its own frequency characteristic (Adams and Howard, 1986).
- The original purpose of DDF/IDF curves was to permit determination of peak discharge from a catchment by means of the Rational equation (Adams and Papa, 2000). Extension of DDF curves to characterize return periods of rainstorm depth, duration, and hyetographs goes well beyond their original purpose; forcing the DDF technique, and making some broad assumptions equating rainfall depth accumulation for a prescribed time with storm depth and duration.
- IDF curves are not measures or characteristics of storm events, so that their current application in design storm modeling may not be fundamentally sound, particularly in characterizing return periods of hydrologic outputs.

Because of the lack of clarity in definition of the time element in conventional rainfall statistical analysis, the term time interval will be used when referring to conventional IDF/DDF analysis, rather than duration. Duration implies measurement of the time elapsed between the start and end of an event, rather than the arbitrary selection of a span of time during which a process, i.e., rainfall, is observed.

In spite of the many drawbacks inherent in the application of DDF curves, their use, combined with the design storm approach is common practice. Alternatives to the DDF approach are based upon the definition of individual storm events. While much research has been conducted on the spatial and temporal distribution of rainfall within individual events (Huff, 1993; Watt et al., 1986), there has been less research on storm-event statistics. The statistical characterization of rainstorms by their external measures of depth, duration, inter-event time, and internal intensity measures has been done by those researchers involved with application of derived probability distribution theory to rainfall-runoff modeling (i.e., Eagleson, 1972; Adams et al.,

1986; Guo and Adams 1998a, b; Adams and Papa, 2000; Goel et al., 2000; Guo, C. Y.J., 2002; Rivera et al., 2005). More recently, Zhang and Singh (2007) developed bivariate rainfall frequency distributions using copulas to address correlation between rainstorm depth, intensity and duration for annual maximum storm-event measures at three sites in Louisiana, U.S.A. Characterization of storm event statistics based upon hourly rainfall data has been carried out for portions of the U.S. Southwest (Asquith et al., 2006). Much of that effort was focused upon developing regional characterization of storm measures of depth, duration, and interevent time. Both Kappa and exponential distributions have been applied in that analysis. In this paper, we apply SEA through threshold-excess techniques in order to provide a new approach to developing design storms.

2. Definition of Rainstorm Events

In order to study the statistics of actual rainstorm events, separate events must first be identified. For the purpose of identifying individual events, an Inter-Event Time Definition (IETD) must be adopted. Individual storm events consist of consecutive hourly records of rainfall preceded and followed by a minimum period of time greater than or equal to the IETD. The IETD used is a function of application, but is usually selected so as to minimize serial correlation between storm events (Restrepo-Posada and Eagleson, 1982). Six hours is used as the IETD in the analysis of hourly rainfall statistics used in this paper. Design storms are often developed for use with small urban catchments where the time of concentration is usually less than six hours. Since the minimum IETD is greater than the time of concentration, the runoff response of successive storm events can be treated independently. Other rationales have been suggested for the selection of appropriate IETDs. These other rationales are primarily based upon treatment criteria and performance requirements applied to stormwater management practices (Wanielista and Yousef, 1993). However, caution needs to be exercised in this regard, since there is a risk of diluting a fair statistical model of storm events to fit a design strategy. Increasing the IETD beyond that required for statistical independence between individual events may result in the lumping of separate real storm events together.

The steps followed in the analysis are summarized below:

- Rainfall data, based upon reported depth during hourly intervals is analyzed.
- If adjacent hourly time blocks with some rainfall are separated by dry times less than the IETD (in this case, 6 hours) then those blocks are aggregated as part of the same rainstorm event.
- When hourly time blocks with rainfall are separated by at least the IETD, then separate events are recorded.
- Each event is characterized by its external measures of storm depth v , storm duration t , and inter-event time b

The fundamental difference between conventional rainfall statistics used to develop DDF curves and SEA is that the former ignores actual storm events, and measures rainfall accumulation within prescribed time intervals. SEA is based on actual storm events which are identified with the adoption of a suitable IETD. This then permits the measurement of the magnitude and duration of individual rain storm events.

Recent work (Guo and Adams, 1998a) has made use of single-parameter exponential distributions of rainstorm event depth, duration, and inter-event time. The typical form of the probability density function (PDF) is:

$$f_v(v) = \zeta \exp(-\zeta v), \zeta = 1/\bar{v}$$

where v is the storm depth as a random variable, \bar{v} is the average of the depths of all events. Rainstorm duration (t) and inter-event time (b) statistics are similarly fitted to exponential PDFs. The exponential distributions of storm depth, duration, and inter-event time are applied to derive the probability distribution of a hydrologic output, such as peak discharge.

From the hourly rainfall data recorded at the Toronto Pearson International Airport (Meteorological Services Canada, Station No.6158733), it was found that the one-parameter exponential distribution underestimates storm depth for extreme

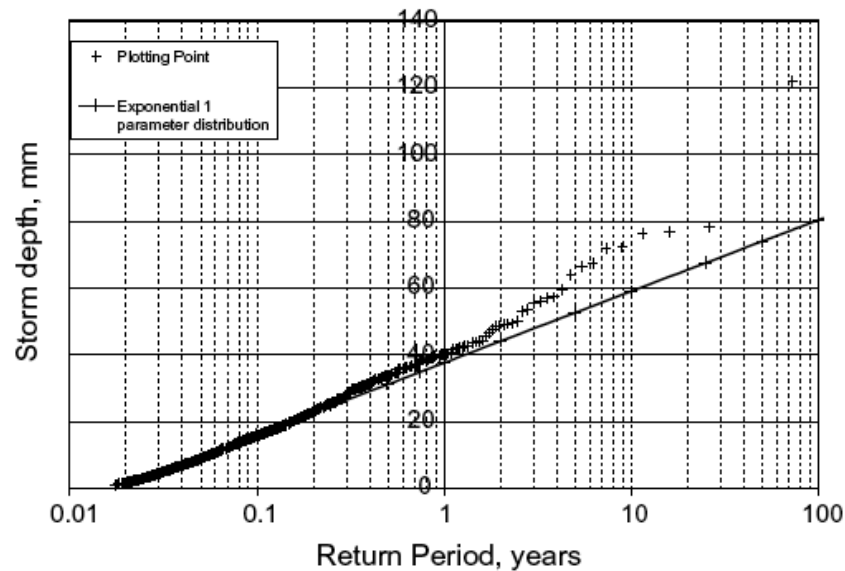


FIGURE 2.1. The plotting point distribution of rainstorm data is compared with the one-parameter exponential distribution. Crosses are used to represent actual measures of storm depth.

events (return periods exceeding 2 years) while providing a good fit for more frequent events. This is indicated in Figure 1. Improvement or redefinition of probability distributions may lead to a better fit between extreme event models and observed (empirical) distributions.

For the development of more representative design storms, the object of this study is the frequency of occurrence and characteristics of extreme events. A better fit of the probabilistic model to extreme events is required and is the first step.

3. Extreme Value Probability Distributions and Parameter Estimation

Generalized Pareto Distributions (GPD), applied through threshold-excess measures of rainstorm depth are used to characterize storm-event depths in this paper. A brief review of applicable forms, and duality with the Generalized Extreme Value (GEV) models follows.

Nomenclature.

| | |
|------------------|---|
| V, v | Rainstorm depth. |
| T, t | Storm duration. |
| $M_n = \max\{\}$ | Maximum value of a set of random variables. |
| $Pr\{X\}$ | Probability |
| $f_X(x)$ | Probability density function |
| ξ | Shape parameter GEV or Generalized Pareto distributions |
| σ | Scale parameter |
| μ | Location parameter |
| u_v | Rainstorm depth threshold parameter |
| n | Total number of rainstorm events |
| m | Number of rainstorm events exceeding threshold |
| J_u | Probability of exceedence of storm depth threshold |
| θ_0 | Average number of rainstorm events per year |
| θ_u | Average number of rainstorm events per year exceeding threshold |
| t_{max} | Maximum value of storm duration |
| k | Number of unique values of ordered measures of storm depth |
| A^2 | Anderson-Darling Statistic |
| ρ | Correlation coefficient |

Extreme value theory models the statistical behavior of large values from series of identically distributed, independent random variables with a common distribution function. If the time block is the calendar year, the annual maxima of the annual blocks of rainfall measurements are modelled. Block maxima are modelled with the GEV distribution function:

$$G_V(v) = \exp \left\{ - \left[1 + \xi \frac{(v-\mu)}{\sigma_v} \right]^{-\frac{1}{\xi}} \right\}.$$
 ξ is the shape parameter, σ_v and μ are the scale and location parameters respectively. The value of the shape parameter provides a means of classification of the GEV into three types:

- Type I or Gumbel distribution, $\xi = 0$, is widely used to characterize hydrologic extremes. The GEV is evaluated in the limit as $\xi \rightarrow 0$. σ_v should be invariant with threshold selection within sampling error.
- Type II or Frechet distribution, $\xi > 0$, the distribution has no upper limit.
- Type III or Weibull distribution, $\xi < 0$, the distribution has an upper bound.

If the block maxima of the set of random variables can be modeled with the GEV, then an alternative approach is to model the behavior of large values of the variable, greater than a high threshold value, from the entire set of random variables. When a high threshold u_v is selected so that large values of the independent random variable are modeled, then the conditional probability of exceedence of those high values is the Generalized Pareto Distribution (GPD):

$$Pr\{V > v|V > u_v\} = \left[1 + \xi \frac{(v - u_v)}{\tilde{\sigma}_v}\right]^{\frac{1}{\xi}}, \quad \xi \neq 0 \quad (2.1)$$

where $\tilde{\sigma}_v$ is the scale parameter for the Pareto distribution. The shape parameter ξ has identical value and meaning in the two distributions (GEV and GPD) and serves to classify the model type in the same fashion. Eq. (1) corresponds to Type II and III distributions. The GPD Type I distribution is obtained by evaluating Eq. (1) in the limit as $\xi \rightarrow 0$,

$$Pr\{V > v\} = \exp[-(v - u_v)/\tilde{\sigma}_v] \quad (2.2)$$

The relationship between Pareto and GEV scale parameters is $\tilde{\sigma}_v = \sigma_v + \xi(u_v - \mu)$. The distinction between the two will be dropped in the balance of the review. The equivalent Pareto distributions will be used exclusively in characterizing threshold excess-based distributions of storm event depth v . It should be noted that for Type I distributions, since $\xi = 0$, GEV and Pareto scale parameters are equal, and that the GPD Type I distribution is a 2-parameter exponential distribution. The Generalized Pareto model is attributable to Pickands (1975), while the threshold approach applied to the generalized Pareto distribution was developed by Davison and Smith (1990). A discussion on the relationship between GEV and GPD can be found in Coles (2001).

Since $Pr\{V > v\} = Pr\{V > u_v\} Pr\{v > v|V > u_v\}$, that is the probability of exceedence of storm depth can be obtained from the conditional probability of exceedence, multiplied by the threshold exceedence probability, then letting $Pr\{V > u_v\} = J_u$ and combining with Eq. (1):

$$Pr\{V > v\} = J_u \left[1 + \xi(v - u_v)/\sigma_v\right]^{\frac{1}{\xi}}, \quad \xi \neq 0 \quad (2.3)$$

For $\xi = 0$, combining J_u with Eq. (2):

$$Pr\{V > v\} = J_u \exp[-(v - u_v)/\sigma_v] \quad (2.4)$$

J_u , the probability of exceedence at the threshold value u_v may be estimated as: $\hat{J}_u = m/n$ where n is the total number of rainstorm events and m is the total number of events with depth exceeding the threshold value.

A common form of expressing risk of occurrence of an extreme event is to use the return period. Thus a quantile may be expressed as the T_v - year return period rainstorm depth, i.e. the depth that will be exceeded on average once every T_v - years. The probability of exceedence of v_T given an average of θ_0 rainstorms per year is $1/(T_v\theta_0)$. Substituting into Eq. (3):

$J_u [1 + \xi(v - u_v)/\sigma_v]^{\frac{1}{\xi}} = 1/(T_v\theta_0)$, then solving for v_T , the following is obtained:

$$v_T = u_v + (\sigma_v/\xi)(T_v\theta_0 J_u)^\xi - 1, \xi \neq 0 \quad (2.5)$$

Or in the limit as $\xi \rightarrow 0$.

$$v_T = u_v + \sigma_v \ln(T_v\theta_0 J_u) \quad (2.6)$$

The total number of events equals the average number of events per year times the number of years of record $n = \theta_0 y_r$. θ_u is the average number of events per year, where storm depth exceeds the threshold value, so that $m = \theta_u y_r$. Therefore $\hat{J}_u = \theta_u/\theta_0$.

The variance of \hat{J}_u is: $Var(\hat{J}_u) = \hat{J}_u(1 - \hat{J}_u)/n$ (Coles, 2001). Expressed in terms of average number of events per year, $Var(\hat{J}_u) = \theta_u(\theta_0 - \theta_u)/(y_r\theta_0^3)$. Provided that a relatively high threshold value is taken, so that $\theta_0 \gg \theta_u$, this expression has a very low value. J_u , and by extension, θ_u , are treated therefore, as constants. Substituting the estimate of J_u into Eqs. (5) and (6):

$$v_T = u_v + (\sigma_v/\xi)(T_v\theta_u)^\xi - 1, \xi \neq 0 \quad (2.7)$$

$$v_T = u_v + \sigma_v \ln(T_v\theta_u), \xi = 0 \quad (2.8)$$

The equivalent expression for the GEV I (Gumbel) distribution, based upon annual maximum statistics (Stedinger et al., 1992) is:

$$v_T = \bar{v}_A - (\sqrt{6}/\pi)[0.5772 + \ln(1/T_v)]\sigma_{v_A} \quad (2.9)$$

Return periods based upon annual maximum statistics differ slightly from those derived from threshold statistics. For the sake of uniformity in this example all return periods are expressed as or converted to those based upon threshold statistics. The relationship between the two methods is $T_v = [\ln(T_{vA}/(T_{vA} - 1))]^{-1}$ (Stedinger et al., 1992) where the subscript A refers to annual maximum statistics.

In order to estimate the values of the parameters of any potential PDF from observed data, two common approaches are the method of moments, and the method of maximum likelihood. Maximum-likelihood estimators are generally agreed to be more efficient than those determined by the method of moments (Kite, 1977). The method of L-moments provides a third alternative, and is used increasingly in the analysis of rainstorm data (Asquith et al., 2006). L-moments are not used in this paper because maximum likelihood estimators are appropriate for GPD I and III distributions (Stedinger et al., 1992).

Since the GPD Type I threshold-based distribution is a 2-parameter exponential distribution, maximum likelihood estimates of distribution parameters have analytical solutions, $\hat{\sigma}_v = \bar{v} - u_v$ (Johnson and Kotz, 1970). Maximum likelihood estimates of the scale and shape parameters for GPD Types II and III may be obtained by maximizing the log-likelihood function:

$$\ell(\sigma_v, \xi) = -m \ln \sigma_v - (1 + 1/\xi) \sum_{i=1}^m \ln[1 + \xi(v_i - u_v)/\sigma_v], \xi \neq 0.$$

Eq. (7) is recast so that σ_v is the dependent variable, $\sigma_v = [(v_T - u_v)\xi]/[(T_v\theta_u)^\xi - 1]$, or noting that $T_v = i/\theta_0$, where $(n-m) < i \leq n$ then $\sigma_v = [(v_i - u_v)\xi]/[(i\theta_u/\theta_0)^\xi - 1]$. Values of v_i are obtained from ordered statistics, and the log-likelihood function may be maximized iteratively to solve for the shape parameter ξ (Coles, 2001).

Probability distributions fitted to the data using parameters estimated with these maximum likelihood techniques may be compared visually with the data using a suitable plotting position equation. The form used was that proposed by Gringorten

(Cunane, 1978) which is unbiased when the true distribution is GEV I or exponential: $F_i = (i - 0.44)/(n + 0.12)$, where F_i is the CDF of the i^{th} ordered statistic, and n is the total number of observations, i.e., $x_1 \leq x_2 \leq \dots x_n$.

4. Example Analysis of Hourly Rainfall Data from Toronto, Canada

4.1. Storm depth.

Forty-two years of hourly rainfall data for the months of March through November inclusive recorded at Toronto L.B.Pearson International Airport (TPIA, Meteorological Services Canada, formerly Atmospheric Environment Service, Station No. 6158733) ending in 2001 were reviewed. Individual storm events were identified, based upon an IETD of 6 hours. Storms of durations greater than 12 hours were excluded. This was done for several reasons.

- Shorter duration storms will have the greatest impact on small, or urban catchments, the object of much of this research.
- Rainstorms at this location are formed by two primary mechanisms; convective storms are of short duration, while cyclonic storms are of longer duration. Long duration cyclonic storms will be excluded from this analysis because different probability distribution models may be required to describe their frequency of occurrence.
- Correlation between storm depth and duration is minimized; when the SEA statistics were analyzed using a storm depth threshold of 25 mm ($u_v = 25$ mm) correlation between storm depth and duration was near zero, ($\rho_{v,t} = 0.028$). Evaluation of scatterplots between v and t did not disclose any relationship, so that v and t were treated as independent random variables. This independence is a prerequisite for the convenient application of design storms.

Maximum likelihood estimates for GPD parameters were made. The value of the shape parameter ξ , for Type II or III ($\xi \neq 0$) was found to be less than zero, indicating a Type III distribution. Two distributions, GPD Type I and GPD Type

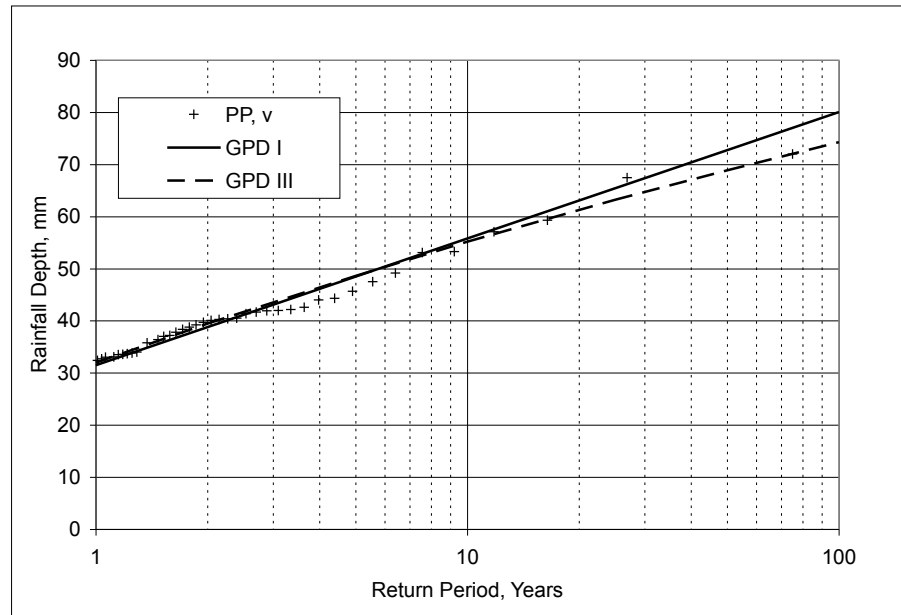


FIGURE 2.2. Comparison of the plotting point distribution with Type I and III distributions, storm threshold depth $uv = 25$ mm. Solid line shows GPD Type I modeled storm depths, dashed line plots Type III.

III were compared to the plotting position distribution for the ordered statistics in Figure 2. Visually, either distribution appears to fit well for return periods less than about 20 years. Beyond that point, the two distributions start to diverge, as expected, since the Type III distribution will have an upper limiting value, while the Type I does not.

Goodness-of-Fit was evaluated by means of the Anderson-Darling-Statistic:

$$A^2 = -(1/k) \left\{ \sum_{i=1}^k (2i-1) [\ln(H(v_i - u)) + \ln(1 - H(v_{k+1-i} - u))] \right\} - k$$
 (Stephens, 1974, 1977; Evans et al., 1995). k is the number of unique, ordered values of the random variable v . A^2 is adjusted, based upon sample size and assumed distribution (see Table 1). The adjusted value is called the modified Anderson-Darling Statistic.

TABLE 2.1. Rainstorm depth parameters and test statistics.

| Parameter | TPIA Sample | Values | Notes |
|------------------------|---------------------|----------|---|
| u_v | 25 | | Storm volume threshold, mm |
| m | 78 | | Number of events exceeding u_v |
| θ_0 | 68.643 | | Avg. number of Rainstorm events per year |
| θ_u | 1.857 | | Avg. number of Rainstorm events per year, exceeding u |
| μ_v | 35.537 | | Estimate of mean Rainstorm volume, mm. |
| $\rho_{v,t}$ | 0.028 | | Correlation of rainstorm depth v , with storm duration t . |
| | | | Value of 1 indicates perfect correlation. Value of 0, random variables are not correlated. |
| | GPD | | |
| | Type I | Type III | |
| $\hat{\sigma}$ | 10.537 | 11.626 | Max. Likelihood estimates of scale parameter (standard deviation). |
| ξ | 0.000 | -0.083 | GEV/GPD shape parameter. |
| k | 64 | 64 | Number of unique values of Rainstorm volume; points in plotting position estimate of CDF. |
| $A^2(1 + 6/10k)$ | 1.504 | | Modified Anderson-Darling Statistic, Type I distribution (Stephens, 1974) |
| $A^2(1 + 0.2/k^{0.5})$ | | 0.980 | Modified Anderson-Darling Statistic, Type III distribution (Evans et al, 1995). |
| Upper tail | hypothesis limit | | Accept at α -level if Modified Anderson-Darling Statistic less than limit value. |
| $\alpha = 0.10$ | 1.062 | 0.626 | Type I rejected, Type III rejected. |
| $\alpha = 0.05$ | 1.321 | 0.744 | Type I rejected, Type III rejected. |
| $\alpha = 0.025$ | 1.591 | 0.846 | Type I accepted, Type III rejected. |
| $\alpha = 0.01$ | 1.959 | 1.019 | Types I and III accepted. |

The modified A^2 is compared to standardized values that represent upper-tail (α) significance levels. The hypothesis is that the assumed distribution H (Type I or Type III in this case) is a good fit to the empirical distribution of the ordered, independent, random variables. It is accepted, if the calculated value of the modified Anderson-Darling statistic is less than the standardized α -level value. The standardized values

are a function of assumed distribution and number of parameters estimated. Table 1 summarizes storm depth parameters and goodness-of-fit tests.

Type I and III distributions provide reasonable representations of probability density functions for extreme rainfall volume statistics from the Toronto Pearson Airport, based upon the depth threshold and duration limits applied. The choice of distribution may be based upon a number of factors:

- Type I provides a better fit on the basis of the Modified Anderson-Darling Statistic.
- Final application While both PDFs are relatively simple mathematical expressions, it may be that Type I provides a more tractable solution in a given application.
- Physical constraints Probable Maximum Precipitation events are estimates of the upper limit of rainfall depth for a given duration over a particular area. Extreme rainfall events in a region are examined, then potential rainfall is calculated by maximizing physical variables, such as moisture content, and lapse rate effects which contribute to the mass of precipitable moisture and the rate of rainfall formation (Smith, 1993). If a theoretical or measured upper limit of rainstorm volume is considered a criterion for fitting of an appropriate GPD distribution, then the Type III upper bound of: $v_{max} = -(u_v - \sigma)/\xi$ could be applied. However, this value is highly sensitive to small differences in the shape parameter estimate. Based upon Type III parameters from Table 1, a calculated upper limit of 161 mm is obtained. This limit has already been exceeded at a nearby meteorological station for a short-duration storm on August 19, 2005 (175 mm at Thornehill Grandview, MSC Station No.6158255) . Further, the probable maximum precipitation for a 6-hour duration in this region is estimated as 559 mm (Hansen et al., 1982).

Since the Type I distribution provides a better fit using the modified Anderson-Darling statistic, and the upper limit of storm depth estimated for the Type III distribution is below observed and estimated maximum rainfall depths estimated

following the probable maximum procedure, Type I is selected as the distribution of storm depths for the TPIA observations.

4.2. Storm Duration.

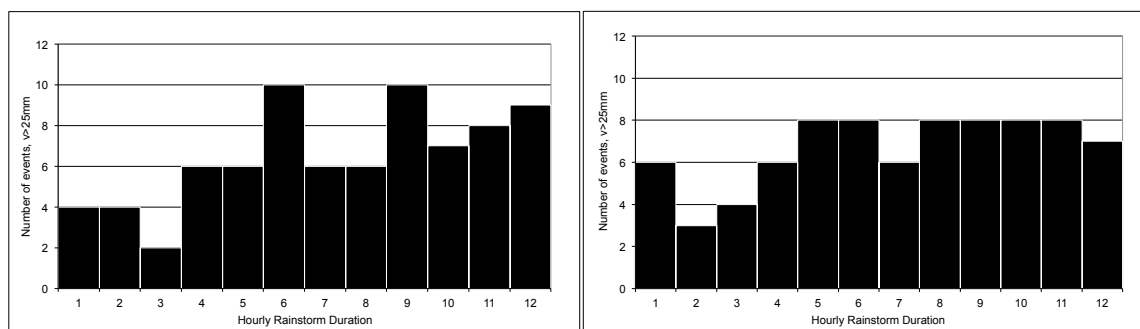


FIGURE 2.3. Figure 3a (left). Storm duration histogram based upon hourlyrainfall records, using $IETD = 6$ hours to define individual events. Figure 3b (right). Storm duration histogram, adjusted for start and finish time uncertainty.

The available rainfall records are reported at 1 hour increments, so that there is no way of knowing when rainfall may have started or stopped within each hourly increment. For that reason, the true rainstorm duration has a range of possible values, between that calculated on the basis of the IETD, and a value up to 2 hours less. A storm event may have started at any time between the beginning and the end of the initial hourly block, and finished at any time between the start and the finish of the final hourly block: $t_{IETD} \geq t > t_{IETD} - 1$, if $t_{IETD} \leq 2$; $t_{IETD} \geq t > t_{IETD} - 2$ if $t_{IETD} > 2$; where t_{IETD} is the storm duration established from analysis of hourly rainfall records. Of course, for durations of one hour, the actual duration cannot be less than zero. The effect of this will be to smooth the distribution, and increase frequency of shorter duration ranges. If the actual start and end of rainfall are assumed to be uniformly distributed within their reported hourly block, then the number of events reported for each IETD-based storm duration range may be redistributed across the range between t_{IETD} and $t_{IETD} - 2$. The IETD-based storm duration histogram is compared to the redistributed true duration distribution in Figures 3a and 3b respectively.

The adjusted distribution appears to be relatively uniform, with no strong evidence of a central tendency.

The uniform distribution has mean, variance, and PDF described by the following equations: $\mu_t = (t_{max} - t_{min})/2$, $\sigma^2 = (1/12)(t_{max} - t_{min})^2$, $f_T = 1/(t_{max} - t_{min})$. Since the lower limit of storm duration t_{min} is zero, these reduce to:

$$\mu_t = t_{max}/2, \sigma^2 = (1/12)t_{max}^2, f_T = 1/t_{max}.$$

In order to evaluate the applicability of the uniform distribution to storm duration, the Chi-squared goodness-of-fit test was performed. This test is based upon a standardized difference between measured and modeled frequencies, comparing the computed difference to critical test statistics (Snedecor and Cochran, 1989). The results are summarized in Table 2. In addition, mean and sample standard deviation determined by conventional method of moments, as well as the central moments of the uniform distribution are compared.

Sample mean value is well within 95% confidence limits of the maximum likelihood value, and estimate of sample standard deviation is within 4% of that for the uniform distribution. χ^2 test shows that the rainstorm duration follows a uniform distribution at all standard significance levels. Therefore, the TPIA SEA-based storm event duration statistics may be modelled with the uniform distribution. The CDF of this distribution is:

$$F_T = t/t_{max} \tag{2.10}$$

where t is a value of storm duration, and t_{max} is 12 hours in this example.

4.3. Comparison of Storm-Event Depths with DDF Accumulations.

Individual storm events are established with the IETD. An individual event is then described by its depth and duration. Any definition of the probability of occurrence of an individual storm must be based upon the joint probabilities of depth and duration. In general, the probability of exceedence of storm depth is of interest. Storm duration is often selected, for design purposes, as a function of catchment response (Marsalek and Watt, 1984). A single point value of storm duration has a zero

TABLE 2.2. Rainstorm duration parameters and test statistics.

| Parameter | TPIA Sample Values | Notes |
|----------------------------|--------------------|---|
| t_{max} | 12 | Maximum storm duration, hours. |
| t_{min} | 0 | Minimum value of storm duration. |
| m | 80 | Number of events exceeding u . Note that this is 2 greater than number used for parameter estimation of v . This is because the IETD storm duration at $t=13$ hours must be included to account for the number of storms with $11 \leq t < 12$ hours. |
| \bar{t} | 6.744 | Estimate of mean Rainstorm duration (hours) using method of moments |
| $\hat{\sigma}_t$ | 3.332 | Estimate of standard deviation, using method of moments |
| $\hat{\sigma}_t/\sqrt{12}$ | 0.962 | Standard error of the estimate of mean |
| Uniform Distribution | | |
| μ_t | 6 | Mean. |
| σ_t | 3.464 | Standard deviation. |
| j | 6 | Number of observed frequency intervals. Observations were grouped into 6, 2-hour intervals. |
| Parameter | TPIA Sample Values | Notes |
| χ^2 | 3.692 | Calculated value of χ^2 Statistic. |
| Degrees of Freedom | 5 | No parameter estimates required for uniform distribution. |
| Upper tail | Hypothesis limit | Calculated χ^2 value must be lower than test limit to accept null hypothesis at given significance level. |
| $\alpha = 0.10$ | 9.236 | Uniform distribution accepted. |
| $\alpha = 0.05$ | 11.070 | Uniform distribution accepted. |
| $\alpha = 0.025$ | 12.830 | Uniform distribution accepted. |
| $\alpha = 0.01$ | 15.090 | Uniform distribution accepted. |

probability of occurrence, and therefore a range of storm durations must be evaluated based upon the appropriate probability distribution. For hydrologic design purposes, the probability of occurrence of storm durations being equal to or less than a selected value is often required. Combining probability of exceedence of storm depth with the CDF of storm duration, the joint probability of storm depth and duration may be established. The joint probability of the CDF of storm duration and probability of exceedence of storm depth is equal to their product since depth and duration are independent random variables:

$$Pr\{(T \leq t) \cap (V > v)\} = Pr\{T \leq t\}Pr\{V > v\}.$$

Substituting Eq. (4), and Eq. (10) the joint probability may be established as follows:

$$Pr\{(T \leq t) \cap (V > v)\} = J_u(t/t_{max}) \exp[-(v - u_v)/\sigma_v] \quad (2.11)$$

Then the return period for a given t and v can be evaluated as:

$$T_{v,t} = \frac{1}{Pr\{T \leq t\}Pr\{V > v\}\theta_0} = \frac{t_{max}}{\theta_u \exp[-(v - u_v)/\sigma_v]} \quad (2.12)$$

Eq. (11) states that the probability that a particular storm depth v will be exceeded, given storm duration being less than or equal to a selected value t is the product of the CDF of storm duration with the probability of exceedence of storm depth, adjusted for the threshold value of storm depth. Eq. (12) is evaluated for durations from 0.5 through 12 hours using parameters determined from TPIA hourly rainfall statistics, and the results are shown in Figure 4, for a return periods of 5, 25, and 100 years.

TABLE 2.3. Statistical moments for conventional DDF annual maximum series.

DDF Annual Maximum Parameters,
TPIA, 1950 - 1998

| parameter | DDF Time Interval, hours | | | | |
|---------------------|--------------------------|------|------|------|------|
| | 1/2 | 1 | 2 | 6 | 12 |
| $\hat{\mu}$, mm | 21.8 | 24.9 | 29.4 | 38.6 | 44.4 |
| $\hat{\sigma}$, mm | 7.9 | 8.7 | 10.8 | 15.6 | 17.9 |

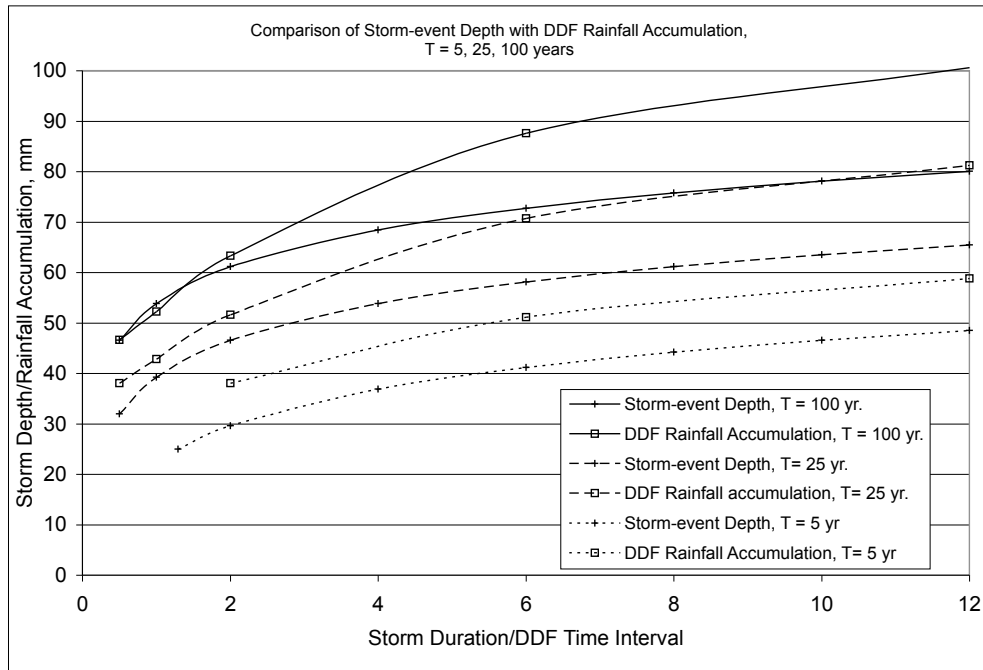


FIGURE 2.4. 100, 25 and 5-year return period storm-event depth-durations are compared with conventional DDF rainfall accumulation. Box symbol indicates conventional DDF GEV I-modeled rainfall accumulation. Cross symbol is used to show SEA GPD Type I-modelled depth.

For comparison, conventional DDF parameters (by method of moments) for TPIA rainfall measures (Meteorological Services Canada/AES, 1998) shown in Table 3 are applied with Eq. (9) (Gumbel annual maximum distribution) to determine rainfall depth/duration combinations for return periods of 5, 25, and 100 years.

The results are plotted in Figure 4. Both SEA/GPD and DDF/GEV curves are monotonically increasing, and have similar values of storm depth/rainfall accumulation at short durations/time intervals. SEA/GPD values at short durations are

lower than DDF/GEV, for short return periods, with differences decreasing with increasing return periods. With increasing storm duration/time interval, the differences between the two techniques increase. Conventional DDF curves model greater rainfall depth accumulations than those of SEA/GPD. This is expected because conventional DDF analysis procedures capture the highest-intensity portion of an actual storm for a pre-selected time interval regardless of the true duration of the actual storm. In order to demonstrate this difference between the two methods of rainfall frequency analysis further, annual maximums from SEA (rather than threshold excess events) are compared to DDF annual maximum rainfall accumulations where there is an overlap in the period of record (1960-1998). In this way, the number of individual storm events actually captured by DDF analysis can be assessed. These records were compared on a cumulative basis for comparable durations or time intervals. While all data are obtained from the same meteorological station, the DDF statistics, curves, and parameters are based upon the period from 1950 to 1998. 1998 was the last year for which the rainfall accumulation data has been analyzed and published at the time of writing. Hourly rainfall data has been archived at this station since 1960, and was last published in 2001.

At the 1 hour SEA duration/DDF time interval only 4 of the 39 values shown in Figure 5 were equal. In all other cases, the DDF values for rainfall depth were much greater than annual maximum storm-event depths, confirming that most short time interval measurements of rainfall depth in conventional analysis are portions of longer storm events. SEA threshold-based storm event analysis excludes non-extreme events below the threshold value (25 mm in this example). Therefore the majority of the SEA 1-hour duration annual maximum storm events plotted in Fig. 5 was excluded. This is the main reason that the two methods still result in similar rainfall depths at short durations/time intervals.

For longer durations, two comparisons between storm event annual maximum depths and conventional DDF rainfall accumulation were made. Storm events less than or equal to 6 hours duration were compared to 6-hour DDF rainfall accumulation measures in Figure 6. Fig. 6 shows that there were 13 of the 39 years of record where storm depth and rainfall accumulation were identical.

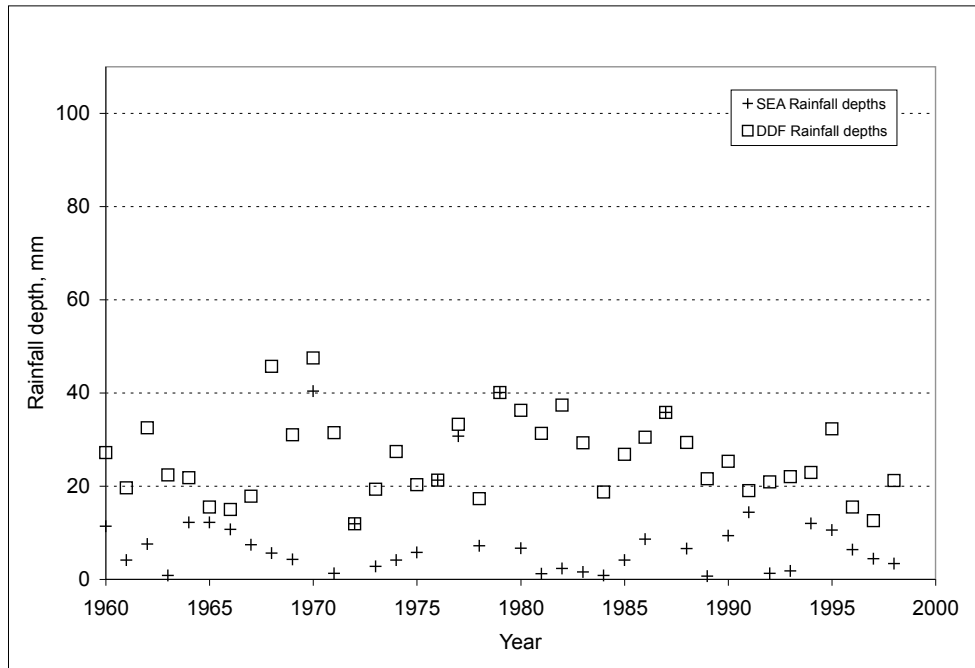


FIGURE 2.5. Comparison of event-based and DDF annual maximum rainfall depths, for durations/time intervals of one hour. Actual conventional DDF depths are shown with a box symbol. SEA measures of storm depth are shown with a cross.

Storm events less than or equal to 12 hours in duration were compared to conventional 12 hour rainfall accumulation measures in Figure 7. 17 of the 39 years of record had identical rainfall depths.

All DDF annual maximum measures equal or exceed SEA measures. It is clear from this review that DDF measures are not composed entirely of single events of duration equal to or less than the standard DDF time intervals. Rather they most often measure rainfall accumulations greater than the depth of individual events for the selected time interval. This is reflected in the DDF over estimation of rainfall

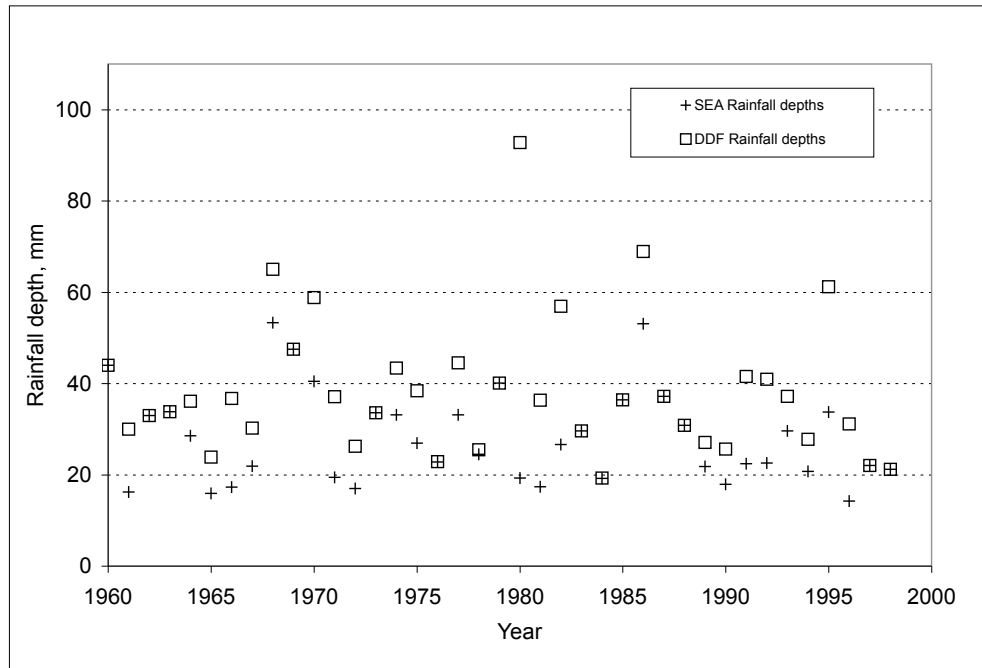


FIGURE 2.6. Comparison of event-based annual maximum storm depths for durations of 6 hours or less and DDF annual maximum depths for the 6-hour time interval.

accumulation, compared to the storm-event model, with increasing duration/time interval. Since DDF time intervals are unrelated to storm duration, a given measure of rainfall accumulation may represent:

- The rainfall of a single storm event of duration less than or equal to the time interval,
- A portion of an event of duration exceeding the time interval,

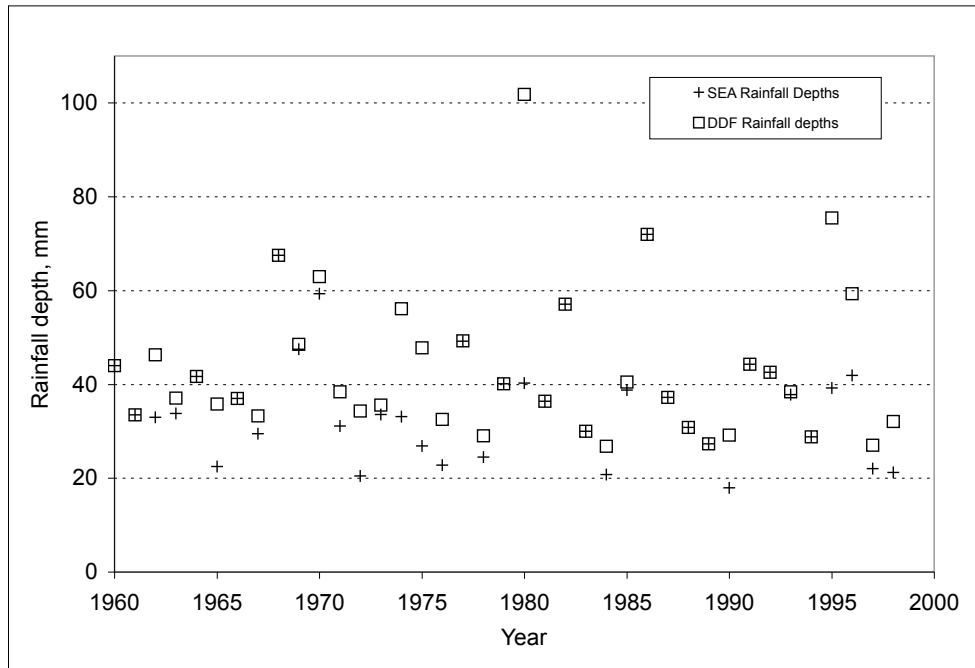


FIGURE 2.7. Comparison of event-based annual maximum storm depths for durations of 12 hours or less, and DDF annual maximum rainfall accumulations for the 12-hour time interval.

- Portions of multiple events, provided that the time interval exceeds the IETD.

Conventional analysis does not explicitly address the joint probability of rainfall accumulation and time interval, but implicitly does so by separate characterization of the extreme value probability distribution at each of the successive time intervals. An example of this implicit cumulative analysis from TPIA statistics is the incorporation of rainfall depths of the same event in 1979 as the annual maximum statistic for 1, 2, 6, and 12 hour time intervals. Since prescribed time intervals are treated with equal

weight in development and application of DDF curves, time interval probability distribution is implicitly assumed to be uniform.

5. Summary and Conclusions

In this paper using the maximum likelihood method for parameter estimation and a goodness-of-fit test, it is demonstrated that the Generalized Pareto Distribution Type I is an acceptable model of rainstorm depth for long-return period events, for the data set examined. The review of storm event identification led to modifications of storm duration estimation, arising from an understanding of the differences between reporting interval and actual storm duration within those reporting intervals. A simple uniform distribution of rainstorm duration may be applied to describe the probability density function. The current practice in the use of design storms is to select the storm duration in accordance with the catchment time of concentration only, with no regard to the probability of occurrence of different duration storms. That is, all durations are assumed to have an equal probability of occurrence, equivalent to a uniform probability density. The finding in this paper that extreme rainstorm even durations have a uniform probability density function provides confirmation that the implicit assumption used in practice is justifiable.

The depths of design storms as determined from conventional DDF curves was found to be much higher than those determined following the SEA/GPD procedure for longer durations.

As shown in this paper, the event-based joint probability of storm depth and duration provides a theoretical basis for a simple storm-event depth-duration-frequency model that explicitly incorporates the probability distributions of both storm depth and duration. Comparing the SEA procedure with the conventional DDF analysis procedure, the following implications arise:

- The prescribed time intervals used in conventional DDF analysis are not often a match to the actual duration of storm events.

- Conventional DDF methods make use of the Gumbel distribution for rainfall depths within each prescribed time interval, and so implicitly incorporate the joint probability of rainfall depth accumulation and time interval.
- Application of the SEA-based depth-duration curve to design-storm rainfall-runoff models may result in lower estimates of runoff volume and peak discharge as compared to the results from conventional DDF curves, for larger catchments where longer duration design storms need to be applied. SEA-based methods are more realistic because the design storms developed are based upon a probabilistic model that considers both depth and duration of actual storms. Conventional DDF techniques do not measure storm events explicitly and their application to design storms assumes concurrence between rainfall accumulations and storm depth. This assumption is not justified based upon the comparisons in this study.

SEA combined with threshold-excess models as described herein provide an immediate means of improving the quality and accuracy of describing design storm depths and durations. Accuracy is improved because more complete use is made of available data. The entire set of rainstorm data is used to describe the probability of exceedence at the storm depth threshold. That starting point for the GPD is firmly established with a low-variance parameter, so that the balance of the distribution is determined by measures of storm depth that are clearly those of extreme events, through appropriate selection of the storm depth threshold. By contrast annual maximum analysis is based upon the assumption of sufficient number of measures within the annual block so that parameter estimates approach asymptotic values (Coles, 2001). This may not be the case if the number of independent measures of rainfall depth in the annual block is insufficient.

Efficient management of runoff quantity and quality requires accurate estimation of peak flows and runoff event volumes of various return periods. Design storms developed using conventional DDF techniques will produce more conservative estimates than SEA methods, incorporating an implicit factor of safety, and so may appear to be initially attractive. However, models applied for design purposes should be as realistic as possible, so that designers, policy makers, and system operators have a clear

understanding of actual system performance and safety limits. With an improved understanding achieved through SEA-based models, costs can be more accurately determined so that design and operational alternatives are properly assessed. The more realistic assessment of runoff volume may be especially important, since runoff volume storage required as a result of urbanization imposes high costs in terms of construction, land occupancy, and treatment. The improvements provided by the threshold-based SEA procedures make it a sound alternative to conventional DDF techniques. It is therefore proposed that this alternative be tested for other locations. Upon successful testing, these threshold techniques may be used for the development of more representative design storms that reflect the frequency of occurrence of short duration convective storms more accurately. Similar methods of analysis are being applied to long duration rainstorm measures ($t > 12$ hours), so that the full range of extreme rainstorm events may be characterized.

5.1. Acknowledgement.

The comments of two anonymous reviewers led to improvements in this paper.

CHAPTER 3

A probabilistic description of rain storms incorporating their peak intensity

1. Introduction

Most day-to-day engineering hydrology involves the use of design storms as input to a rainfall-runoff model. Design storms are prescribed distributions of rainfall intensity. Rainstorms have wide variation in intensity within their durations, and in order to describe or model this variation, a number of design storm intensity distribution patterns or hyetographs have been developed and applied (e.g., Marsalek and Watt, 1984). Some of the common design storm hyetographs include the Chicago Storm, the NRCS storm, and the Canadian AES (Atmospheric Environment Service, now Meteorological Services Canada) storm distributions. Some of these hyetographs are based upon the analysis of actual storm intensity distributions (Watt et al., 1986; Huff, 1967, 1993). Others, such as the Chicago Storm distribution (Kiefer and Chu, 1957) are constructs that make use of curve fitting equations. Once the Design Storm hyetograph is selected for a total rainfall depth and duration, then the return period of the event is that of the selected storm depth and duration. Typically, Depth-Duration-Frequency (DDF) curves, or related Intensity-Duration-Frequency (IDF) curves are used to establish the return period of total depth accumulation over the duration of a design storm.

In application, the effect of the storm hyetograph upon the frequency of the event is usually ignored. Provided that the storm depths and durations are equal, there is no difference in the frequency of occurrence between a Chicago, Huff, or AES event. While convenient, this assumption, when examined critically, is not plausible. This aspect was recognized early in the development of design storms (Kiefer and Chu, 1957). The DDF curves used as the basis for determination of return period for

design storm depth/duration combinations themselves do not provide measures of actual storm depth. The time intervals selected for design storm durations are not based upon storm event durations, but are in fact moving time-windows which are unrelated to the measurement of the start and end of actual storms (Palynchuk and Guo, 2008). In conventional rainfall frequency analysis, rainfall amounts contained within a moving time-window with fixed duration may in fact fall throughout the duration or any sub-duration within the moving window. The rainfall data used to develop probability distributions as the basis of DDF curves are based upon a mix of rainfall accumulation within actual events, or parts of multiple storm events within prescribed time intervals.

In order to improve upon the design storm approach, Storm-Event Analysis (SEA) (Adams et al, 1986; Restrepo-Posado and Eagleson, 1982), employing a minimum inter-event time or dry period definition (IETD), has been used in order to identify individual rain storm events at a meteorological station near Toronto, Canada (Palynchuk and Guo, 2008). The depth and duration measures of those events were then screened. Storms less than a selected upper duration limit (i.e. 12 or 24 hours), but with depths exceeding a high threshold (i.e. 25mm) were analyzed, in order to determine the distributions and dependencies of those measures. Storms with depths exceeding a high threshold are selected, in order to establish an appropriate tail distribution. Generalized Pareto Distribution (GPD) (Coles, 2001) were examined, because of their appropriate application to threshold statistics. Applying goodness-of-fit tests GPD Type I was found to provide the best fit from within the GPD family. The bounded empirical distribution of the storm durations (between 1 and 24 hours) were found to fit the uniform distribution. The frequency distribution of storms of various magnitudes was then characterized by the joint probability distribution of storm depth and storm duration.

The threshold-based probabilistic model of storm depth and duration is constructed as follows. First, the probability of exceedence for storm depth is:

$$Pr \{V > v\} = J_u \exp [-(v - u_v)/\sigma_v] \quad (3.1)$$

where $J_u = Pr\{V > u_v\}$ is the probability of storm depth (V, v) being greater than the threshold value u_v . The threshold value is selected on the basis of a number of factors; statistical independence between storm depth and duration and stability in estimation of the shape parameter σ_v being the two most important criteria. J_u is estimated as the ratio between the number of storm events exceeding the depth threshold and the total number of events.

Second, the probability density function (PDF) of storm duration (T, t), given storms with depth greater than u_v , and duration less than or equal to the maximum duration considered (t_{max}), is modeled with a uniform distribution. The probability that storm duration is less than or equal to a particular value, t is:

$$Pr\{T \leq t | T \leq t_{max}\} = t/t_{max} \quad (3.2)$$

Since V and T were found to be statistically independent for events exceeding the selected threshold, the joint probability of depth and duration is:

$$Pr[(T \leq t)(V > v)] = (t/t_{max})J_u \exp[-(v - u_v)/\sigma_v] \quad (3.3)$$

This work as detailed in Palynchuk and Guo (2008), advances the design storm approach by:

- characterizing depth and duration of actual individual events,
- developing explicitly their joint probabilities.

Conceptually, this work clearly expresses the severity of a rainstorm event in both probabilistic and practical terms. For drainage design purposes, rainstorm events increase in severity with increasing depth and decreasing duration. This is reflected in Eq. (3), which is the joint probability of storm depth exceeding a given value, and storm duration being less than or equal to a selected value. In a similar fashion, in the development of conventional design storms, when a storm duration is selected, in the ensuing frequency analysis, the occurrence of events with durations less than or equal to the selected duration are actually evaluated. For purposes of design, the designer establishes the likelihood of a given event, together with all more serious events.

Design storms are used as input for rainfall-runoff modelling. Peak rainfall intensity is a key factor in the determination of time of concentration and peak discharge from a catchment. Analysis of actual and modeled rainfall-runoff data leads to similar conclusions. For example, Fig. 1 below shows results of regression analysis of actual hydrograph data from the Mimico Creek catchment in Toronto, Ontario, Canada (Environment Canada, Canada Centre for Inland Waters, Mimico Creek Stage-Discharge data, Station 02HC033, 2009). The dependent variable is peak discharge (Q_p) in mm/h, with independent variables of runoff volume (v_r) and peak hourly rainfall intensity (i_p):

$Q_p = c_1 v_r + c_2 i_p$, where c_1 and c_2 are coefficients of regression. For this particular data set, $R^2 = 0.975$.

While it is clear that peak intensity is an important variable needed to describe design storms (since it has an important influence on hydrologic outputs), neither the conventional probabilistic models of rainfall employing DDF curves nor the joint probability model of Palynchuk and Guo (2008) explicitly address the distribution of intensity within rainstorms as a random variable. Since peak intensity is itself a random variable, the probabilistic description of storm frequency based solely upon storm depth and duration is incomplete. In order to improve the probabilistic description of design storms, the joint probability of storm depth, duration and peak intensity is required. This is the primary objective of this paper.

Some research has been carried out examining the influence of peak intensity upon frequency of storm events. Yue (2000a, 2000b) has applied bivariate Normal and bivariate GEV I distributions to develop joint and conditional return periods of storm depth and peak daily intensity for very long-duration (several days) storms in Japan. Another line of research has examined peak intensity within extreme rainfall events identified with a prescribed IETD from hourly rainfall data (Zhang and Singh, 2007a). The marginal distributions of storm variables were established first. Bivariate frequency distributions were then developed using copulas to relate the distributions of any two variables. Both of these approaches have been applied to annual maximum statistics, expanding from the conventional univariate approach to estimate rainfall event return periods.

A further refinement has been described by both Grimaldi and Serinaldi (2006) and Zhang and Singh (2007b), where one-parameter 3-copula functions are used to relate the marginal distributions of three rainstorm variables. Kao and Govindaraju

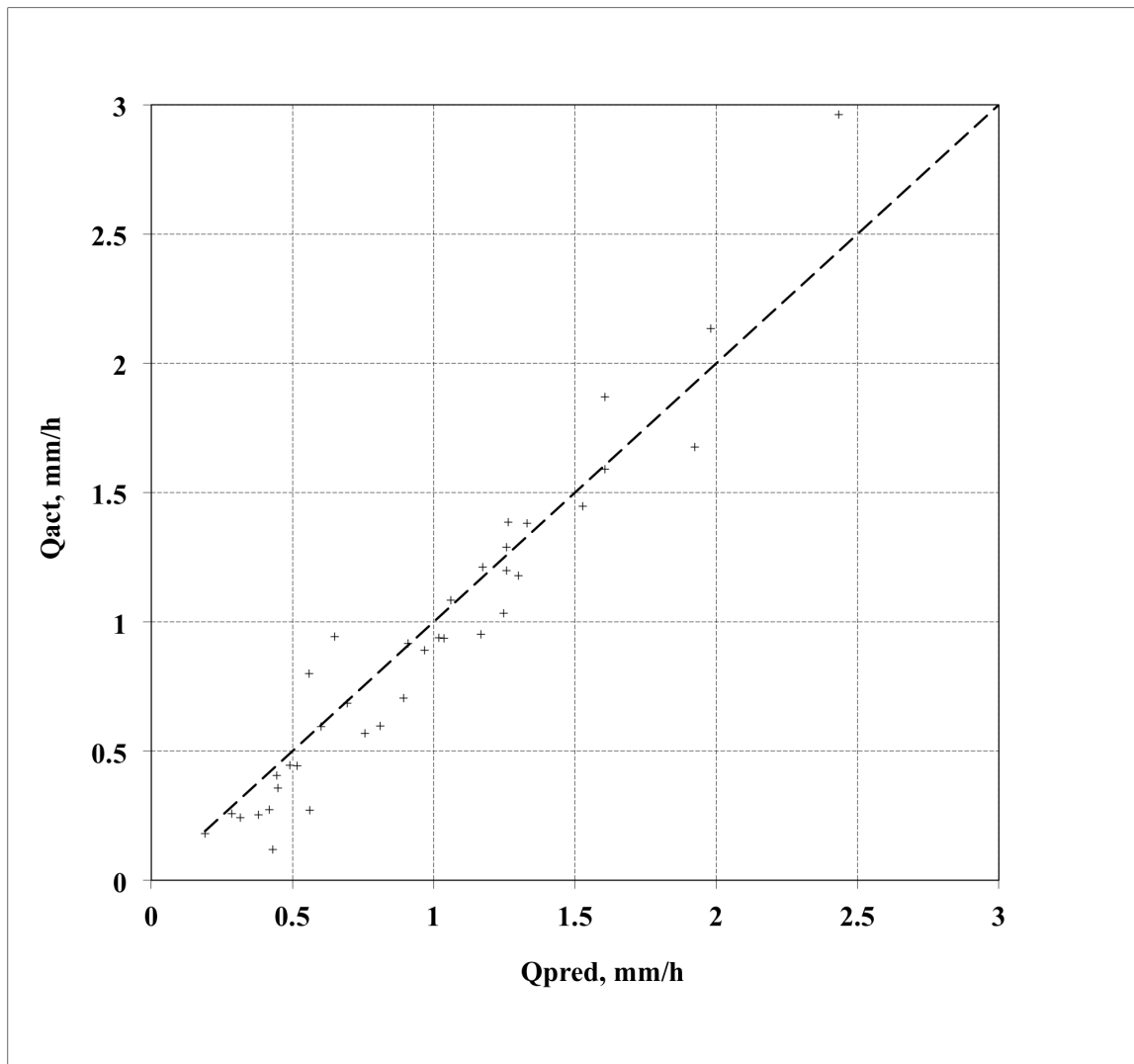


FIGURE 3.1. Plot showing actual peak discharge for Mimico Creek (Ontario, Canada) catchment on y-axis, and predicted by regression equation on x-axis. Independent variables for regression equation are runoff depth and peak hour intensity.

(2008) have applied the Plackett family of copulas in order to develop trivariate distributions of rainstorm variables. These approaches will be discussed and compared later with the techniques developed in this paper.

The conventional DDF approach is to estimate return period from the cumulative distribution function for rainfall depth (usually from annual maximum statistics), for a particular rainfall interval. The SEA-threshold-based approach applies Eq. (3) to determine storm return period $T_{v,t}$, based upon the joint probabilities of storm depth and duration: $T_{v,t} = 1/\{Pr[(V > v)(T \leq t)]\theta_0\}$ where θ_0 is the average number of storm events each year.

The bivariate distribution approaches make use of bivariate cumulative distribution functions (CDFs) or copulas and marginal distributions of two random variables to determine joint return periods (Yue, 2000a, 2000b): $T_{v,i} = 1/[1 - F_{V,I}(v, i)]$, where $F_{V,I}(v, i) = Pr[(V \leq v)(I \leq i)]$; and conditional return periods: $T_{v|i} = 1/[1 - F_{V|I}(v|i)]$, where $F_{V|I}(v|i) = Pr[V \leq v|I \leq i]$; so that the joint effects of storm depth and intensity may be considered. Trivariate copula methods incorporate information upon the greatest number of random variables. Each technique calculates the annual probability that a storm of a particular combination of measures will be exceeded. The return period is then the inverse of the annual probability of exceedence. Conventional DDF approaches incorporate the least amount of information on storm descriptors (i.e., rainfall depth for a selected time interval). The SEA-threshold approach incorporates storm depth and duration in its formulation. The bivariate frequency distributions can incorporate any two storm variables. The 3-copula joint frequency distributions have the potential to incorporate any 3 storm measures, but the focus has been primarily upon development of the underlying mathematics, together with techniques for parameter estimation. None of the copula techniques is well suited at this point, to advancing and improving the design storm approach as used in day-to-day engineering hydrology since they do not incorporate the key measures of rainstorms. Clearly, the next development must be of frequency distributions that incorporate those rainstorm variables that impact directly upon hydrologic outputs, and that lends itself to consistent application by practitioners familiar with the conventional design storm approach.

The SEA approach, using threshold analysis to examine extreme rainfall events, results in rainfall data, organized or grouped on the basis of individual storm events. While peak intensity within individual events was not previously evaluated, the information is available as a result of the analysis process. Building upon previous work, hourly rainstorm data from two meteorological stations near Toronto, Canada were analyzed, in order to develop probability distributions for storm depth and duration, and to begin the characterization of storm peak intensity. The results of the analysis are presented in detail in the Appendix to this paper. A summary of the results is as follows:

- Storm depth is well described using the GPD I distribution, judged by the modified Anderson-Darling test statistic at $\alpha = 0.05$;
- Storm duration, for $t \leq 24$ hours may be fitted to a uniform probability distribution, judged by the χ^2 test statistic at $\alpha = 0.05$;
- storm depth and duration are uncorrelated at $\alpha = 0.05$;
- Storm peak intensity and storm duration are negatively correlated;
- Storm peak intensity and storm depth are positively correlated.

The balance of this paper will examine the following:

- An alternative approach for characterization of peak-storm intensity;
- The fitting of a probability distribution to a new measure of peak intensity;
- Development of the joint probability of storm depth, duration, and the new measure of peak intensity.

2. Alternative Approaches to Rainstorm Peak Intensity Characterization

So far, characterization of the frequency distribution of storm peak intensity has followed an approach similar to those of Yue (2000a, b), Zhang and Singh (2007a, 2007b), Grimaldi and Serinaldi (2006), and Kao and Govindaraju (2008).

In these works, direct measures of the peak intensity are fitted to probability distributions.

Conventional design storm approaches rely on the assumption that hyetograph shape can be characterized independently of storm depth (Huff, 1967; Yen and Chow, 1980; Watt et al, 1986). Some effort should be spent on determining whether this traditional practice has some validity. A description of storm shape should bear a direct relationship to peak storm intensity and provide some indication of relative concentration of rainfall within the storm. These characteristics would facilitate application to design storm techniques, and provide a means of direct comparison with traditional design storm patterns.

Available rainfall data in the region of interest and of sufficient period of record are archived on an hourly basis, so that depth recorded for a given hour is the average hourly intensity. The peak hourly intensity, in the context of a storm event, has upper and lower bounds. The lower bound of peak intensity is the average storm intensity; $i_{low} = v/t$. The upper limit of peak storm intensity would correspond to the case where nearly all of the storm depth occurs within a single hourly interval; $i_{up} = v/1$. Peak hourly storm intensity on its own does not aid in characterizing storm hyetograph shape. A measure incorporating the upper and lower bounds of peak intensity as well as the relative concentration of total storm depth within the peak hour would permit such a description. Using the bounded nature of hourly peak intensity, a reduced variate (I_{pf} , i_{pf}) on $[0, 1]$ may be established by substituting the upper and lower bounds of hourly peak intensity into the standard expression for the reduced variate of a bounded variable, $i_{pf} = (i_p - a)/(b - a)$; where a and b are lower and upper bounds respectively:

$$i_{pf} = \frac{i_p - v/t}{v/1 - v/t} = \frac{(i_p/v)t - 1}{t - 1}, t > 1 \quad (3.4)$$

The reduced variate is defined as intensity peak factor, which is a relative measure of the "peakiness" of a given rainstorm event. Note that for a storm duration of one hour, then the upper and lower values of peak storm intensity are identical. For that reason, the evaluation of the reduced variate is only valid for storm durations greater than one hour.

TABLE 3.1. Correlation of intensity peak factor with storm depth and duration.

| | Toronto (MSC 6158350) | TPIA (MSC 6158733) |
|---|--------------------------|-----------------------|
| Correlation coefficient ($I_{pf} - T$) | -0.552 | -0.585 |
| Correlation coefficient ($I_{pf} - V$) | 0.099 | 0.033 |
| Upper tail limit $\alpha = 0.05$ | 0.126 | 0.141 |
| Accept/reject independence ($I_{pf} - V$) | Accept | Accept |

The intensity peak factor is a new concept introduced in this paper. It is a reduced variate describing the peak hourly intensity in terms of its position between minimum and maximum possible values. The minimum and maximum values of peak hour intensity are not independent of storm depth and duration. Rather, within this framework, storm intensity is correctly described in terms of the limits imposed by the external measures of storm depth and duration and basic principals of continuity. The balance of much of this paper is the consequence of applying this concept to the probabilistic description of rainstorm events.

When the intensity peak factor was evaluated for correlation with storm depth and duration, it was found to be uncorrelated with storm depth, and negatively correlated with storm duration. The values for the two meteorological stations for which data have been analyzed are shown in Table 1, together with corresponding critical values for correlation coefficient ρ at $\alpha = 0.05$. The correlations of $I_{pf} - T$ are high in relation to the critical value of ρ , so those two variables are correlated. The correlations of $I_{pf} - V$ are below the critical value of ρ , so are independent at the selected α value.

The independence of the form of rainfall distribution (hyetograph) with storm depth has only been used in the past as a simplification to aid in the prescription of standardized forms of storm events, and not as a means of enhancing their probabilistic description. The implicit assumption of independence of storm depth and hyetograph form continues to be applied. Al-Rawas and Valeo (2009) applied the techniques originally developed by Huff (1967) in characterization of the temporal distribution of rainfall depth within rain storms in Oman wherein the possible effect of storm depth on distribution of rainfall within a storm is neglected. In the past,

this independence was assumed, but the results in Table 1 provide statistical confirmation that a measure of the relative concentration of rainfall depth within a storm is independent of storm depth.

A bounded plotting position equation was applied to I_{pf} , for storm durations greater than 1 hour ($t > 1hr$):

$$F_{pp}\{I_{pf} \geq i_{pf}\} = \begin{cases} 0, & i_{pf} = 0 \\ \frac{k}{n+2}, & 1 < k \leq n \\ 1, & i_{pf} = 1 \end{cases} \quad (3.5)$$

where n is the sample size and k is the rank of the variate i_{pf} . The lower and upper bounds of the reduced variate necessarily have cumulative probabilities of 0 and 1 respectively, and so upper unbounded plotting position formulas such as the Weibull plotting position ($\frac{1}{n+1}$) cannot be applied.

The bounded nature of intensity peak factor limits the selection of probability distributions. The sample moment estimators presented in Table 2 indicate that the distribution is not symmetric, ruling out a number of distributions (bounded normal, raised cosine, Irwin-Hall, U-quadratic). Many bounded distributions are simply particular forms of the Beta distribution (uniform, triangular, Kumaraswamy). Therefore, the Beta distribution was selected and fitted to the plotting point distribution, using sample moment estimators. The results are shown in Fig. 2 below for the Toronto station.

The Beta distribution CDF (Johnson et al., 1994) has the following form:

$$F_{I_{pf}}(i_{pf}) = \frac{\int_0^{i_{pf}} x^{p-1} (1-x)^{q-1} dx}{\beta(p, q)} \quad (3.6)$$

where $p, q > 0$ are distribution parameters. $\beta(p, q)$ is the beta function, and x is a dummy variable of integration.

The distribution parameters p and q were estimated using the method of moments (MM) (National Institute of Standards and Technology, 2006):

$$p = \bar{i}_{pf}(\bar{i}_{pf}(1 - \bar{i}_{pf})/\hat{\sigma}_{i_{pf}}^2 - 1)$$

$$q = (1 - \bar{i}_{pf})(\bar{i}_{pf}(1 - \bar{i}_{pf})/\hat{\sigma}_{i_{pf}}^2 - 1)$$

TABLE 3.2. Beta distribution parameters for intensity peak factor.

| Parameter | Toronto MSC 6158350 | TPIA MSC 6158733 |
|--------------------------------------|------------------------|---------------------|
| \bar{i}_{pf} | 0.317 | 0.321 |
| $\sigma_{\hat{I}_{pf}}$ | 0.214 | 0.210 |
| p | 1.190 | 1.262 |
| q | 2.562 | 2.667 |
| Kolmogorov-Smirnov test statistic | 0.0994 | 0.1000 |
| Critical value, 5% $1.36/\sqrt{n+1}$ | 0.1037 | 0.1388 |
| Accept/Reject | Accept | Accept |

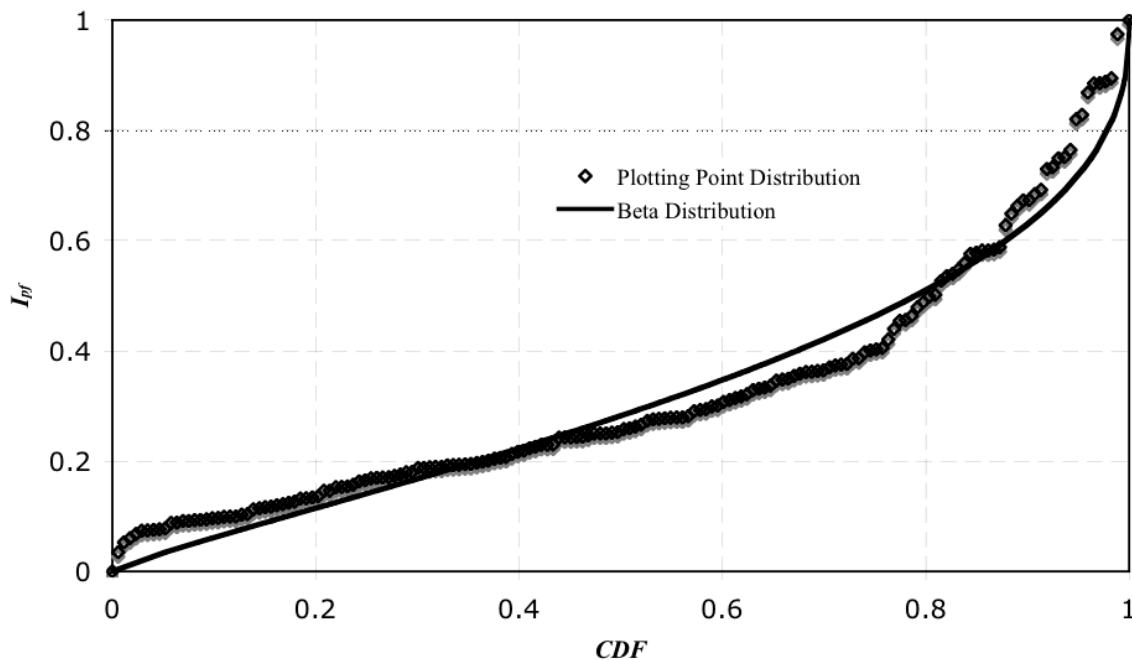


FIGURE 3.2. Plotting point or empirical distribution of intensity peak factor (I_{pf} , i_{pf}), based upon Eq. (5), together with Beta distribution in solid line, fitted by method of moments.

Where \bar{i}_{pf} and $\hat{\sigma}_{i_{pf}}$ are respectively, the mean and standard deviation of the sample of i_{pf} . The estimated Beta distribution parameters are shown for the two meteorological stations in Table 2. In addition, Kolmogorov-Smirnov (K-S) test statistics and critical test values for the 5% level of significance are shown, providing an assessment of the goodness-of-fit of the Beta distribution to the empirical distribution of the ordered statistics.

The close visual fit between the Beta and plotting position distributions, and the K-S goodness-of-fit statistic suggest that Beta distributions are suitable models for the frequency distribution of the intensity peak factor, for storm durations greater than one hour, i.e., the time interval for rainfall measurement. Other researchers (Kao and Govindaraju, 2008) apply Beta distributions to summary measures of rainfall accumulation and relative peak temporal location within storm events, recognizing the bounded nature of such measures.

3. Joint Probability of Storm depth, duration and Intensity Peak Factor

3.1. Joint probability model and its assumptions.

Eq. (6) can be used for the determination of the CDF of intensity peak factor. Eqs. (1) and (2) are used to determine the marginal distributions of storm depth and duration respectively. The joint probability of storm intensity peak factor, storm depth, and storm duration, in the context of describing increasing storm severity may be expressed as:

$$Pr\{(V > v)(I_{pf} > i_{pf})(1 < T \leq t)\} = Pr\{(V > v)[(I_{pf} > i_{pf})(1 < T \leq t)]\}$$

Note that storms with $t \leq 1$ are excluded by virtue of the definition of I_{pf} . Applying the conditional probability theorem (Ang and Tang, 1975):

$$\begin{aligned} & Pr\{(V > v)[(I_{pf} > i_{pf})(1 < T \leq t)]\} \\ &= Pr\{(V > v)[(I_{pf} > i_{pf})(1 < T \leq t)]\}Pr\{(I_{pf} > i_{pf})(1 < T \leq t)\} \end{aligned}$$

That is, the probability of storm depth conditional upon intensity peak factor and storm duration, times the joint probability of intensity peak factor and storm duration equals the joint probability of all three events. Furthermore, if $Pr\{V > v\}$ is independent of the joint event $\{(I_{pf} > i_{pf})(1 < T \leq t)\}$, then,

$$Pr\{(V > v)(I_{pf} > i_{pf})(1 < T \leq t)\} = Pr\{(V > v)\}Pr\{(I_{pf} > i_{pf})(1 < T \leq t)\} \quad (3.7)$$

The probability terms in the right-hand side of Eq. (7) are:

- the probability of exceedence of V , Eq.(1) if V is independent of the joint event of intensity peak factor and duration; and
- the joint probability of $I_{pf} > i_{pf}$ and $1 < T \leq t$.

3.2. Initial test of the assumption of independence between V and the joint event of I_{pf} and T .

TABLE 3.3. Correlation of intensity peak factor with storm depth ($I_{pf} - V$) for three separate ranges of storm duration..

| Duration Range | Toronto MSC 6158350 | TPIA MSC 6158733 |
|---|------------------------|---------------------|
| 2 to 9 hours | 0.066 | -0.020 |
| - Upper tail limit $\alpha = 0.05$ | 0.220 | 0.235 |
| 10 to 15 hours | 0.095 | 0.153 |
| - Upper tail limit $\alpha = 0.05$ | 0.216 | 0.251 |
| 16 to 24 hours | 0.051 | 0.074 |
| - Upper tail limit $\alpha = 0.05$ | 0.224 | 0.254 |
| Accept/reject independence ($I_{pf} - V$) | Accept | Accept |

Although earlier analyses showed that V is independent of the marginal distributions of both I_{pf} and T , this is still not sufficient to ensure that V is independent of the joint probability distribution of T and I_{pf} . Since it is not possible to theoretically prove if V is independent of the joint probability distribution of I_{pf} and T , an initial empirical test was performed to verify the validity of an assumed independence. The rainfall data were split into three different groups according to storm duration.

Three groups were used in order to ensure that sample size remained large; increasing the number of groups reduces the size of each sample and leads to poor estimates. Correlation between V and I_{pf} was calculated for each of the three storm duration groups, for the two meteorological stations. If the correlation coefficient is very low for each group (as it is for the whole set of data), then it would be an indication that the assumption of independence is valid. The results of this test are shown in Table 3, together with the critical value of the correlation coefficient for acceptance of the null hypothesis that correlation coefficient $\rho = 0$ corresponding to $\alpha = 0.05$.

Results of this first test show that correlation is not significant, regardless of the storm duration range. The assumption of independence of V with respect to the joint distribution of I_{pf} and T is supported since grouping by storm duration leads only to small, statistically insignificant changes in correlation. Further testing of the assumption of independence will be performed, following development of a joint probability distribution, in order to confirm the validity of the assumption of independence for both stations.

3.3. Joint Probability of I_{pf} and T .

An approach for determining the joint distribution of two marginal distributions is through the application of Copulas. A copula function has the following general form (Balakrishnan and Lai, 2009):

$$F(x, y) = C_{\alpha} [F_X(x), F_Y(y)] \quad (3.8)$$

where $F(x, y)$ is the joint CDF of X and Y , $F_X(x)$ and $F_Y(y)$ are respectively the marginal CDFs of X and Y , and C_{α} is the copula function with parameter α . In order to simplify presentation, $F_X(x)$ will be represented by F_x , and $F_Y(y)$ by F_y in the development and formulation of copulas.

Eq. (8) states that there is a unique copula function C that relates the marginal CDFs of two correlated random variables, such that the result is the joint CDF of the two (i.e., Sklar Theorem; see, e.g. Nelson, 2006). In hydrology, the Archimedean class of copulas is frequently applied, because of their relative simplicity and successful

application to problems of joint probability. This class has the general form of:

$$C_\alpha(F_x, F_y) = \psi^{-1} [\psi(F_x) + \psi(F_y)] \quad (3.9)$$

where ψ is a generator function which is strictly decreasing and convex. Given the negative correlation of intensity peak factor and storm duration, there are two particular groups of Archimedean copulas that apply (Zhang and Singh, 2007a): the Ali-Mikhail-Haq (AMH) and Frank families. The AMH family of copulas (following reduction of the general form) is:

$$C_\alpha(F_x, F_y) = \frac{F_x F_y}{1 - \alpha(1 - F_x)(1 - F_y)} \quad (3.10)$$

for which the parameter α is estimated from Kendall's τ (Balakrishnan and Lai, 2009):

$$\tau = \left(\frac{3\alpha - 2}{\alpha} \right) - \frac{2}{3} \left(1 - \frac{1}{\alpha} \right)^2 \ln(1 - \alpha) \quad (3.11)$$

The Frank family of copulas has the following reduced form:

$$C_\alpha(F_x, F_y) = -\frac{1}{\alpha} \ln \left[1 + \frac{(\exp(-\alpha F_x) - 1)(\exp(-\alpha F_y) - 1)}{\exp(-\alpha) - 1} \right] \quad (3.12)$$

for which the parameter α is estimated from Kendall's τ :

$$\tau = 1 - \frac{4}{\alpha} [D_1(-\alpha) - 1] \quad (3.13)$$

where D_1 is the Debye function, $D_1(\alpha) = \frac{1}{\alpha} \int_0^\alpha \frac{z}{e^z - 1} dz$, $D_1(-\alpha) = D_1(\alpha) + \frac{\alpha}{2}$, and z is a dummy variable of integration.

One of the objectives of this paper is to evaluate the joint probability, $Pr[(I_{pf} > i_{pf})(1 < T \leq t)]$ of intensity peak factor and storm duration per Eq. (7). Both distributions describe the probability of more severe occurrences; greater intensity peak factor and shorter storm events. The copula evaluates the joint probability of the CDFs of two dependent random variables. To evaluate the joint probability, the CDFs of I_{pf} and of cT must be substituted into the the copula, where $cT = t_{max} - T$ is the complementary of T . These probability distributions will be abbreviated as F_i

and F_{ct} respectively. The copula, is then in its turn, substituted within the following expression (Balakrishnan and Lai, 2009) in order to evaluate the joint probability of exceedence of the two dependent random variables, I_{pf} and cT :

$$Pr[(I_{pf} > i_{pf})(cT > ct)] = 1 - F_i - F_{ct} + C_\alpha(F_i, F_{ct}) \quad (3.14)$$

Note that, to be consistent with the definition of intensity peak factor, then values of $cT \leq 23$ are only considered, which is equivalent to values of $T > 1$. Values of $T \leq 1$, or $cT > 23$ will be considered later in the paper.

TABLE 3.4. Kendall's τ for intensity peak factor and storm duration ($I_{pf} - T$), Ali-Mikhail-Haq and Frank copula parameters α .

| Parameter | Toronto | TPIA |
|------------------|-------------|-------------|
| | MSC 6158350 | MSC 6158733 |
| Kendall's τ | -0.4191 | -0.4562 |
| AMH α | 0.5219 | 0.5149 |
| Frank α | -4.433 | -4.993 |

Values of the copula parameter α for each meteorological station, and for each of the AMH and Frank Copulas are shown in Table 4.

The tail dependence coefficient for upper-tail dependence (Joe, 1997), $\lambda_U = \frac{\lim_{F_x \rightarrow 1^-} [1 - 2u + C(F_{i_{pf}}(u), F_{cT}(u))]}{(1 - u)}$ was evaluated for both Frank and AMH copulas, and were found to both approach 0 in the limit. This indicates that both copulae are upper tail independent. This further supports the suitability of either of the Frank or AMH copulae, for the degree of dependence between the two random variables.

Based upon Eq. (7), substituting the expressions for the probability of exceedence of V and the copula-based joint probability of exceedence of I_{pf} and of cT , the following expressions are obtained.

For the AMH Copula:

$$\begin{aligned} & Pr\{(V > v)(I_{pf} > i_{pf})(1 < T \leq t)\} \\ & = J_u \exp[-(v - u_v)/\sigma_v] \left[1 - F_i - F_{ct} + \frac{F_i F_{ct}}{1 - \alpha(1 - (F_i))(1 - F_{ct})} \right] \end{aligned} \quad (3.15)$$

For the Frank Copula:

$$\begin{aligned}
& Pr\{(V > v)(I_{pf} > i_{pf})(1 < T \leq t)\} \\
& = J_u \exp[-(v - u_v)/\sigma_v] \\
& \left\{ 1 - F_i - F_{ct} - \frac{1}{\alpha} \ln \left[1 + \frac{(\exp(-\alpha F_i) - 1)(\exp(-\alpha F_{ct}) - 1)}{\exp(-\alpha) - 1} \right] \right\} \quad (3.16)
\end{aligned}$$

The distributions of I_{pf} and cT applied in both cases are:

$$F_i = \frac{\int_0^{i_{pf}} x^{p-1} (1-x)^{q-1} dx}{\beta(p, q)} \quad (3.17)$$

$$F_{ct} = 1 - (t - 1)/t_{max} \quad (3.18)$$

The uniform distribution is used as the marginal distribution of T , but 1 hour events are excluded, so $Pr[1 < T \leq t] = t/t_{max} - 1/t_{max}$ which reduces to $Pr[1 < T \leq t] = (t - 1)/t_{max}$. Since decreasing storm duration is associated with increasing storm severity and decreasing probability, then the CDF of cT must be used in the copula function. This will have the form of $Pr[cT \leq t_{max} - t | cT \leq 23] = Pr[T > t | T > 1] = 1 - Pr[1 < T \leq t]$, leading to Eq. (18).

Since the probability distribution of I_{pf} applies only to storm durations greater than 1 hour, the joint probability must also account for cases when $T < 1$. The total probability should be:

$$\begin{aligned}
& Pr\{(V > v)(I_{pf} > i_{pf})(T \leq t)\} \\
& = Pr(V > v)\{Pr[(I_{pf} > i_{pf})(1 < T \leq t)] + Pr[(V > v)(T \leq 1)]\}
\end{aligned}$$

For a storm duration of 1 hour or less, I_{pf} is always equal to 1 and is independent of T , therefore $Pr[(I_{pf} > i_{pf})(T \leq 1)] = Pr(T \leq 1) = 1/t_{max}$. The expression for the total joint probability of exceedence of storm depth, intensity peak factor, and CDF of storm duration is, after reducing:

$$Pr\{(V > v)(I_{pf} > i_{pf})(T \leq t)\}$$

$$= J_u \exp[-(v - u_v)/\sigma_v] \left\{ 1 - F_i - F_{ct} + \frac{F_i F_{ct}}{1 - \alpha (1 - F_i)(1 - F_{ct})} + 1/t_{max} \right\} \quad (3.19)$$

for the AMH copula model and:

$$\begin{aligned} & Pr\{(V > v)(I_{pf} > i_{pf})(T \leq t)\} \\ &= J_u \exp[-(v - u_v)/\sigma_v] \\ & \left\{ 1 - F_i - F_{ct} - \frac{1}{\alpha} \ln \left[1 + \frac{(\exp(-\alpha F_i) - 1)(\exp(-\alpha F_{ct}) - 1)}{\exp(-\alpha) - 1} \right] + 1/t_{max} \right\} \end{aligned} \quad (3.20)$$

for the Frank copula model.

3.4. Second test of the assumption of independence between V and the joint distribution of I_{pf} and T .

A second empirical test was performed in order to determine whether the assumption of the independence between V and the joint distribution of I_{pf} and T was acceptable for practical applications. This test compares the empirical joint frequency distribution of I_{pf} , T and V based upon plotting positions of the joint event, applying techniques described by Yue (2001), with the joint probability for the same values calculated using the theoretical distribution models as shown in Eq. (19) and Eq. (20).

The following plotting position equation was used to estimate a conditional probability first:

$$\begin{aligned} & Pr\{[(V > v)(I_{pf} > i_{pf})(T \leq t)] | [(V > u_v)(T \leq t)]\} \\ &= (l + 0.56)/(n + 0.12), l \leq n \end{aligned} \quad (3.21)$$

In Eq. (21), n is the total number of events in a subset of data, where $T \leq t$ and $V > u_v$; and l is the number of events within that subset where $V > v$ and $I_{pf} > i_{pf}$. The empirical probability estimated this way is the conditional exceedence probability of a selected storm event with particular values of v , i_{pf} , and t . The Gringorten plotting position equation was selected as being appropriate to variables described by Generalized extreme value Type I (GEV I), or GPD I extreme value distributions (GPD I is used as the theoretical distribution for storm depth).

Events for which $V > v$, $I_{pf} > i_{pf}$, and $T \leq t$ was extracted from the full set of threshold rainstorm data. For a particular event of duration t having storm intensity peak factor i_{pf} and storm depth v , the number of events with $T \leq t$, $I_{pf} > i_{pf}$, and $V > v$ was counted. The number of such events meeting these criteria was then l .

In order to remove the conditions from Eq.(21), $Pr\{V > u_v\}$, the probability of exceedence of the storm depth threshold u_v , and the CDF of storm duration, $Pr\{T \leq t\}$, must be estimated. $Pr\{V > u_v\} = J_u$ is estimated directly from the storm frequency parameters in Table 1. To estimate the CDF of storm duration, the following plotting position equation was applied to the full set of rainstorm data:

$$Pr\{T \leq t\} = k/N, k \leq N, \quad (3.22)$$

where k is the total number of storm events with $T \leq t$, and N is the total number of storm events in the entire set of storm data for a given station as obtained from Table 1. This plotting position equation is consistent with design storm modelling where storm duration is treated as having uniform distributions. The estimates of $Pr\{T \leq t\}$ and $Pr\{V > u_v\}$ were applied to Eq.(21) as follows given the independence between V and T :

$$\begin{aligned} & Pr\{[(V > v)(I_{pf} > i_{pf})(T \leq t)]|[(V > v)(T \leq t)]\}Pr\{V > u_v\}Pr\{T \leq t\} \\ &= Pr\{(V > v)(I_{pf} > i_{pf})(T \leq t)\} \\ &= [(l - 0.44)/(n + 0.12)]J_u[k/N] \end{aligned} \quad (3.23)$$

The conditional joint probability of occurrence of v , i_{pf} , and t estimated on the basis of the plotting position Eq.(21) is then combined with the plotting position estimates of probability of exceedence of storm depth threshold and $Pr\{T \leq t\}$.

This exercise was carried out for storm events of 6, 12, 14, and 23 hours. Empirical plotting position distribution results are compared with results from the use of the theoretical distributions, applying both AMH and Frank Copulas, and are shown below in Figure 3a for the Toronto station, and Figure 3b for the TPIA station. For comparison, simple joint probabilities, assuming complete independence between storm depth, duration, and intensity peak factor is also shown for each station:

$$\begin{aligned} & Pr\{(V > v)(I_{pf} > i_{pf})(T \leq t)\} \\ & = Pr\{V > v\}Pr\{I_{pf} > i_{pf}\}Pr\{1 < T \leq t\} + Pr\{V > v\}Pr\{T \leq 1\} \quad (3.24) \end{aligned}$$

The results based upon the theoretical distributions are plotted on the x-axis, while those based upon the plotting positions (for the same event) are plotted on the y-axis. Should a given theoretical method produce identical results with the empirical distribution, then the points on the chart would appear on the 45-degree line. A higher probability of exceedence from the theoretical model than that estimated from the empirical model places the point for a particular event below the 45-degree line. Where the Frank copula is used to model the joint distribution of storm duration and intensity peak factor, the theoretical and plotting position methods produce very similar results. The bias of the simple joint probability model (i.e., Eq. (24)) is visually apparent, and the AMH copula produces results between those of the Frank copula and the simple joint probability. As a measure of goodness-of-fit, several standard ranking criteria were considered:

- AIC - The primary value of this ranking criteria is for comparison of models with varying number of parameters. This is not applicable in this case.
- The $RMSE = \sqrt{\frac{1}{n} \sum_{i=1}^n (x_i - \hat{x}_i)^2}$ is a relative measure of goodness-of-fit applied in this case by comparing differences between plotting point distribution probabilities and those of the theoretical models. Lower RMSE

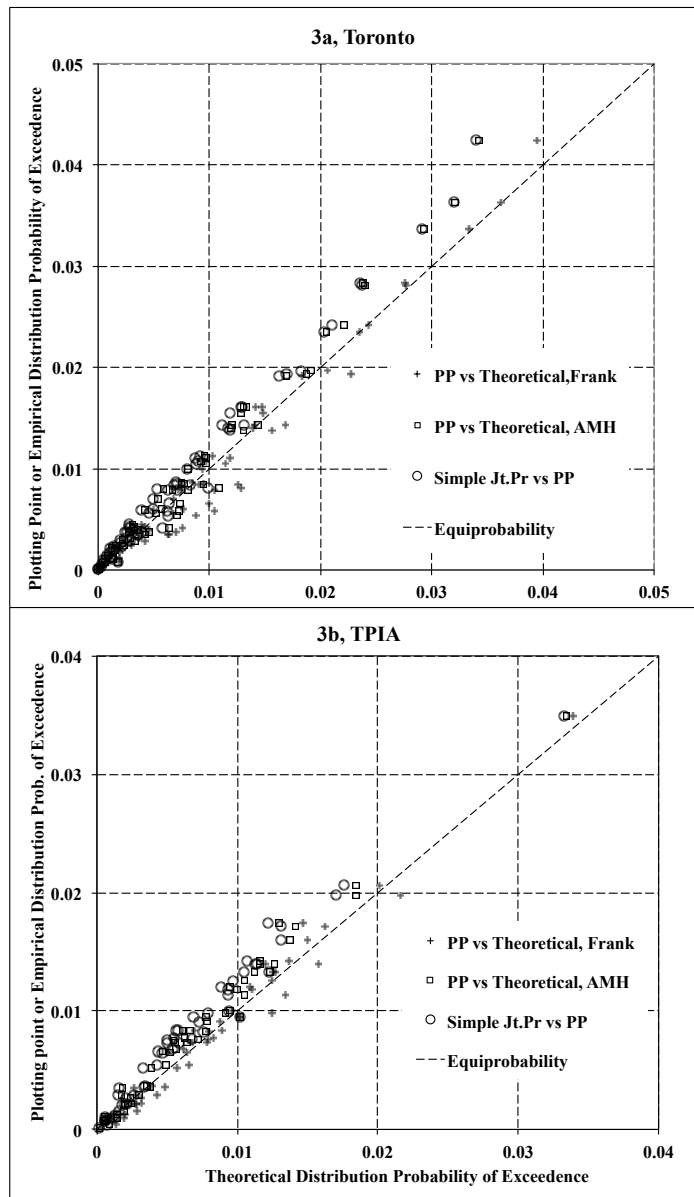


FIGURE 3.3. Comparisons of plotting position and theoretical joint probability distributions. Plotting position empirical distribution established with Eq. (23) plotted on y-axis. Theoretical distributions based upon Eq. (19) for AMH copula, Eq. (20) for Frank copula, and Eq. (24) for simple joint probability plotted along x-axis. Figure 3(a) for Toronto station, Figure 3(b) for TPIA. Points falling closest to 45-degree line indicate best fit between empirical and theoretical models.

values for a particular theoretical model compared to another would indicate a better fit with the empirical distribution. There is no indication of bias provided by this measure.

- The Nash-Sutcliffe model efficiency coefficient E_f provides a measure of reduction in variance. $E_f = 1 - [\sum_{i=1}^n (x_i - \hat{x}_i)^2 / \sum_{i=1}^n (x_i - \bar{x})^2]$, so that an increasing value of E_f up to a value of 1, indicates better predictive power for a theoretical model in comparison to observed values.
- A simple measure of difference between empirical and theoretical models was also adopted: $\delta = \frac{1}{n} \sum_{i=1}^n (x_i - \hat{x}_i)$. With this, bias can be estimated.

For each of the above goodness-of fit criteria, n is the total number of events evaluated for both their empirical and theoretical probabilities and i is the counter that identifies individual events. The joint probability of exceedence of each event considered, $Pr\{(V > v)(I_{pf} > i_{pf})(T \leq t)\}_i = x_i$ for the observed values established by means of the plotting point distribution, and \hat{x}_i for the modeled joint probabilities.

Table 5 provides RMSE, E_f , and average difference for theoretical joint probabilities based upon AMH and Frank copulas, as well as for the simple joint probability expressed in Eq. (24).

- RMSE provides differentiation between the three theoretical models applied to data for the two stations, and provides some indication that the theoretical model incorporating the Frank Copula provides a closer fit to the plotting point distribution than either the AMH Copula or simple joint models. The RMSEs for the Frank copula model are 82.8% and 70.9% of that for the AMH model for the Toronto and TPIA data respectively.
- E_f provides an indication of reduction in variance between each of the three models and the observed plotting point joint distribution. While differences are small, the Frank copula model leads to the largest values of E_f for rain-storm data from both stations, indicating the greatest reduction in variance when compared to the plotting position model. The AMH copula model has

a greater reduction in variance than the simple joint model, when each is compared to the plotting position model.

- The average difference, δ , between empirical and predicted estimates of joint probability provides clear indication that for data from both stations, the model incorporating the Frank copula has the lowest average difference in comparison to the plotting position event joint probabilities. The Frank copula model slightly overestimates the joint probability, but in absolute terms, the performance of the Frank copula model is much better than that of the AMH model. The absolute values of δ for the Frank copula is 60.8% and 6.2% of those for the AMH model for the Toronto and TPIA stations respectively. AMH and simple joint probability both underestimate the joint probability of exceedence in comparison to the empirical, or plotting position joint probabilities.

TABLE 3.5. Relative Goodness-of-fit, Theoretical models compared to Empirical Plotting Point Distribution.

| Parameter | Toronto MSC 6158350 | TPIA MSC 6158733 |
|-----------------------|---------------------|------------------|
| RMSE Frank | 0.00116 | 0.000829 |
| RMSE AMH | 0.00140 | 0.00117 |
| RMSE Simple Joint | 0.00164 | 0.00160 |
| E_f Frank | 0.967 | 0.976 |
| E_f AMH | 0.955 | 0.950 |
| E_f Simple Joint | 0.944 | 0.909 |
| δ Frank | -0.000572 | -0.0000648 |
| δ AMH | 0.000940 | 0.00104 |
| δ Simple Joint | 0.00144 | 0.00152 |

The visual comparisons in Fig. 3a and Fig. 3b support the selection of the GPD I distribution for storm depth with the Frank copula linking the uniform distribution for duration, and Beta distribution for intensity peak factor, as providing the best model for the joint probability distribution of storm depth, duration, and intensity peak factor in comparison to the empirical joint probability distribution. The close match to the plotting position and improvement compared to simple joint probabilities confirms the applicability of the independence assumption invoked (that of storm depth being independent of the joint event of intensity peak factor and duration).

Thus, Eq. (20), completed by Eq. (17) and Eq. (18) is an acceptable model for the joint probability distribution of the three rainstorm measures at least for two stations in Toronto, Canada.

4. Conclusions

Intensity peak factor, as defined in this paper, shows promise as a simple but general measure of the degree to which rainstorm depth is concentrated in a peak hourly interval within a storm. This variable has upper and lower bounds; for two stations in Toronto, Canada it is correlated with storm duration but has no correlation with storm depth. Intensity peak factor was found to follow well the Beta probability distribution. Although the hourly archiving interval for rainstorm depth accumulation sets some limits upon characterizing true storm durations and peakedness, the application of the intensity peak factor still allows a practical description of a storm's peak intensity. In fact, it takes advantage of the averaging effect of hourly archiving.

The findings about the statistical independence between storm depth and duration, as well as between storm depth and intensity peak factor, partially support some aspects of the current approach in specifying design storms. The joint probability distribution of storm depth, duration, and intensity peak factor developed in this paper provides a better probabilistic description of rainstorm events than that proposed by other researchers since all measures having an important effect upon peak discharge from a catchment are considered in characterizing the frequency of occurrence of different storm events. This new approach also avoids a priori determination of annual maximum events. In order to explain these assertions, some contrast with other techniques follows.

The one-parameter 3-copulae methods developed by Grimaldi and Serinaldi (2006) and by Zhang and Singh (2007b) are not applicable to the case of negative correlation between storm intensity and duration found for the two Toronto area sets of rainfall data (Kao and Govindaraju, 2008).

The application of Plackett 3-copulas by Kao and Govindaraju (2008) does not have the limitation imposed by the single-parameter 3-copula. They select the annual maximum rainstorm events on the basis of plotting point estimation of the maximum joint probability of storm depth and peak intensity. The use of annual maximum statistics reduces the sample size, and may bias the selection of annual maximum events, since annual maxima are selected on the basis of an empirical joint probability of two of the three measures. They applied Beta distributions to hyetograph shape variables (relative location of storm peak, cumulative proportions of storm depth accumulation), in recognition of the bounded nature of such measures, in a similar fashion to the techniques developed in this paper. This paper has established the statistical independence of storm depth with respect to the joint event of intensity peak factor and storm duration, based upon the rainfall data examined for two meteorological stations in Toronto, Canada. Because of this independence, there is no need to apply the more complex 3-copula.

Other researchers have not recognized that storm peak intensity is necessarily bounded in the context of the external measures of storm depth and duration. With the recognition of this necessary relationship and the inclusion of a bounded measure of peak storm intensity as a random variable, all major measures of rainstorm events having significant effects on catchment peak discharge and runoff depth have been incorporated into the probabilistic description of storm events in this paper. The combination of threshold analysis of rain storm data together with the multivariate plotting point estimation of joint probability eliminates the shortcomings of annual maxima data used by others. Further, the random variables are employed in everyday practice, or may be easily derived from available rainfall data. Thus, the storm variables of interest to designers and planners are addressed. Three joint probability distributions incorporating the marginal distributions of storm depth, duration, and intensity peak factor were developed and compared to an empirical distribution. As expected, joint distributions incorporating 2-copulas provided a better fit than a simple joint distribution. The intensity peak factor variable is a unique development that incorporates the fundamental limits upon peak storm intensity within a rainstorm event, and creates a measure that addresses one of the key assumptions in traditional design storm practice: the heuristic that storm hyetograph shape is

invariant with storm depth. While this is an oversimplification, the measure of storm peak introduced in this paper, intensity peak factor, is indeed independent of storm depth. This characteristic lends itself well to application of the methods developed in this paper to the advancement of design storm techniques, and facilitating their adoption by practitioners familiar with traditional concepts.

Apart from development of practical applications in design and risk assessment, further research will include evaluation of data from different climatological zones, in order to broaden the geographic range over which these techniques may be employed. Refinement of the techniques presented in this paper are merited. Although at an early developmental stage, a concise, probabilistic description of storm peak characteristics has been presented. The easy-to-implement method leads to a more comprehensive and practical characterization of storm frequency that can be readily incorporated into the current design storm-based engineering practice.

5. Acknowledgements

The authors are grateful to Drs. R.Zhu and S. Feng, professors of probability and statistics at McMaster University, for the thought-provoking discussions that helped greatly in the completion of this work. The comments of two anonymous reviewers led to much improvement in this paper.

6. Appendix Rainfall Data Analysis

Hourly rainfall data from two nearby stations in Toronto, Canada, operated by Meteorological Services Canada were obtained. The two stations were Toronto, MSC6158350, and Toronto Pearson International Airport (TPIA), MSC6158733. The data from the two stations were subject to SEA using an Intervent Time Definition (IETD) of 6 hours. That is, individual storm events are defined by minimum dry periods of 6 hours between hourly intervals recording rainfall. The identified rain-storm events were then subject to threshold analysis. Events exceeding a threshold of 25 mm, with durations less than or equal to 24 hours were fitted to The Generalized Pareto Distribution Type I (GPD I) for storm depth (see Eq.1). The upper limit

of duration was selected for a variety of reasons. Longer duration events are of less interest in urban stormwater management, the numbers of events exceeding both 24 hours in duration and 25 mm in depth are relatively few, and the average intensities at this threshold are very low, so of little direct interest in stormwater management. These long duration events will require some other method of analysis.

Following procedures described in Palynchuk and Guo (2008), storm durations were found to fit a uniform distribution (Eq.2). Because of the limitations inherent in the use of hourly archived rainfall, the finest temporal definition for storm duration is one hour. Thus, the durations established for individual events must be viewed as an interval. In particular, a one-hour duration rainstorm must be understood to be a storm up to one hour in duration, but may be of shorter duration greater than zero.

Peak hourly intensities within each storm event were identified and then reviewed for correlation with storm depth and duration.

The results of this analysis are summarized in Table A1.

This analysis showed that:

- for the two stations, GPD I probability distribution parameters, mean and standard deviation of storm depth, are very similar in value.
- GPD I (two-parameter exponential distribution) is a good fit for storm depth, applying the Anderson-Darling test statistic to data from both stations.
- Similarly, the χ^2 test showed that the uniform distribution is acceptable at both sites for storm duration. The fitting of a uniform distribution to the durations of extreme rainfall events is consistent with conventional design storm practice, wherein rainstorm duration may be selected for design purposes based upon some measure of catchment response, such as time of concentration. Effectively, current application assumes that all storm durations less than the maximum duration have an equal likelihood of occurrence.

TABLE 3.6. Table A1. Summary of statistical analysis results for two stations in Toronto, Canada.

| | Toronto (MSC 6158350) | TPIA (MSC 6158733) |
|---|-----------------------|---------------------|
| Period of record | 1939 - 1998, 56 yrs | 1960 - 2001, 42 yrs |
| Annual coverage | April-October | March-November |
| Maximum storm duration, t_{max} | 24 hours | 24 hours |
| Threshold storm depth, u_v | 25 mm | 25 mm |
| Location μ | 35.549 mm | 35.094 mm |
| Scale σ_v | 10.549 mm | 10.094 mm |
| GPD I fit, V calculated A^2 | 0.236 | 0.636 |
| Upper tail limit, $\alpha = 0.05$ | 1.321 | 1.321 |
| Accept/reject | Accept | Accept |
| Uniform distribution, T , calculated χ^2 | 13.034 | 7.569 |
| Upper tail limit $\alpha = 0.05$, d.f.=11 | 19.68 | 19.68 |
| Accept/reject | Accept | Accept |
| Storms/year, θ_0 | 64.446 storms/yr | 77.286 storms/yr |
| Storms/year, $V > u_v$, θ_u | 3.071 storms/yr | 3.357 storms/yr |
| Correlation ($V - T$) | -0.043 | -0.016 |
| Upper tail limit $p = 0.05$ | 0.126 | 0.139 |
| Accept/reject independence | Accept | Accept |
| Correlation ($I_p - T$) | -0.579 | -0.555 |
| Correlation ($I_p - V$) | 0.519 | 0.479 |

- Storm depth and duration are uncorrelated. The critical test value of correlation for $\alpha = 0.05$ is included. Sample correlation values less than the test value are uncorrelated, with an $\alpha = 0.05$ risk of false rejection of the null hypothesis. The physical explanation for the lack of correlation may be due to the two major rainstorm producing mechanisms present in this region. Cyclonic events tend to produce long duration, low average intensity storms, while convective storms are of relatively shorter duration and higher average intensity. Both processes result in events within a similar range.
- Peak hourly storm intensity (I_p, i_p) is positively correlated with storm depth, and negatively correlated with storm duration.

A review of some of the parameters from Table A1 for the purpose of characterizing extreme rainfall events on the basis of threshold analysis is merited, since

most similar approaches make use of annual maximum statistics. Storm depths exceeding a threshold of 25mm of storm depth occur between 3 and 4 times per year in the Toronto area. The sample size is therefore larger than that available under the annual maximum approach, and provides information on arrival time between significant rainfall events. The threshold "filters" out minor events in a way that annual maximum statistics may not. Annual maximum statistical analysis is predicated upon the assumption that there are sufficient numbers of annual rainstorm events so that the selection of the maximum value from among the set of all annual events satisfies the asymptotic requirements inherent in the Generalized Extreme Value family of probability distributions (Gumbel, 1958). This last assumption may not be met, and in fact, would not be met in the Toronto Area, since there are only between 64 and 78 total rainstorm events per year, while Gumbel suggests that greater than 100 events per year would be desirable. The use of threshold statistics permits determination of return periods of rainstorm events of less than one year. Effectively threshold statistics, applied through appropriate probability distributions provide a greater range of frequency prediction than do annual maximum statistics, while at the same time providing other important measures, such as time between large events.

The combined application of IETD for identifying individual rainstorm events with threshold-based analysis of extreme events provides a major advantage in examining the probabilistic behaviour of rainstorms, in comparison to the use of annual maximum rainstorm statistics. If univariate analysis is being carried out, then the identification of annual maximum data is straightforward. In the context of evaluating joint probabilities of several measures of rainstorms, then it becomes difficult to define the annual maximum rainstorm event. Two alternatives exist: 1) An a priori definition must be employed in order to determine a combination of, say, storm depth and peak intensity, in advance of statistical analysis; 2) Make use of statistics based solely upon a single measure, typically storm depth. Either alternative risks bias to the subsequent examination of joint probabilities of measures of storms. No such limitation exists when threshold statistics are employed, so that the marginal distributions of each storm variable may be evaluated, without any predetermination of annual maximum criteria for joint events.

CHAPTER 4

Changes in heavy rainstorm characteristics with time and temperature at four locations.

1. Introduction

There has been much speculation with regards to the effect of climate change upon changing patterns of rainfall. One of the major assertions has been that rainfall intensity will increase, or that severe events will become more frequent (IPCC, 2007). This prediction has arisen, in part as a result of modelling studies, as well as from analysis of rainfall statistics. A brief review of recent research, organized upon the basis of evaluation of modeled results versus statistical analysis of trends in rainfall data follows. A further discussion of the definitions of statistical rainfall events is presented.

1.1. Model-based predictions.

Modelling based results include downscaling of GCM results. Kharin and Zwiers (2000) used the results of GCMs to predict changes in extreme daily accumulated rainfall in future climate scenarios. Guo (2003) used 24-hour accumulated rainfall predicted by CGCM1, under the IS92a forcing scenario for the period from 2000 to 2100 to obtain annual maximum rainfall data. 24-hour annual maximum rainfall from Toronto, Canada between 1938 and 2001 for a station from within the same GCM grid square was compared, using a standard plotting position equation. The results showed an increase in rainfall depth for a given frequency between the historical and modelled data.

Mailhot et al. (2007) regionalized available moving-window annual maximum rainfall depth accumulation data (as used in conventional DDF analysis) from Southern Quebec in order to compare to rainfall modelled by a regional climate model with 45 km grid-cell size. The Canadian Regional Climate Model was used, under the SRES-A2 GHG scenario. Results compared reasonably well with annual maximum, moving-window rainfall accumulation statistics, with a bias towards larger rainfall depths for station data, attributable to characteristic storm size reduction with decreasing storm duration. Modelled control and future rainfall depths were compared, showing a future trend of increasing storm depth for annual maximum events for comparable moving-window durations. Simulated data from individual grid squares was aggregated in order to upscale to a regional level.

Douville et al. (2001) used rainfall precipitation modelling from the Centre National de Recherche Météorologique (CNRM) of Météo-France. A base case using 1950 Green-House Gas (GHG) concentrations was modelled. A second case, based upon the SRES-B2 GHG scenario was run. The time spans of both model runs was 150 years, and there was some validation of modelling against current climatology. Rainfall results were compared, and model prediction was about a 5 percent increase beyond current average rainfall, with some indications of seasonal shifts, depending upon the region. The results of the modelling further lead to an inference that an increase in atmospheric moisture content combines with a decreased efficiency in the hydrologic cycle leading to a modest increase in rainfall. The dwell time of atmospheric moisture increases.

Rosenberg et al. (2010) used Regional Climate Models to project possible changes in rainfall in Washington State, and as a basis of comparison to historical records. While increases in rainfall precipitation were predicted at some locations, results were not statistically significant.

1.2. Statistical analysis of historic rainfall data.

1.2.1. *Statistical events as daily rainfall.*

Angel and Huff (1997) used 24-hour annual maximum rainfall accumulation statistics from the U.S. Midwest, for time spans of 1901-1947 and 1949-1994 and found a statistically significant difference. Greater accumulations were found in the second half of the Century. Guo (2006) used the results of this analysis, applying techniques developed in his 2003 paper referenced above, to develop a temporal downscaling technique, based upon a widely accepted empirical intensity-duration-frequency equation. The objective of this analysis was to demonstrate the impact of climate change upon urban stormwater infrastructure, and to propose a technique for applying the results of climate change research to the design of stormwater infrastructure.

Groisman (2010) has recently reported the results of analysis of rainfall data from the Continental US. Patterns of more frequent extreme rainstorms were reported. No statistically significant increase in total rainfall was detected when two 30-year spans of data over a total 60-year block were compared. Rosenberg et al (2010) performed analysis of trends based upon rainfall records from several Pacific-Northwest US rainfall stations, but found few significant trends; potential decreases in the numbers of events, and possible increases in storm depth for medium duration events. Earlier analysis by Karl and Knight (1998), projected increasing trends in heavy rainfall.

1.2.2. *Moving-window statistical analysis.*

Adamowski et al (2009) reviewed conventional annual maximum Intensity-Duration-Frequency (IDF) analysis from Ontario in Eastern Canada and found statistically significant trends over relatively short durations (10 to 20 years). However, there are decadal and multidecadal cycles in rainfall which put into question the validity of any rainfall trend analysis over single and double decade time spans (Yang and Goodrich, 2008).

1.3. Objectives of this chapter.

There have been predictions made, on the basis of increased atmospheric GHG concentrations, that extreme rainfall events would increase in frequency and severity. Extreme rainstorms need some high-level definition. Broadly, they are events that exceed norms, and that do not occur very frequently. Extreme rainfall events occur on an annual, or less frequent basis, and result in runoff events that result in hillside and streambank erosion, with peak stream and sewer flows that will tax the capacity of channels and conduits.

Climate models themselves are effective at describing long term trends and average rainfall, but their physical scale does not adapt them very well to modelling relatively small geographic and time scale individual storm events (Groisman et al., 2004). Even the finer scale of regional climate models requires upscaling of point rainfall data in order to permit comparisons of modelled and actual data (Mailhot et al., 2007). Statistical analysis of rainfall data suffers from a variety of event definitions, which, particularly in the case of moving-window analysis, may prevent the identification of rainstorm event variables. For example, the use of a fixed moving window prevents the identification of storm duration, and because storm duration is not defined, then individual event-based description of storm depth and peak intensity are not identified either. The 24-hour event definition may lead to the aggregation of multiple short, but separate events.

Standard techniques of trend analysis, typically making use of the Mann-Kendall Test (Mann, 1945; Kendall, 1955) are sensitive to the starting point of the analysis, and so may give inaccurate indication of trends, depending upon the time-span of the data set, as well as the starting point of the trend analysis in comparison to decadal and multi-decadal climate cycles (Chen and Grasby, 2009). This is described in greater detail in Section 4. of this chapter.

In order to examine possible changes in rainstorm characteristics with time, or with changes in temperature, an alternate storm event definition, Inter-Event Time Definition (IETD) will be used to identify individual, infrequent, rainstorm events. This technique separates records of rainfall based upon a minimum time interval between hourly archived rainfall records. The individual rain storm events may

then be characterized by their total depth, duration, and peak intensity. Because of the comparative granularity of event definition produced by this technique, these random variables may then be analyzed in terms of their probability distributions and associated statistical parameters. From that analysis, the effects of climate scale temperature on mean values of storm variables may be evaluated. As well, potential changes over time will be assessed. The duration of rainfall data of sufficient precision is limited to 50 to 60 years in many areas of North America, so that trend analysis is at risk of being distorted by multi-decadal cycles. Indeed, initial Mann-Kendall trend analysis using a moving-window approach simply reflected those same cycles. A basic approach will be taken, with the objectives of assessing:

- The effects of temperature, on a climatic basis, upon storm variables
- Shifts in mean values of storm variables, between major time spans within the period of record of the selected meteorological stations
- The relationship between climatological measures of atmospheric temperature, and shifts in rainstorm frequency.

The over-arching objective is to employ a storm-event definition that identifies the key variables of individual storm events, assess the potential changes in storm parameters over time, and the effects of climatic temperature upon those variables. With that assessment, the underlying assumption of stationarity may be tested. Changes in rain storm parameters with time and temperature may be used to project future directions in rainstorm variable analysis.

2. Storm event definition and analysis

2.1. Threshold analysis under the assumption of stationarity.

Rainstorms are observed as discrete events; they have a start, a finite duration, then an end. Identification and measurement of individual events from rainfall data is unfortunately, subject to a variety of definitions. Conventional probabilistic definitions of rainfall as applied through Depth-Duration-Frequency (DDF) and Intensity-Duration-Frequency (IDF) curves ignore the identification of individual events. They instead make use of a moving window of prescribed duration, then measure the annual maximum depth of rainfall occurring within that moving window. Some definitions use a daily or 24-hour window as the basis for describing a rain storm (Karl and Knight, 1998).

A common definition for many researchers is the Inter-Event Time Definition (IETD). Rainfall records are examined, and individual storms are defined by means of a minimum period of time between recorded rainfall. One of the earliest descriptions of this was by Eagleson (1972), (Restrepo-Posada and Eagleson, 1982). Other researchers have employed this definition for a variety of purposes. Adams et al., (1986) examined the basis for selection of the IETD, and applied the concept for the purpose of characterizing the marginal distributions of rain storm depth, duration, and inter-event time. Other researchers (Guo and Adams, 1998a, 1998b; Goel et al., 2000) have used this definition of rainstorm events to characterize the marginal distribution or rainstorm random variables in order to develop derived probability distributions of hydrologic outputs such as peak discharge, or runoff depth. More recently, the technique has been used to characterize the probability distribution of extreme storm events. Storm data is analyzed by application of threshold exceedance analysis to storm depth (Palynchuk and Guo, 2008). The probability distribution of high values of storm depth is determined by applying Generalized Pareto Distributions, and the marginal distributions of storm duration is determined for those events as well. Similar techniques have been applied to include measures of peak storm intensity (Palynchuk and Guo, 2011).

TABLE 4.1. Station Descriptions, Threshold Analysis of Rainstorm Events March-November, ≤ 24 hours

| - Description | Name/ Sta. ID | Springfield IL8719 | Peoria IL6711 | O'Hare IL1549 | Pearson 6158733 |
|---------------------------|------------------|-----------------------|------------------|------------------|--------------------|
| Latitude, degrees N | | 39.848° | 40.668° | 41.995° | 43.677° |
| Longitude, degrees W | | 89.664° | 89.684° | 87.934° | 79.631° |
| Years, hourly rainfall | | 1949-2006 | 1949-2006 | 1962-2006 | 1960-2003 |
| Total no. rainstorms, m | | 4567 | 4615 | 3777 | 3172 |

In this work, hourly-archived rainfall data was analyzed for 4 stations; airport stations at Peoria, Springfield, Chicago(O'Hare), all in the State of Illinois, USA, as well as Pearson, the international airport serving Toronto, Canada. Peoria and Springfield were selected as being relatively rural meteorological stations, but with long continuous records. Chicago and Toronto were selected for relatively long records in urbanized areas. Basic information on each station is shown in Table 1. Data for Pearson has been obtained from Meteorological Services Canada, as referenced in Chapters 2 and 3. U.S. weather data has been sourced through Earthinfo, Inc., assembled from U.S. National Weather Service and other data providers.

The entire record for each station was subject to threshold analysis, in order to develop the dataset of extreme events. The techniques are fully described in the author's previous work, but are summarized as follows for convenience:

- Hourly-archived rainfall data is separated into individual events, using the IETD. The start of a storm event is separated by at least the IETD from the end of the last rainfall record. This current analysis used a minimum inter-event time definition of 6 hours.
- Limit storms to durations less than or equal to 24 hours. This selection is made for several reasons:
 - 1) The analysis of the probability distribution of storm duration is simplified,

- 2) in the context of urban hydrology (the objective of much of this investigation) events of long duration but low average intensity are of less interest because of the lower level of risk of damage,
 - 3) storms of durations exceeding 24 hours must be characterized separately, because of their infrequent nature, and low average intensity.
- Select a high storm depth threshold u_v , so that there are about 3 to 5 events per year on average exceeding this depth.
 - Evaluate statistical parameters of storm depth (V, v) , duration (T, t) , and peak intensity (I_p, i_p)
 - Fit Generalized Pareto Distribution Type I (GPD I) to storm depth, and a bounded distribution to storm duration:

$$Pr\{V > v\} = J_u \exp[-(v - u_v)/\sigma_v] \quad (4.1)$$

(Where u_v is the selected storm depth threshold, and J_u is a natural estimator of the probability of exceedance of u_v)

$$Pr\{T \leq t | T \leq t_{max}\} = t/t_{max} \quad (4.2)$$

where t_{max} is the selected maximum duration of storms under consideration, in this case, 24 hours. A uniform distribution is shown in this case, but other bounded equations in the Beta family may be fitted as appropriate.

- Normalize peak hourly intensity, calculating the Intensity peak factor, following Eq. (3):

$$I_{pf} = [(I_p/v)t - 1]/(t - 1) \quad (4.3)$$

then calculate moments of this reduced variate, to fit to a bounded distribution, usually from the Beta family:

$$F_{i_{pf}} = \frac{\int_0^{i_{pf}} x^{p-1} (1-x)^{q-1} dx}{\beta(p, q)} \quad (4.4)$$

where I_{pf} , i_{pf} is the dimensionless index of peak-hour storm intensity. p and q are Beta distribution parameters, $p = i_{pf}^- \left(i_{pf}^- \frac{(1-i_{pf}^-)}{\sigma_{i_{pf}}^2} - 1 \right)$, and $q = (1 - i_{pf}^-) \left(i_{pf}^- \frac{(1-i_{pf}^-)}{\sigma_{i_{pf}}^2} - 1 \right)$

- Statistical parameters were estimated by Maximum Likelihood for storm depth, method of moments for storm duration (because hourly archiving results in values that can only be estimated as being within a range, and so must be treated as discrete), and method of moments for intensity peak factor (Johnson et al, 1994).
- Goodness-of-Fit was established by comparison of each marginal distributions with empirical distributions. The Modified Anderson-Darling test was used for V, v , χ^2 for T, t , and Kolmogorov-Smirnov for I_{pf}, i_{pf} .
- Depending upon the type of engineering problems, the marginal distributions of V , T , and I_{pf} may be combined into joint probabilities in order to assess the return periods of extreme storm events. Generally, it has been found that storm depth V is independent of storm duration T as well as intensity peak factor I_{pf} , while T and I_{pf} are correlated, in previous analysis carried out at two Toronto, Canada stations. That correlation is addressed with an Archimedean Copula (Palynchuk and Guo, 2011).

TABLE 4.2. Threshold statistics

| Parameter | Springfield IL8719 | Peoria IL6711 | O'Hare IL1549 | Pearson 6158733 |
|---|-----------------------|------------------|------------------|--------------------|
| Storm depth threshold, u_v, mm | 39 | 37 | 37 | 25 |
| Total no. of rainstorms, $n, v > u_v$ | 184 | 238 | 172 | 144 |
| Average storm depth, \bar{v} | 58.298 | 51.543 | 52.881 | 34.962 |
| Standard deviation, $\hat{\sigma}_v$ | 19.298 | 15.543 | 15.881 | 9.962 |
| Average duration, \bar{t} | 13.201 | 12.036 | 12.034 | 11.927 |
| Standard deviation, $\hat{\sigma}_t$ | 6.091 | 8.668 | 5.800 | 6.287 |
| Average intensity peak factor, i_{pf} | 0.294 | 0.299 | 0.296 | 0.339 |
| Standard deviation, $\hat{\sigma}_{pf}$ | 0.187 | 0.191 | 0.171 | 0.229 |

This brief review is to simply establish that standard techniques are applied to ensure that there are probability distributions that model well the marginal distributions of the random variables that describe rainstorm events. Table 2. provides a summary of the parameters estimated for each of the four meteorological stations for which data was evaluated, over the entire time duration for which hourly-archived rainfall data was available.

2.2. Methods.

The following sections evaluate differences between mean values, correlations between variables, and differences between distributions. Comparisons are between storm events divided into time spans within the overall period of record, or temperatures associated with storm events. P-values will be used to assess significance. The p-value is the risk of falsely rejecting the null hypothesis, which is the hypothesis that there is no difference between test parameters. The p-value threshold for statistical significance will be taken as $p < 0.10$, but higher values will be shown as well so that the possibility of a trend may be considered, even though statistical significance acceptance criteria are not otherwise met. In some instances, when p-values are in excess of 0.20, the values may be omitted altogether for clarity. Tests will be for differences between means of storm variables, χ^2 tests for differences between distributions, product moment correlation significance, and differences of percentages of numbers of events between temperature categories. The tests are all in routine use, described in many texts on probability and statistics, and largely based upon normality of the estimates of means. In the case of product-moment correlation, the z -statistic is approximated by $z = r\sqrt{(n - 1)}$, where n is the sample size, and r is the product-moment correlation.

2.3. Storm-event analysis - time spans.

2.3.1. Storm variables.

The full set of extreme events were broken into two subsets; events occurring prior to 1980, and those occurring in 1980 through to the end of the available data. This division of data provided relatively large sample sizes for early and later events.

TABLE 4.3. Difference in values, pre- and post-1980, of statistical parameters.

| Parameter | Time Span | Springfield IL8719 | Peoria IL6711 | O'Hare IL1549 | Pearson 6158733 |
|---|---|-----------------------|------------------|------------------|--------------------|
| Avg. storm depth, \bar{v} | ≤ 1979 | 58.495 | 51.305 | 51.410 | 34.667 |
| Avg. storm depth, \bar{v} | ≥ 1980 | 58.091 | 51.922 | 53.720 | 35.188 |
| Avg. duration, \bar{t} | ≤ 1979 | 13.154 | 11.670 | 12.105 | 11.896 |
| Avg. duration, \bar{t} | ≥ 1980 | 13.244 | 12.522 | 11.968 | 11.957 |
| Avg. intensity peak factor, \bar{i}_{pf} | ≤ 1979 | 0.307 | 0.303 | 0.283 | 0.372 |
| \bar{i}_{pf} | ≥ 1980 | 0.280 | 0.294 | 0.304 | 0.313 |
| Significance of differences | post-1980 >pre-1980 or post-1980 <pre-1980 | IL8719 | IL6711 | IL1549 | 6158733 |
| Avg. storm depth, \bar{v} | | | | > | |
| p-value | | | | 0.173 | |

The same statistical parameters were estimated as was done for the full dataset, and simple, single-sided tests of the significance of the difference of means were performed. Table 3 provides the values of the parameters, the hypothesis of differences in means between the two time periods, and p-value, only when $p < 0.20$.

There has been no significant shift in mean values of storm variables describing depth, duration, or intensity peak factor (V , T , I_{pf}). There may be a trend of increasing mean storm depth at the O'Hare station, but the p-value is larger than normally applied levels of significance.

2.3.2. *Threshold-event frequency.*

The parameter J_u is the estimator of the probability of exceedence of the storm depth threshold, u_v . It is simply:

$$J_u = n/m \quad (4.5)$$

where n and m are the total number of events exceeding the threshold of storm depth, u_v , and the total number of rainstorm events, respectively.

The variance of J_u is (Coles, 2001):

$$Var(J_u) = J_u(1 - J_u)/m \quad (4.6)$$

TABLE 4.4. J_u , average probability of exceedence of u_v , pre- and post-1980.

| Parameter | Time Span | Springfield IL8719 | Peoria IL6711 | O'Hare IL1549 | Pearson 6158733 |
|----------------------------|---------------------------------------|-----------------------|------------------|------------------|--------------------|
| Total no. of storms, m | ≤ 1979 | 2446 | 2430 | 1480 | 1416 |
| Total no. of storms, m | ≥ 1980 | 2121 | 2185 | 2297 | 1756 |
| Total storms, $n, v > u_v$ | ≤ 1979 | 94 | 146 | 62 | 63 |
| Total storms, $n, v > u_v$ | ≥ 1980 | 90 | 92 | 110 | 81 |
| $J_u = n/m$ | ≤ 1979 | 0.038 | 0.060 | 0.0419 | 0.044 |
| $J_u = n/m$ | ≥ 1980 | 0.042 | 0.042 | 0.047 | 0.046 |
| Significance | post 1980 > pre or post 1980 < pre | IL8719 | IL6711 | IL1549 | 6158733 |
| $J_u = n/m$ | | | < | > | |
| p-value | | | 0.003 | 0.199 | |

The significance in the change in the estimate of J_u is evaluated in Table 4., where this parameter is estimated for the two major time spans.

There is a significant decrease in the frequency of occurrence of extreme events exceeding the storm depth at Peoria, where the p-value of the test of the difference of means is well below accepted levels for determination of significance ($p < 0.10$). At O'Hare, there is an apparent trend of increasing frequency of extreme events, but the p-value is 0.199, well above normally accepted levels of significance.

2.3.3. Empirical distributions of storm variables.

Storm variables were clustered into groups by 3-hour ranges of storm duration values, i.e., 21 to 24 hours, 18 to 20 hours, etcetera. The frequency of occurrence of all of the events were compared between events occurring pre- and post-1980.

The 3-hour ranges of duration were selected in order to ensure that there were sufficient threshold exceedence events in each grouping for sufficient sample size testing requirements.

TABLE 4.5. χ^2 analysis of difference between pre- and post-1980 empirical distributions of storm variables.

| Variable | Equation/test $\{\sum_{i=1}^n [(O_i - E_i) / \sqrt{E}]^2\}$ | Springfield IL8719 | Peoria IL6711 | O'Hare IL1549 | Pearson 6158733 |
|------------------------------------|--|-----------------------|------------------|------------------|--------------------|
| Storm Depth, V | χ^2 p-value | 9.080 0.106 | 2.790 | 12.822 0.025 | 5.678 |
| Storm Duration, T | χ^2 p-value | 17.552 .007 | 5.476 | 24.192 0.0005 | 9.16 0.156 |
| Intensity Peak Factor, I_{pf} | χ^2 p-value | 1.141 | 9.998 0.040 | 13.961 0.007 | 10.421 0.034 |

The results of one of the time spans were used to estimate the expected frequency in the other, then the differences in the expected and observed frequencies were compared using the χ^2 test, with the significance expressed as a p-value. The results are shown in Table 5, but only displaying p-values less than 0.20. This comparison provides a non-parametric basis for comparing the empirical distributions as measured pre- and post-1980. The χ^2 test provides a statistical test of the significance of the difference. Thus, no assumption of probability distribution is required, other than normality of the differences.

There has been only one significant shift in the empirical distribution of storm depth V , as indicated in Table 5, and that is for O'Hare. One of the primary contributors to that significant difference is a series of storms, 2 in 1987-88, and 2 in 2001-02 each of which exceeded 100mm. The largest event was 246mm occurring in 1987.

Table 5 results indicate that there has been significant change in the empirical probability distribution of storm durations at Springfield and O'Hare, to a high degree of significance, reflected in very low p-values. There is some indication of a change in distribution of storm durations between periods prior to 1980, and the

period since that time at Pearson, but the p-value nonetheless exceeds the values normally accepted as indicating statistical significance. Both Springfield and O'Hare show similar patterns of a reduction in the frequency of storms in the 7 to 9 hour duration range, with increases in shorter duration ranges, as shown in Figure 1.

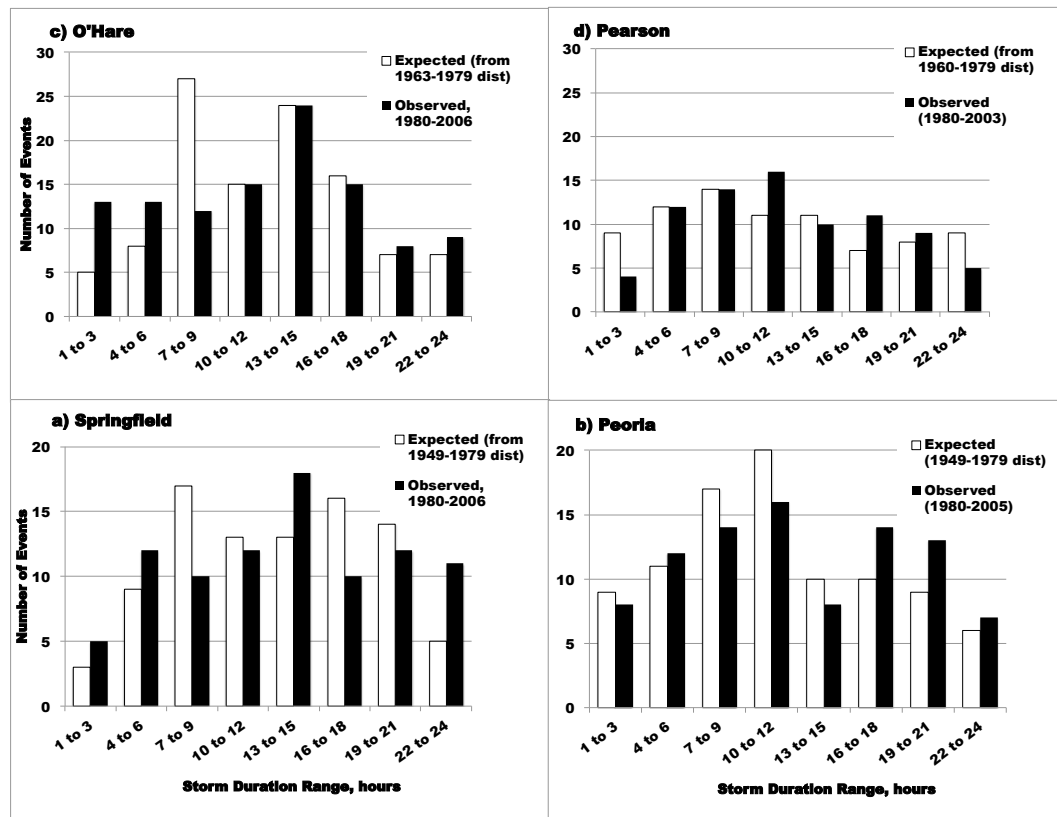


FIGURE 4.1. Storm duration frequency by 3-hour duration increments, pre- and post-1980

A significant change between the empirical distributions of intensity peak factor is apparent from the p-values in Table 5 for all stations, except Springfield. There is no clear pattern of changes in intensity peak factor among the frequencies for stations at Peoria, O'Hare, and Pearson.

2.3.4. Correlation between storm variables.

One of the key steps in developing a joint probability distribution between storm variables is the determination of the degree of dependence between them. Pearson's r , the product-moment correlation coefficient, was determined for correlations of V and T , V and I_{pf} , and I_{pf} with T , with results shown in Table 6.

Correlation between I_{pf} and T is strongly negative and significant at all stations under both time spans examined. Correlation between V and I_{pf} is low, and not significant in most cases. Where the correlation is significant at $p < 0.10$, it would not be at $p < 0.05$.

TABLE 4.6. Correlation analysis between V , T , and I_{pf} , pre-1980 and post-1980.

| Test, Parameter | Time Span | Springfield IL8719 | Peoria xxIL6711 | O'Hare IL1549 | Pearson 6158733 |
|-----------------|-------------|-----------------------|--------------------|------------------|--------------------|
| $r, V-T$ | ≤ 1979 | 0.201 | 0.043 | -0.115 | -0.047 |
| p-value | | 0.026 | 0.277 | 0.186 | 0.355 |
| $r, V-T$ | ≥ 1980 | -0.214 | 0.159 | 0.134 | 0.055 |
| p-value | | 0.021 | 0.081 | 0.096 | 0.311 |
| $r, V-I_{pf}$ | ≤ 1979 | -0.111 | -0.128 | -0.066 | 0.176 |
| p-value | | 0.142 | .061 | 0.304 | 0.083 |
| $r, V-I_{pf}$ | ≥ 1980 | 0.115 | -0.149 | -0.104 | -0.071 |
| p-value | | 0.139 | .077 | 0.140 | 0.264 |
| $r, I_{pf}-T$ | ≤ 1979 | -0.652 | -0.546 | -0.593 | -0.677 |
| p-value | | 0.0000 | 0.0000 | 0.0000 | 0.0000 |
| $r, I_{pf}-T$ | ≥ 1980 | -0.419 | -0.538 | -0.572 | -0.604 |
| p-value | | 0.000 | 0.000 | 0.000 | 0.0000 |

The results for correlations between V and T between the two time spans are more mixed. For 3 of the 4 stations, Peoria, O'Hare, and Pearson, correlation increases, but individual r values are not significant, or marginally significant at $p = 0.10$, and would not be significant at $p = 0.05$. For Springfield, there is a change from a positive, to a negative correlation between early and later time spans, with p values indicating that correlation is significant in both cases.

2.4. Storm-event analysis - temperature.

2.4.1. Storm variable - temperature correlation.

TABLE 4.7. Correlation analysis between the mean monthly temperature (MMT) when storm events occur and V , T , I_{pf} , pre- and post-1980.

| Test, Parameter | Time Span | Springfield IL8719 | Peoria IL6711 | O'Hare IL1549 | Pearson 6158733 |
|-------------------|-------------|-----------------------|------------------|------------------|--------------------|
| $r, V - MMT$ | ≤ 1979 | 0.112 | 0.164 | 0.277 | 0.148 |
| p-value | | 0.141 | .024 | 0.0147 | 0.122 |
| $r, V - MMT$ | ≥ 1980 | 0.252 | 0.093 | 0.165 | -0.038 |
| p-value | | 0.009 | .187 | 0.096 | |
| $r, T - MMT$ | ≤ 1979 | -0.341 | -0.486 | -0.434 | -0.456 |
| p-value | | 0.0004 | .0000 | 0.0003 | 0.0001 |
| $r, T - MMT$ | ≥ 1980 | -0.461 | -0.538 | -0.324 | -0.455 |
| p-value | | 0.00000 | .00000 | 0.005 | 0.00000 |
| $r, I_{pf} - MMT$ | ≤ 1979 | 0.361 | 0.504 | 0.202 | 0.417 |
| p-value | | 0.0002 | .00000 | 0.056 | 0.0005 |
| $r, I_{pf} - MMT$ | ≥ 1980 | 0.356 | 0.538 | 0.304 | 0.500 |
| p-value | | 0.0003 | .00000 | 0.008 | 0.00000 |

The mean monthly temperature (MMT) for the month of occurrence of any given extreme rainstorm was obtained, and storm variables were assessed against this climatological measure, using the product-moment correlation statistic, r . Table 7. provides the values of correlation coefficients and the p-values, when they are less than 0.20.

All stations show similar patterns of significant ($p < 0.10$) negative correlation between temperature and storm duration, and significant positive correlation between intensity peak factor (I_{pf}) and mean monthly temperature, regardless of time span. Three of the four stations show a decrease in correlation between storm depth and mean monthly temperature. r values in the time span of post 1980, as compared to pre-1980 decrease, and p-value increased for Peoria, O'Hare, and Pearson. One station only, Springfield, shows an increased correlation between V and mean monthly Temperature.

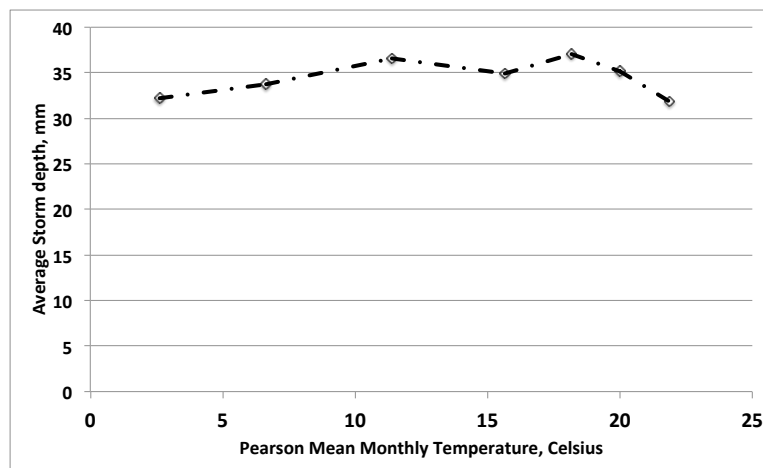
2.4.2. *Temperature range analysis and time-spans.*

FIGURE 4.2. Mean storm depth versus mean monthly temperature

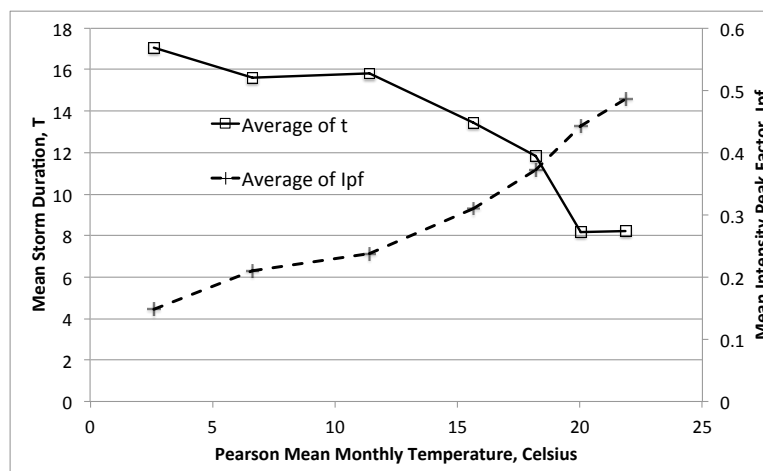


FIGURE 4.3. Mean storm duration and mean intensity peak factor, versus mean monthly temperature

The events were grouped into temperature ranges, where the ranges were selected so as to ensure that there are more than 10 samples in each range. Mean values of V , T , and I_{pf} in each range were calculated, and the results are shown in Figures 2 and 3 for the Pearson station, as a typical example. Product-moment correlation tests first led to indications of strong positive correlation between mean monthly temperature

and Intensity peak factor, with strong negative correlation between storm duration and temperature. Fig. 2 shows visually, little correlation between mean storm depth and mean monthly temperature. Fig. 3 confirms the negative correlation between mean storm depth and temperature, and the positive correlation between mean storm intensity peak factor and mean monthly temperature.

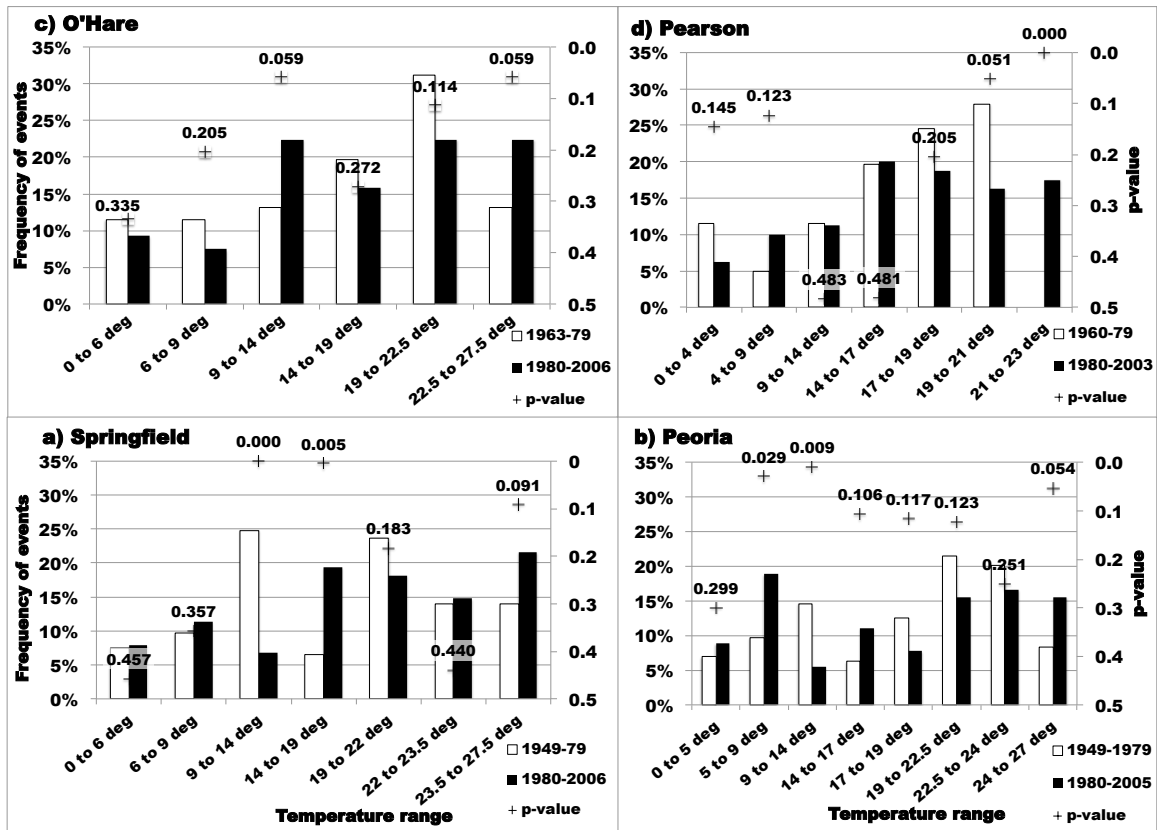


FIGURE 4.4. Storm frequency versus temperature ranges. p-value of difference in proportions shown on reverse scale, significance assessed as $p < 0.10$

Using these same temperature ranges, the proportions of storms within these temperature ranges were examined for the two time spans under investigation. Fig. 4 shows bar charts for each of the stations comparing the frequency of storms for each time span (pre-1980 and post-1980). The p-values of the differences between

frequencies for a given temperature range are shown in a reverse scale. This was done to visually compare the relative significance of the difference of the frequencies of storms between the two time spans. Thus, a low p-value appears near the top of the chart area, indicating a highly significant difference between proportions of events between the two time spans.

For all stations, the frequency of occurrence of storms is significantly higher in the highest temperature range for each station post-1980. There is a corresponding reduction in frequency (between earlier and later time spans) in the next two lower temperature ranges. While a reduction in the proportion of events occurring in the lowest temperature ranges might be expected, this is not always the case, and there is no consistent pattern in change in the proportions of storms occurring in the lowest temperature ranges, between the two time spans among the 4 stations examined.

2.4.3. Average of Mean Monthly Temperature (*MMT*).

TABLE 4.8. Average of mean monthly temperature when threshold-excess storm events occurred, pre- and post-1980.

| Parameter | Time Span | Springfield IL8719 | Peoria IL6711 | O'Hare IL1549 | Pearson 6158733 |
|----------------|-------------|-----------------------|------------------|------------------|--------------------|
| <i>MMT</i> | ≤ 1979 | 16.430 | 17.091 | 16.104 | 15.213 |
| $\hat{\sigma}$ | ≤ 1979 | 7.087 | 6.821 | 6.678 | 5.668 |
| <i>MMT</i> | ≥ 1980 | 17.653 | 16.498 | 16.350 | 15.609 |
| $\hat{\sigma}$ | ≥ 1980 | 6.686 | 7.436 | 6.543 | 5.871 |
| p-value | | 0.116 | 0.270 | 0.408 | 0.343 |

The mean monthly temperature associated with each threshold-excess event has been used as a means of evaluating the relationships between storm variables and average temperature. The average of this mean monthly temperature was calculated for the two time spans, and the significance of the difference between the averages is presented in Table 8.

None of the differences is significant at $p < 0.10$. Three of the four stations show a small increase in the average of mean monthly temperature. One of the stations, Peoria, indicates a decrease in the average of mean monthly temperature when threshold-excess events occurred. This is associated with a significant increase in the proportion of storm events occurring in the 5 to 9 degree temperature range.

3. Review of analysis - rainstorm parameter changes with time and temperature

3.1. Summary of statistical test results.

- Section 4.3 Storm-event analysis - time spans:
 - Table 3 - Means of storm variables did not show any significant change between the time span prior to 1980, and that following.
 - Table 4 - Average probability of exceedance of threshold events was not significantly different between the two time spans, with the exception of Peoria, where a significant decrease in the frequency of occurrence of threshold events appears.
 - Table 5 - Empirical distributions - O'Hare storm depth indicates a significant difference between earlier and later time spans, but that difference is driven by 4 storms of depth exceeding 100 mm occurring in the later time span. In spite of the results shown in Table 3, two of the four stations, Springfield and O'Hare, have significantly different distributions of storm duration between the time span pre-1980, and post-1980. The Pearson and Peoria stations χ^2 test results indicate that there is no significant difference in storm duration distributions between the two time spans. The intensity peak factor empirical distribution is significantly different for 3 of the 4 stations between the two time spans.
 - Table 6 - Strong correlations between storm duration and intensity peak factor were unchanged between time spans. Correlations, or lack of correlation between storm depth and intensity peak factor did not change between time spans. Correlations between storm depth and duration increased negatively for Springfield and positively for Peoria.
- Section 4.4. Storm-event analysis - temperature correlation:

- Table 7 - Significant 1) negative correlation between mean monthly temperature and storm duration, and 2) positive correlation between intensity peak factor and mean monthly temperature are common across all stations and time spans. Storm depth has a low positive correlation with temperature at all four stations prior to 1980. Post-1980, correlation decreased to insignificant levels at two of the stations, Peoria and Pearson, and decreased at O’Hare to a marginally significant level. Only at Springfield did correlation increase and reach a level that was significant ($p \ll 0.10$).
- Fig. 4 - All stations have a significant increase ($p < 0.10$) in the proportion of storms occurring at the highest mean monthly temperature ranges, with decreases, or no significant change, in the next two lower temperature ranges.
- Table 8 - Average of mean monthly temperatures associated with threshold excess storm events has not changed between early and late time spans significantly. Three of the four stations have an increase, while one station, Peoria has a decrease in the average of mean monthly temperature.

Table 9 summarizes qualitatively the significant changes in statistical characteristics between time spans, and in relation to MMT. Small and insignificant changes have been omitted. Some added statistical testing was performed on changes in the product-moment correlation coefficient, r . In particular, where a change in sign of r between time-spans was noted, the statistical significance of the change was tested. Double-shafted arrows are used to indicate the direction of change for significant changes, single shaft arrows show the direction of changes that are not statistically significant. "NC" stands for no change, Δ stands for changes between time spans. $\%n$ is the proportion of total threshold exceedence events in the highest temperature range of mean monthly temperature evaluated for each station.

TABLE 4.9. Summary of major time-span and temperature changes and trends

| Section | - | Springfield | Peoria | O'Hare | Pearson |
|---------------------------|-----------------------------|-------------|--------|--------|---------|
| Subsection | Test, Change | IL8719 | IL6711 | IL1549 | 6158733 |
| 4.3 Storm-event analysis | - time spans | | | | |
| Threshold-event freq. | ΔJ_u | NC | ↓ | NC | NC |
| Empirical Dist V | $\Delta f_V; \chi^2$ | NC | NC | Change | NC |
| Empirical Dist T | $\Delta f_T; \chi^2$ | Change | NC | Change | NC |
| Empirical Dist I_{pf} | $\Delta f_{I_{pf}}; \chi^2$ | NC | Change | Change | Change |
| Correl. storm var. | $\Delta r; V - T$ | ↑ (-) | ↑ | NC | NC |
| 4.4. Storm-event analysis | - temp. | | | | |
| v, T, I_{pf} - MMT | $\Delta r, V$ | ↑ | ↓ | ↓ | ↓ |
| correl | - MMT | | | | |
| Temp. range vs. time | $\Delta \%n,$ top MMT | ↑ | ↑ | ↑ | ↑ |
| Avg. of MMT | $\Delta MMT(NS)$ | ↑ | ↓ | ↑ | ↑ |

3.2. Discussion and comparison.

Mean values of storm variables did not change significantly between earlier and later time spans, but the empirical distributions of some storm variables at each of the stations did change significantly. In particular:

- The distribution of storm depth at O'Hare changed significantly between pre-1980, and the later time span. That difference in distribution is driven in part by the temporal location of a few very large storms in the post-1979 time span. While this may be an indication of climate change effects, it may also be simply due to the division of the overall rainfall record into 2 spans at the end of 1979. The years of record prior to 1980 is relatively short, 17 years, which is a short period of time in which to assess the statistical characteristics of extreme rain storms.
- Storm durations did change significantly at two of the locations, Springfield and O'Hare. There were common elements between the two stations, a shift

from 7 through 9 hour duration events to shorter durations. However, the relatively short duration of the span of rainfall records prior to 1980 may call into question the validity of the comparison between the two time spans, particularly in assessing the probability distributions of extreme rain storm events. Care in fitting of an appropriate probability distribution would need to be exercised, as more data becomes available.

- The distribution of intensity peak factor changed significantly between the two time spans, for Peoria, O'Hare, and Pearson stations. There was no discernible pattern of changes among the three stations. Again, the short period of record prior to 1980 for O'Hare and Pearson in particular may be a factor.

There is a significant increase in the frequency of storms at the highest temperature ranges into which each span of records was divided. Storms occurring at higher temperatures will, on average be of shorter duration, and have a greater concentration on storm depth within the peak hour. This conclusion is supported by both the correlation analysis summarized in Table 7, and the results of estimates of means of storm variables as a function of temperature ranges shown in Fig. 2 and Fig. 3. This is further supported by the summary of Karl and Trenberth (2003) where they stated that:

...whereas additional atmospheric water vapour increases the risk of heavy precipitation events (14). Basic theory (15), climate model simulations (2), and empirical evidence (Fig. 2) all confirm that warmer climates, owing to increased water vapor, lead to more intense precipitation events even when the total precipitation remains constant, and with prospects for even stronger events when precipitation amounts increase (16-18).

Note that references within quotation are:

- (14) Trenberth et al 2003
- (15) Clausius Clayperon Equation (Wark, 1988)
- (2) Haughton et al, 2001
- (16) Katz, 1999
- (17) Groisman, 1999
- (18) Karl and Knight, 1998

Fig. 2 in Karl and Trenberth (2003) provides empirical evidence that greater daily depths of rain fall in heavy ($> 40\text{mm}$) and extreme ($> 100\text{mm}$) categories as temperature regime increases.

The review of Karl and Trenberth (2003) still suffers from a lack of clear storm definition. The original research in this thesis provides the first clear evidence of the changes in intensity within storms over time. Further, it is demonstrated that, for these mid-North-American stations, the primary effects of increasing climatic temperature are decreasing storm duration, and increasing peak-hour intensity. It is not clear that storm depth increases with temperature. There is, in fact, a decreasing correlation between storm depth and temperature between pre- and post-1980 storms at 3 of the 4 stations examined. This may be a result of increasing CO_2 leading to a decrease in the intensity of the hydrological cycle, because of a reduction in the rate of upward radiation of latent heat flux through the troposphere released by precipitation (Allen and Ingram, 2002).

Some of the anomolous effects, particularly in rural Illinois, may be due to non-GHG climate change effects. Groisman (2010) and Changnon et al (2003) have both provided evidence that changes in crop practices may have a greater impact upon changes in rainfall than GHG-driven warming. This may account for the contrary changes at Springfield and Peoria.

3.2.1. Sensitivity of storm variables to temperature change.

The product-moment correlation statistics and their associated p-values provide some indication of average sensitivity of storm variables to changes in mean monthly temperature. Using the Springfield station as an example, then the r -values from Table 7, for the time span post-1980 provide a measure of the average change in storm variables per degree-change in MMT . Thus, a one degree increase in mean temperature would lead, on average, to a .252 mm increase in average threshold storm depth at Springfield, while that same increase in temperature would lead to a reduction in average storm duration of 0.461 hours. That same change in temperature would lead to an increase in intensity peak factor of 0.356. Thus, generally, temperature increases will lead to greater change in storm duration and intensity peak factor, than to increase in average storm depth. In fact, based upon Table 7, mean monthly temperature increase will lead to significant increases in average intensity, because of reduction in storm duration, coupled with significant increases in peak intensity, as measured by I_{pf} . Those results are consistent between the two time spans into which storm data was divided. Storm depth, on the other hand, is either not correlated with temperature, or the average rate of increase of storm depth is low, and the rate of increase of storm depth with temperature has decreased in the time span after 1979, at 3 of the 4 stations examined.

4. Time series trend analysis - Background

As stated in Sub-section 1.3 of this chapter, initial attempts were made to evaluate potential trends in storm variables, by use of the the Mann-Kendall trend test. The test statistic is relatively simple; i.e., the double summation of the sign of differences between successive values in a time series, as expressed in the following equation

$$S = \sum_{l=1}^j \sum_{k=1}^i (a_{ij}), i < j, a_{ij} = \text{sgn}(x_i - x_j) = \begin{cases} -1 & x_i - x_j < 0 \\ 0 & x_i - x_j = 0 \\ 1 & x_i - x_j > 0 \end{cases} \quad (4.7)$$

where a_{ij} is the sign of the difference between successive values of a random variable x . As the size of the sample increases, the distribution of the Mann-Kendall statistic S tends towards normality. This characteristic forms the basis of tests for significance of trends.

It has long been recognized that hydrological variables, both rainfall inputs and discharge outputs follow long-cycle climatological trends. Because of this, statistical parameters, in particular, mean values are non-stationary. The standard error of the estimate of means is, as a result, not as "narrow" as for independent, identically distributed random variables. The estimate of the standard error is then

$$StD[\bar{X}] = \sigma/n^{(1-H)} \quad (4.8)$$

where \bar{X} is the mean value of a hydrologic variable, StD is the standard error of the estimate of the mean, σ is the standard deviation of the variable X , n is the sample or population size, and H is the Hurst parameter, which has a value between 0.5 and 1.

At a value of 0.5, Eq. (4.8) becomes the conventional standard error of the estimate of the mean. As H increases towards 1, then the standard error value increases, for a given value of the standard deviation of the random variable X . Because the test for significance of trends is essentially based upon normality of the distribution of the Mann-Kendall statistic S , then as the value of the Hurst parameter increases, the confidence in the assessment of positive trends decreases. The Hurst parameter increases with an increasing degree of non-stationarity of the mean of a given random variable.

Trend testing, making use of the Mann-Kendall statistic S as the method of analysis was not conducted in this thesis for a variety of reasons:

- Significance of trends was marginal, and the direction of trends depended upon the starting point, as noted earlier in this chapter.
- Literature reviews pointed towards an overestimation of positive trends, because the effect of the Hurst phenomenon was not always taken into account

when assessing the significance of trends in hydrologic time series (Hamed, 2008; Koutsoyannis, 2006).

- Application of the Mann-Kendall tests for trends requires an annualization of data, in order to filter out seasonality, leading to a reduction in the granularity provided by threshold statistics. This makes the assessment of the effects of climatic oscillations, by estimation of the Hurst parameter, more difficult.
- Some estimation of the Hurst parameter was carried out, but the combined effects of annualization of data, and the short overall time span of data did not permit accurate estimation of the Hurst parameter H .
- A 20-year moving window calculation of the S statistic showed variation, and change in trend direction on a decadal cycle for all stations. An example of this analysis is illustrated in Fig. 4.5.

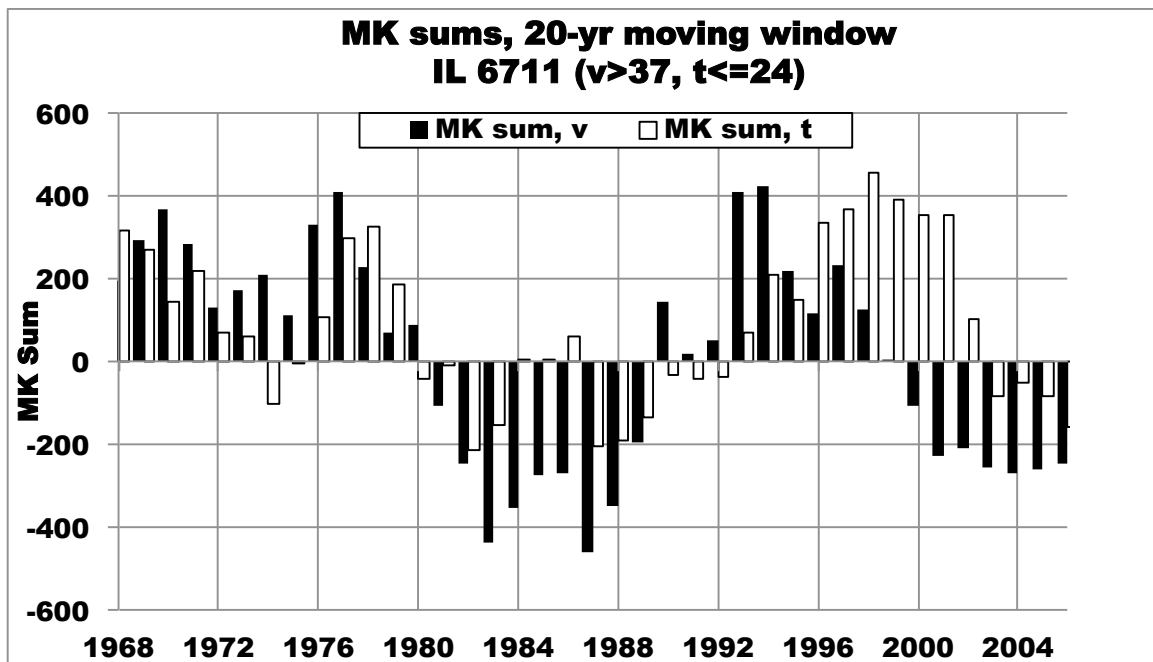


FIGURE 4.5. Mann-Kendall test statistic for Peoria station, on a 20-year moving window basis.

5. Conclusions

There is a clear increase in the frequency of rainstorms occurring at the highest values of mean monthly temperature in the period post- 1980, as compared to the period pre- 1980. However, in spite of strong correlations between mean monthly temperature/storm duration and MMT/intensity peak factor, there has not been a shift in mean values of storm variables between the two time spans. The only significant change between the two time spans are changes in the shape of the empirical probability density functions of some storm variables at some locations. The average of mean monthly temperatures associated with occurrence of heavy rainstorms has not changed significantly, indicating that despite the clear increase in frequency of rainstorm occurrence at the highest temperatures, increases in frequency at lower temperatures results in little increase in the average of mean monthly temperature of extreme or severe storms between the two time spans.

Correlation of storm variables with temperature is relatively low for storm depth V in all cases, but negative correlation between mean monthly temperature and storm duration T , and positive correlation with intensity peak factor I_{pf} are both significant. It is clear that increases in mean monthly temperatures for months during which heavy rainfall occurs will lead to reductions in average storm duration, and increases in mean intensity peak factor.

Section 4 summarizes concerns with the use of the Mann-Kendall test for trends in hydrologic data. The problems were encountered in initial attempts to make use of the widely used technique. The conclusion reached is that the test will provide evidence of trends over the time span of the available data, and because there is indication of a series of overlapping climatic cycles over a variety of periods, then the relatively short duration of accurate rainfall data may be insufficient on it's own, to provide conclusive evidence of changes in rainfall characteristics. For that reason, simpler statistical tests were performed upon rainstorm data in this chapter. The strengths of these simple test of differences in rainstorm parameters are multiple and include:

- Clear definitions of rainstorm variables, rather than the vague accumulations of storm depth used by most researchers
- Expansion upon clear relationships between storm duration and intensity peak factor established in Chapter 3 as a means of detecting potential differences in storm characteristics over time.
- The start of an assessment of the influence of climatic temperature upon rainstorm variables, that will ultimately lead to linkages with the underlying physics of the formation of rainstorms.

CHAPTER 5

Example applications

1. Introduction

In chapter 3, a joint probability distribution model is developed to estimate the true return period of rainstorms, based upon the three most important variables describing extreme storm events. Incorporating all of the important measures of rainstorms in a probabilistic framework advances several major concepts in hydrologic design:

- Assessment of the true level of protection: Event return period is used to specify the level of protection provided by a given design. Until now, that specification has been incomplete. In conventional DDF-based design storm applications, only storm depth, conditioned upon duration has been incorporated. Using other probabilistic approaches, planning and design risk assessment are not fully developed. Now three measures, depth, duration and peak intensity, may be evaluated and incorporated in an approach that addresses risk assessment in a more complete sense. Alternative design concepts may be compared so as to determine the true level of protection provided.
- Assessment of uncertainty in design: All of the important measures of storm events may now be incorporated in the evaluation of an output function that expresses a measure of hydrologic output with a desired return period. This output, recognized as having the same return period, may now be maximized, to identify critical combinations of inputs. The potential range of output values and the levels of uncertainty may be objectively assessed.

In the following two sections, two potential applications of the theory and methods developed in Chapters 2 and 3 are demonstrated. The first section illustrates

the effect of hyetograph shape upon storm-event return period. In the subsequent section, an example of maximization of a catchment's response function is provided, taking full advantage of the joint probability of rainstorm inputs.

2. Application of the joint probability distribution to evaluate conventional design storm hyetographs

As noted in the introduction, the effect of the actual shape of the storm hyetograph upon design storm frequency is currently not taken into account in conventional design practice. In order to evaluate the effect of different standard hyetographs, two examples were evaluated; a simple symmetric triangular intensity distribution (Yen and Chow, 1980) and the Chicago storm distribution (Kiefer and Chu, 1957). Design storms are six-hours in duration, with a 100-year return period for storm depth, estimated using the GPD I - uniform distribution joint probability, for the Toronto and Pearson (Toronto, Canada) rainstorm data. A 6-hour event with a storm depth of 71 mm was determined to have a 100-year return period for Toronto and 70 for Pearson.

The triangular hyetograph has a peak-hour intensity occurring on the hourly interval centred on the storm peak which occurs at a time of one-half of the storm duration. The depth of rainfall occurring during the peak hour of the storm is:

$$v_{peakhour} = \frac{v(2t - 1)}{(t - 1)}$$

Substitution this expression into Eq. (3.4) for the intensity peak factor then the following equation results:

$$i_{pf} = \frac{[(2t - 1)/t^2] - 1}{(t - 1)} \tag{5.1}$$

The Chicago design storm distribution is based upon the Modern Sewer Design fitting equation parameters (AIS, 1980). This equation is a fitting equation used to relate average rainfall intensity to a prescribed time interval t for a given return

period. The form of this equation is:

$$i = A/(t + C)^B \quad (5.2)$$

Where A is constant for a given return period, while B and C are constants independent of return period (Wenzel, 1982). Storm depths and durations between 1 and 24 hours, for the 100-year return period estimated based upon Eq. (4.3) from Chapter 4 for the Toronto data, were fitted to Eq. (2). The values for Toronto are: $A = 54.7$, $B = 0.856$, and $C = 0.067$. The form of the Chicago storm is then obtained from the following equation for the rising limb of the storm.

$$i_{before} = A[(1 - B)t_{before}/r + C]/(t_{before}/r + C)^{1+B} \quad (5.3)$$

where i_{before} is the intensity of the design storm before the peak intensity, calculated as a function of t_{before} , $t_{before} = t_{peak} - t_{fromstart}$ and r is the peak location ratio; t_{peak} and $t_{fromstart}$ are the time to peak rainfall intensity and the time from the start of the storm respectively. A symmetrical distribution will be used, so that $r = 0.5$. The descending limb of the Chicago storm is described by.

$$i_{after} = A[(1 - B)t_{after}/(1 - r) + C]/[t_{after}/(1 - r) + C]^{1+B} \quad (5.4)$$

where i_{after} is the intensity of the design storm after the peak intensity, calculated as a function of t_{after} , $t_{after} = t_{fromstart} - t_{peak}$. Since $r = 0.5$, the rising and descending limbs are identical in shape, for this example. The intensity peak factor was determined for the 6-hour, 71 mm event, for the 1-hour interval centered on the storm peak. The equations were solved and integrated numerically, and the peak-hour intensity was substituted into Eq. (3.4) in order to determine the intensity peak factor.

Return period may be calculated using Eq.(3.20), restated as.

$$T_{t,v,i_{pf}} = \frac{1}{J_u \exp[-(v - u_v)/\sigma_v] \left\{ -\frac{1}{\alpha} \ln \left[1 + \frac{(\exp(-\alpha(1-F_i))-1)(\exp(-\alpha F_t)-1)}{\exp(-\alpha)-1} \right] + \frac{1}{t_{max}} \right\} \theta_0} \quad (5.5)$$

where θ_0 is the average number of storm events per year. Refer to Chapter 2, section 3 for full details.

TABLE 5.1. Intensity peak factor and return periods of different design storm hyetographs.

| Parameter/Station | Toronto | Pearson |
|--|---------|---------|
| Station Number | 6158350 | 6158733 |
| v , for $t = 6$ and $T_{v,t} = 100$ | 70.8 | 69.7 |
| Triangular Storm Distribution i_{pf} | 0.167 | 0.167 |
| Triangular Storm Distribution $T_{i_{pf},v,t}$ | 105 | 100+ |
| Chicago Storm Distribution i_{pf} | 0.688 | 0.688 |
| Chicago Storm Distribution $T_{i_{pf},v,t}$ | 316 | 246 |

Table 1 summarizes the results of evaluating storm intensity peak factor and return period arising from applying Eq. (5.5) for the two design storm distributions. It is clear that incorporating the probability distribution of intensity peak factor results in significantly different frequencies for the two design storms, where conventional analysis, incorporating only storm depth and duration (i.e., rainfall depth and prescribed time interval) attributes the same frequency to both storms, in spite of their significantly different distributions of rainfall intensity over the same duration.

The fact that the triangular hyetograph has a return period relatively close to 100 years suggests that it is a better design storm model for the Toronto region. The Chicago Storm hyetograph, or intensity peak factor values arising from the Chicago Storm does not occur very frequently in this region, so that the return period calculated from the joint probability of storm depth, duration, and intensity peak factor is significantly greater than that calculated from the joint probability of storm depth and duration alone. In fact, because the return period is so large, compared to the period of record available, the calculated value of return period should simply be taken as confirmation that the data available for this station does not support the use of the Chicago Design Storm. Measured intensity peak factors of sufficient magnitude to match those produced in the Chicago design storm hyetograph occur very rarely at the Toronto and Pearson stations. The triangular hyetograph intensity peak factor occurs frequently enough that the return period calculated from the joint

probability of storm depth, duration, and intensity peak factor is not very different from the return period calculated from storm depth and duration alone.

3. Application of the joint probability distribution to identify critical combinations and levels of uncertainty

Inspection of Eq. (5.5) indicates that there will be a variety of combinations of storm depth, duration, and intensity peak factor which will lead to the same joint probability of exceedence. Assessing the effect resulting from variations in storm intensity peak factor, depth, and duration requires some basis for evaluation. In order to identify critical combinations of variables, some output function needs to be identified first. One of the common objectives of design hydrology is the evaluation of catchment response, arising from rainfall inputs. Accordingly, a regression equation for Mimico Creek catchment in Toronto, Ontario, Canada (discussed previously in the introduction of Chapter 4) was used. This equation has peak discharge as the dependent (i.e., response or output) variable, with runoff depth and peak hour intensity as independent variables:

$$Q_p = 0.088(v_r) + 0.012(i_p) \quad (5.6)$$

Runoff depth is storm depth less total abstractions, while peak hour intensity is intensity peak factor times storm depth. Eq. (5.5) was evaluated using a range of intensity peak factor values, applying Beta distribution parameters developed for intensity peak factor, and storm depth and duration distributions for the Toronto meteorological station data. Return period was kept constant over the range of intensity peak factor values and storm depths. Storm duration was kept constant at 6 hours. The resulting peak catchment discharge was then calculated with Eq. (5.6); v_r was calculated by subtracting a total abstraction from storm depth (for all storms) of 25 mm (selected as being representative for the catchment), and i_p by substituting i_{pf} , v , and t into Eq. (3.4) from Chapter 3. The results are shown in Fig. 1, where intensity peak factor is plotted along the x-axis, and peak discharge along the y-axis. Storm depth is also plotted against a second y-axis.

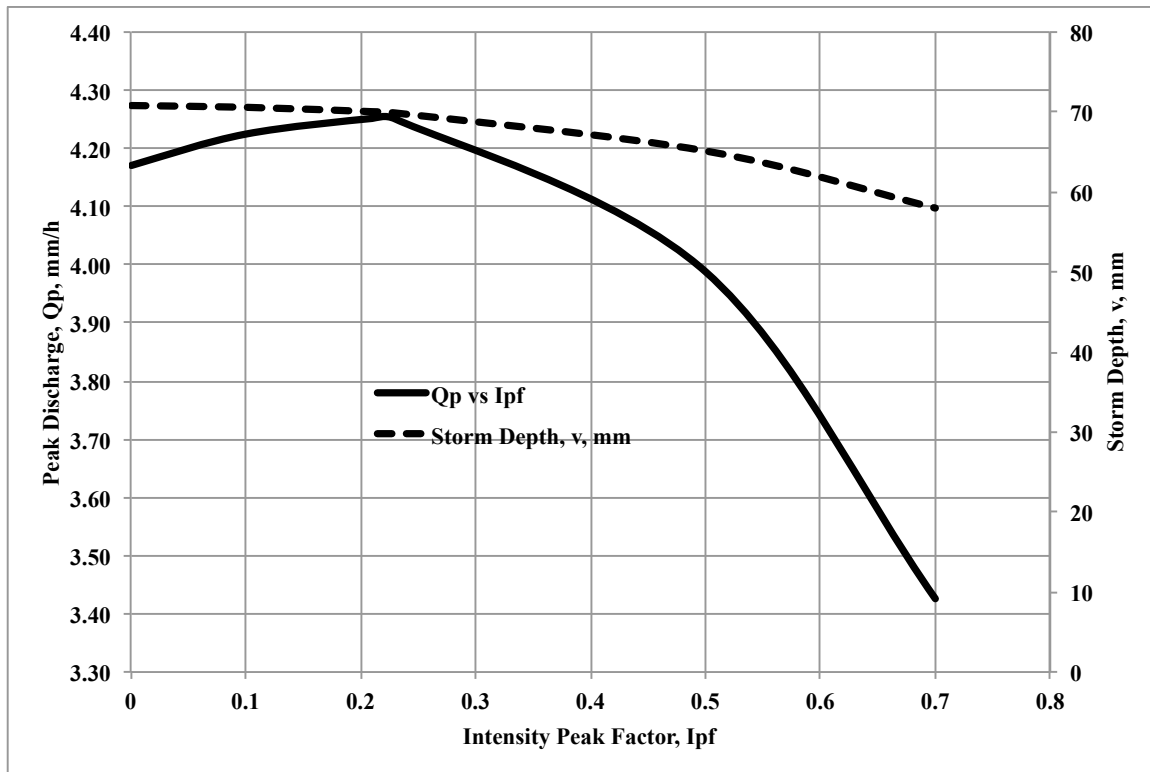


FIGURE 5.1. Maximization of peak discharge for 100-year joint return period.

There are a range of storm depths and intensity peak factors that result in the same joint return period, as shown by the dashed line in Fig. 1 relating i_{pf} to v for the same return period of 100 years. The catchment output varies, as shown by the solid line in Fig.1, reaching a maximum value at a critical combination of storm depth and intensity peak factor of about 70.05 mm and 0.21.

Fig. 1 shows that, output peak discharge (Q_p) can vary widely, even though all input rainstorms have the same joint return period of 100 years. A range of intensity peak factors typically employed in design storms, can lead to a range in storm depths from about 58 mm to 71 mm, or a range width of 18% of the maximum storm depth. The Q_p values range from 3.43 mm/hr to 4.25 mm/hr; the width of the range is 19% of the maximum value. Comparable variations in runoff volume are expected. These

results demonstrate quantitatively the level of uncertainties that may be expected if intensity peak factor is not incorporated as a measure of design storms.

4. Conclusions

The example developed in Section 2 provides clear evidence that, in order to provide an assessment of the true input or load upon a hydrological system, the joint effects of storm depth, duration, and peak intensity must be evaluated. Therefore, the assessment of level of risk must incorporate the joint probability of those inputs. If the effect of peak intensity upon return period is ignored, there is risk of understating the value of the return period of the storm event. While using conservative values for load upon a system is prudent, gross overstatement is misleading and sometimes wasteful.

Section 3 illustrates that the response of a system must be carefully evaluated; presumed use of input values, without understanding of the system response, and the frequency of occurrence of the combination of inputs may lead to serious underestimation of the output values. In the particular example, there is clear indication that the presumption by some practitioners that the Chicago Design Storm provides the maximum peak-discharge response of a catchment is shown to not be the case in this case at least.

CHAPTER 6

Conclusions and Recommendations

1. Approach

Chapters 2 and 3 were written as stand-alone articles and have been published in the Journal of Hydrology, and Chapter 4 is drafted with a view towards submission as an article as well. Therefore, conclusions and recommendations form parts of each of those chapters. The material in this final chapter will limit repetition, and focus upon the interactions between the research presented in the three primary chapters, as well as over-arching results and directions for future research.

2. Threshold Analysis of Rainstorm Depth and Duration Statistics at Toronto, Canada

The theory and methods developed in chapter 2 are being incorporated by others into new means of design storm event definition (Jobin et al., 2010). Opportunities in this regard should be developed and pursued.

The independence of storm depth and duration determined in this chapter for the Pearson rainfall station data was confirmed in Chapter 3 for a second, nearby station, then the analysis performed in Chapter 4 provides strong indication that, at three stations in Illinois, storm depth and duration are uncorrelated, or the correlation coefficient is low, for events exceeding a high threshold. One of the key findings is that the predicted storm depth and duration combinations are lower than those predicted by conventional DDF analysis, in spite of the fact that identical data has been used for the two methods of analysis. While those differences are thoroughly reviewed and explained in Chapter 2, the consequence would be generally lower runoff

depth, and possibly, lower peak discharge. This consequence, having important policy implications, would merit much further investigation.

3. A probabilistic description of rain storms incorporating their peak intensity

The development of an index measure of peak-hour storm intensity is a major contribution to the characterization of the joint probability of storm depth, duration, and Intensity peak factor. The independence of I_{pf} with respect to storm depth V , established for the two Toronto, Canada stations in Chapter 3, and the strong indications of independence provided in Chapter 4 simplify the development of joint probability models. Another key contribution is the establishment of the combinations of storm variables that constitute extreme events. It is clear that increasing storm depth and increasing peak intensity lead to the risk of flooding and damage from runoff. In fact increases in the values of storm depth v and intensity peak factor i_{pf} , with decreasing storm duration t leads to the most severe consequences in small to medium-sized catchments. The probabilistic models developed in Chapter 3, the joint probability of increasing v and i_{pf} , and decreasing t , allows modelling of the corresponding physical phenomena. Chapter 2 started the development of the probabilistic model, developing the joint probability of storm depth, and storm duration. The full expression, in probabilistic terms, was completed in Chapter 3. Indeed, the otherwise under-examined relationship between storm depth and duration is tied to the false paradigm among many researchers and practitioners of assumed strong correlation between depth and duration for severe rainstorms.

The dependency between I_{pf} and storm duration T is essentially strong and invariant with time and temperature, as demonstrated in Chapter 4. Some examination of the physical basis for this would lead to improvements in modelling, and prediction of potential climate change impacts.

Other areas of research which are suggested by the results of Chapter 3, together with the trends suggested in Chapter 4 include:

- Examination of alternative probability distributions that may be applicable to storm duration and intensity peak factor;
 - the analysis of empirical distributions suggests that there may be some shift, as a result of changes with time, driven by changes in temperature associated with storm events, between the time spans analyzed;
 - this may apply to both storm duration and intensity peak factor.
- Application of these techniques to a broader range of output functions that are of interest in hydrologic design.

Dunkerley (2008) has raised concerns with the wide variation in definition or identification of individual storm events. The selection of IETD (called minimum inter-event time in his paper) has a significant influence on other measures of rain-storm events, in particular, the variability of intensity within an event increases with rising IETD. The intensity peak factor would provide a standardized measure of rainfall variability within an event, providing a means of comparison between storm-events identified with varying IETD..

4. Changes in heavy rainstorm characteristics with time and temperature at four locations

In general, mean values of storm variables and threshold event frequency estimators (J_u) did not change significantly between the time spans into which the time-range of available data was subdivided. The two time spans ranged between 1949 to 1979, and 1980 to 2006. Comparison of empirical distributions between the two data sub-sets showed some significant differences, but differences in distributions between the two time spans did not follow any common patterns across all stations examined. Because the sizes of the data sets are reduced, and the time spans shorter, there is a risk that the effects of decadal and multi-decadal climactic trends may either cause an apparent trend that does not exist, or alternatively, hide a trend within long-period cycles.

It is clear that there has been a trend towards an increasing frequency of occurrence of storm events occurring during the highest mean monthly temperatures, when early and late time spans are compared. Storm depth correlations with temperature have decreased with time in most cases.

The remaining primary question can only be answered with time: Is the increasing frequency of warmer rainstorm events a long-term trend, or part of a cyclical climatic pattern?

5. Overall conclusions

This thesis uniquely combines several key concepts developed by others, namely, inter-event time definition, threshold excess statistics, and the Generalized Pareto distribution (GPD). The major unique contributions of this thesis are the application of bounded distributions to appropriate rainstorm variables, the identification of an index measure of rainstorm peak intensity (intensity peak factor), and the correct formulation of the joint probabilities of rainstorm depth, duration, and intensity peak factor. Future research should investigate and solve remaining theoretical problems. The major objective, and challenge, will be to work with practitioners in order to provide understandable and useable tools, so that the evaluation of uncertainty in design and modelling is improved beyond the current state.

APPENDIX A

References

Chapter 1

Adams, B.J. and Howard, C.D.D., 1986. Design Storm Pathology. Canadian Water Resources Journal, Vol.11, no.3, 49-55.

Flannery, T., 2005. The Weather Makers. The Text Publishing Company, Australia.

Groisman, P., 2010. Changes in intense precipitation over the central U.S. - Manifestation of global climate change, regional land use, or both? AGU Hydrology Section Newsletter, july 2010.

Groisman, P., Karl, T.R., Easterling, D.R., Knight, R.W., Jamaso, P.F., Hennessy, K.J., Suppiah, R., Page, C.M., Wibilg, J., Fortuniak, K., Razuvaev, V.N., Douglas, A., Forland, E, Zhai, P-M., 1999. Changes in the Probability of Heavy Precipitation: Important Indicators of Climatic Change (42), Number 1, 243-283.

Kao, S-C, Govindaraju, R., 2008. Trivariate statistical analysis of extreme rainfall events via the Plackett family of copulas. Water Resources Research, Vol.44 WO2415.

Karl, T.R., Knight, R.W., 1998. Secular trends of precipitation amount, frequency, and intensity in the United States. Bulletin of the American Meteorological Society 79(2):231 - 241.

Karl, T.R., Trenberth, K.E., 2003. Modern global climate change. *Science* 302, 17191723.

Chapter 2

Adams, B.J. and Howard, C.D.D., 1986. Design Storm Pathology. Canadian Water Resources Journal, Vol.11, no.3, 49-55.

Adams, B.J., Fraser, H.G., Howard, C.D.D., Hanafy, M.S., 1986. Meteorological Data Analysis for Drainage System Design. Journal of Environmental Engineering, 112 (5), 827-848.

Adams, B.J., Papa, F., 1999. Urban Stormwater Management with Analytical Probabilistic Models. John Wiley and Sons, Inc. Toronto, Ontario.

Asquith, W.H., Roussel, M.C., Cleveland, T.G., Fang, X., Thompson, D.B., 2006. Statistical Characteristics of Storm Interevent Time, Depth, and Duration for Eastern New Mexico, Oklahoma, and Texas. Texas Department of Transportation and U.S. Geological Survey, Austin, Texas.

Atmospheric Environment Service (now Meteorological Services Canada), 1998. Rainfall Intensity-Duration Frequency Values, Gumbel - Method of Moments - 1998 Toronto Pearson International Airport, Station No. 6158733.

Boni, G., Parodi, A., Rudari, R., 2006. Extreme rainfall events: Learning from rain-gauge time series. Journal of Hydrology 327, 304-314.

Carr, D., 1987. Program IDF87HA Compute IDF Statistics (Moments). Atmospheric Environment Service (now Meteorological Services Canada), Environment Canada, Downsview, Ontario.

Chow, V.T., Maidment, D.R., Mays, L.W., 1988. Applied Hydrology. McGraw-Hill Book Company, New York.

Coles, S., 2001. An Introduction to Statistical Modeling of Extreme Values. Springer-Verlag London Limited.

Cunnane, C., 1978. Unbiased Plotting Positions - A Review. *Journal of Hydrology* 37, 205-222.

Davison, A.C., Smith, R.L., 1990. Models for Exceedence over High Thresholds. *Journal of the Royal Statistical Society B* 52 (3), 393-442.

Eagleson, P.S., 1972. Dynamics of Flood Frequency. *Water Resources Research* 8 (4), 878-897.

Evans, J.W., Johnson, R.A., Green, D.W., 1995. Goodness-of-Fit Tests for Two-Parameter and Three-Parameter Weibull Distributions, Chapter 9, *Advances in the Theory and Practice of Statistics*, Johnson, N.L., Balakrishnan, N., Editors, John Wiley and Sons, Inc., New York.

Goel, N.K., Kurothe, R.S., Mathur, B.S., Vogel R.M., 2000. A derived flood frequency distribution for correlated rainfall intensity and duration. *Journal of Hydrology* 228, 56-67.

Guo, C.Y.J., 2002. Overflow Risk Analysis for Stormwater Quality Control Basins. *Journal of Hydrologic Engineering* 7 (6), 428-434.

Guo, Y. and Adams, B.J. 1998a. Hydrologic analysis of urban catchments with event-based probabilistic models 1.Runoff volume. *Water Resources Research* 34 (12), 3421-3431.

Guo, Y. and Adams, B.J. 1998b. Hydrologic analysis of urban catchments with event-based probabilistic models 2. Peak discharge rate. *Water Resources Research* 34 (12), 3433-3443.

Hansen, E.M., Schreiner, L.C., Miller, F.F., 1982. Application of Probable Maximum Precipitation Estimates - United States East of the 105th Meridian, NOAA Hydrometeorological Report No.52, National Weather Service, Washington, D.C.

Hershfield, D.M., 1961. Rainfall frequency atlas of the United States for durations from 30 minutes to 24 hours and return periods from 1 to 100 years, technical paper 40, U.S. Department of Commerce, Weather Bureau, Washington, D.C.

Huff, F.A., 1993. 100-Year Rainstorms in the Midwest: Design Characteristics. Illinois State Water Survey, Champaign, Circular 176.

Johnson, N.L., Kotz, S., 1970. Continuous Univariate Distributions - 1. Houghton Mifflin Company, Boston.

Kite, G.W., 1977. Frequency and Risk Analyses in Hydrology. Water Resources Publications, Fort Collins, Colorado.

Marsalek, J. and Watt, W.E., 1984. Design storms for urban drainage design. Proceedings of 6th Hydrotechnical Conference, Canadian Society for Civil Engineering, Ottawa, Ontario. II, 574-584.

Pickands, J., 1975. Statistical Inference Using Extreme Order Statistics. *The Annals of Statistics* 3 (1), 119-131.

Restrepo-Posada, P.J., Eagleson, P.S., 1982. Identification of Independent Rainstorms. *Journal of Hydrology* 55, 303-319.

Rivera, P., Gironas, J., Montt, J.P., Fernandez, B., 2005. An analytical model for hydrologic analysis in urban watersheds. 10th International Conference on Urban Drainage, Copenhagen, Denmark.

Smith, J.A., 1992. Precipitation, Chapter 3, *Handbook of Hydrology*, Maidment, D.R., Editor-in-Chief, McGraw-Hill Companies Inc. New York.

Snedecor, G.W., Cochran, W.G., 1989. *Statistical Methods*, Eighth edition, Iowa State University Press, Ames, Iowa.

Stedinger, J.R., Vogel, R.M., Foufoula-Georgiou, E., 1992. Frequency Analysis of Extreme Events, Chapter 18, *Handbook of Hydrology*, Maidment, D.R., Editor-in-Chief, McGraw-Hill Companies Inc. New York.

Stephens, M.A., 1974. EDF (Empirical Distribution Function) Statistics for Goodness of Fit and Some Comparisons. *Journal of the American Statistical Association* 69 (347). Theory and Methods Section.

Stephens, M.A., 1977. Goodness of fit for the extreme value distribution. *Biometrika* 6 (3), 583-588.

U.S. National Weather Service, Office of Hydrologic Development, 2002. Ohio River Basin Precipitation Frequency Study; Update of Technical Paper No.40, NWS HYDRO-35, and Technical Paper No.49, Ninth Progress Report 1 October 2001 through 31 December 2001.

Wanielista, M.P., Yousef, Y.A., 1993. Stormwater Management, John Wiley and Sons, Inc. New York.

Watt, W.E., Chow, K.C.A., Hogg, W.D., Lathem, K.W., 1986. A 1 h design storm for Canada, Can.J of Civil Eng. 13 (3), 293-300.

Wenzel, H.G., 1982. Rainfall for urban stormwater design, Chapter 2, Urban Stormwater Hydrology, Kibler, D.F., Editor, American Geophysical Union, Washington, D.C.

Zhang, L., Singh, V.P., 2007. Bivariate rainfall frequency distributions using Archimedian copulas. Journal of Hydrology 332, 93-109.

Chapter 3

Adams, B.J., Fraser, H.G., Howard, C.D.D., Hanafy, M.S., 1986. Meteorological Data Analysis for Drainage System Design. *Journal of Environmental Engineering* 112 (5), 827-848.

Al-Rawas, G.A., Valeo, C., 2009. Characteristics of rainstorm temporal distributions in arid mountainous and coastal regions. *Journal of Hydrology*, 376, 318-326.

Ang, A.H-S., Tang, W.H., 1975. *Probability Concepts in Engineering Planning and Design, Volume I Basic Principles*. John Wiley and Sons, Inc. New York.

Balakrishnan, N., Lai, C.D., 2009. *Continuous Bivariate Distributions*. Springer Science, Amsterdam.

Coles, S., 2001. *An Introduction to Statistical Modeling of Extreme Values*. Springer-Verlag London Limited.

Environment Canada, Canada Centre for Inland Waters, 2009. *Mimico Creek Stage-Discharge Data, 1966-2003*.

Grimaldi, S., Serinaldi, F., 2006. Design heightograph analysis with 3-copula function. *Hydrological Sciences Journal* 51 (2), 223 - 238.

Gumbel, E.J., 1958. *Statistics of Extremes*. Columbia University Press, New York.

Huff, F.A., 1967. Time distribution of rainfall in heavy storms. *Water Resources Research* 3 (4), 1007 - 1019.

Huff, F.A., 1993. 100-Year Rainstorms in the Midwest: Design Characteristics. Illinois State Water Survey, Champaign, Circular 176.

Joe, H, 1997. *Multivariate Models and Dependence Concepts*. Chapman & Hall, London.

Johnson, N.L., Kotz, S., Balakrishnan, N., 1994. *Continuous Univariate Distributions 2*. John Wiley and Sons, Inc., New York.

Kao, S-C, Govindaraju, R., 2008. Trivariate statistical analysis of extreme rainfall events via the Plackett family of copulas. *Water Resources Research*, Vol.44 WO2415.

Kiefer, C.J. and Chu, H.H., 1957. Synthetic storm pattern for drainage design. *Journal of the Hydraulics Division, ASCE*, Vol.83, no.HY4 1332-1 - 1332-25.

Marsalek, J. and Watt, W.E., 1984. Design storms for urban drainage design. *Proceedings of 6th Hydrotechnical Conference, Canadian Society for Civil Engineering, Ottawa, Ontario 2*, 574-584.

Meteorological Services Canada (formerly Atmospheric Environment Service), 1998. Hourly rainfall statistics - 1934-1998 Toronto Bloor Street, Station No. 6158350.

Meteorological Services Canada (formerly Atmospheric Environment Service), 2001. Hourly rainfall statistics - 1961-2001 Toronto Pearson International Airport, Station No. 6158733.

National Institute of Standards and Technology/SEMATECH, 2006. e-Handbook of Statistical Methods, <http://www.itl.nist.gov/div898/handbook>.

Nelson, R.B., 2006. An Introduction to Copulas, 2nd Edition. Springer Science, New York.

Palynchuk, B.A. and Guo, Y., 2008. Threshold analysis of rainstorm depth and duration statistics at Toronto, Canada. *Journal of Hydrology* 348, 535-545.

Restrepo-Posada, P.J., Eagleson, P.S., 1982. Identification of Independent Rainstorms. *Journal of Hydrology* 55, 303-319.

Watt, W.E., Chow, K.C.A., Hogg, W.D., Lathem, K.W., 1986. A 1 h design storm for Canada, *Can.J of Civil Eng.*13 (3), 293-300.

Yen, B.C., Chow, V.T., 1980. Design Hyetographs for Small Drainage Structures. *Journal of the Hydraulics Division, Proceedings of the American Society of Civil Engineers* 106 (HY6), 1055 - 1076.

Yue, S., 2000a. Joint probability distribution of annual maximum storm peaks and amounts as represented by daily rainfalls. *Hydrological Sciences Journal* 45 (2), 315 - 326.

Yue, S., 2000b. The Gumbel Mixed Model Applied to Storm Frequency Analysis. *Water Resources Management* 14, 377-389.

Yue, S., 2001. A bivariate gamma distribution for use in multivariate flood frequency analysis. *Hydrological Processes* 15, 1033-1045.

Zhang, L., Singh, V.P., 2007a. Bivariate rainfall frequency distributions using Archimedian copulas. *Journal of Hydrology* 332, 93-109.

Zhang, L., Singh, V.P., 2007b. Gumbel-Hougaard Copula for Trivariate Rainfall Frequency Analysis. *Journal of Hydrologic Engineering* 12(4), 409 - 419.

Chapter 4

Adamowski, K., Prokoph, A., and Adamowski, J., 2009. Development of a new method of wavelet aided trend detection and estimation. *Hydrological Processes*, 23(18): 2686-2696.

Adams, B.J., Fraser, H.G., Howard, C.D.D., Hanafy, M.S., 1986. Meteorological Data Analysis for Drainage System Design. *Journal of Environmental Engineering* 112 (5), 827-848.

Allen, M.R., Ingram, W.J., (2002). Constraints on future changes in climate and the hydrologic cycle. *Nature*, 419, 224-232.

Ang, A.H-S., Tang, W.H., 1975. *Probability Concepts in Engineering Planning and Design, Volume I Basic Principles*. John Wiley and Sons, Inc. New York.

Angel, J.R., Huff, F., 1996. Changes in Heavy Rainfall in Midwestern United States. *Journal of Water Resources Planning and Management*, 123(4):246-249.

Balakrishnan, N., Lai, C.D., 2009. *Continuous Bivariate Distributions*. Springer Science, Amsterdam.

Chagnon, D., Sandstrom, M., Schaffer, C., 2003. Relating changes in agricultural practices to increasing dew points in extreme Chicago heat waves. *Climate Research*, (24): 243 - 254.

Chen, Z., Grasby, S., 2009. Impact of decadal and century-scale oscillations on hydroclimate trend analyses. *Journal of Hydrology*, 365(1-2): 122 - 133.

Coles, S., 2001. An Introduction to Statistical Modeling of Extreme Values. Springer-Verlag London Limited.

Douville, H., Chauvin, F., Planton, S., Royer, J-F., Salas-Melia, D., Tyteca, S., 2002. Sensitivity of the hydrological cycle to increasing amounts of greenhouse gases and aerosols. *Climate Dynamics*, 20, 45 - 68.

Eagleson, P.S., 1972. Dynamics of Flood Frequency. *Water Resources Research* 8 (4), 878-897.

Groisman, P., Knight, R., Easterling, D., 2004. Trends in precipitation intensity in the climate record. *Journal of Climate*....

Groisman, P., 2010. Changes in intense precipitation over the central U.S. - Manifestation of global climate change, regional land use, or both? *AGU Hydrology Section Newsletter*, July 2010.

Groisman, P., Karl, T.R., Easterling, D.R., Knight, R.W., Jamaso, P.F., Hennessy, K.J., Suppiah, R., Page, C.M., Wibilg, J., Fortuniak, K., Razuvaev, V.N., Douglas, A., Forland, E, Zhai, P-M., 1999. Changes in the Probability of Heavy Precipitation: Important Indicators of Climatic Change (42), Number 1, 243-283.

Goel, N.K., Kurothe, R.S., Mathur, B.S., Vogel R.M., 2000. A derived flood frequency distribution for correlated rainfall intensity and duration. *Journal of Hydrology* 228, 56-67.

Guo, Y. and Adams, B.J. 1998a. Hydrologic analysis of urban catchments with event-based probabilistic models 1.Runoff volume. *Water Resources Research* 34

(12), 3421-3431.

Guo, Y. and Adams, B.J. 1998b. Hydrologic analysis of urban catchments with event-based probabilistic models 2. Peak discharge rate. *Water Resources Research* 34 (12), 3433-3443.

Guo, Y., 2006. Updating Rainfall IDF Relationships to Maintain Urban Drainage Design Standards. *Journal of Hydrologic Engineering*, pages 14.

Hamed, K.H., 2008. trend detection in hydrologic data: The Mann-Kendall trend test under the scaling hypothesis. *Journal of Hydrology* (349): 350 - 363.

Haughton, J.T., Ding, Y., Griggs, D.J., Noguera, M., van der Linden, P.J., Dai, X., Maskell, K., Johnson, C.A., 2001. *Climate Change 2001: The Scientific Basis*. Cambridge University Press, Cambridge, MA.

IPCC, 2007. The physical science basis contribution of working group I to the fourth assessment report of the intergovernmental panel on climate change 13:245259IPCC. In: Solomon S, Qin D, Manning M, Chen Z, Marquis M, Avery A, Tignor M, Miller HL (eds) Cambridge University Press, Cambridge, UK and New York, USA, p 996

Johnson, N.L., Kotz, S., Balakrishnan, N., 1994. *Continuous Univariate Distributions 2*. John Wiley and Sons, Inc., New York.

Kao, S-C, Govindaraju, R., 2008. Trivariate statistical analysis of extreme rainfall events via the Plackett family of copulas. *Water Resources Research*, Vol.44 WO2415.

Karl, T.R., Knight, R.W., 1998. Secular trends of precipitation amount, frequency, and intensity in the United States. *Bulletin of the American Meteorological Society* 79(2):231 - 241.

Karl, T.R., Trenberth, K.E., 2003. Modern global climate change. *Science* 302, 1719-1723.

Katz, R.W., 1999: Extreme value theory for precipitation: Sensitivity analysis for climate change. *Advances in Water Resources*, 23, 1331-1339.

Kendall, M. G., 1955. Rank correlation methods. Charles Griffin and Company: London. Second edition. Kendall, M.G., 1975. Rank Correlation Methods. Griffin, London.

Kharin, V., Zwiers, F., 2000. Changes in the Extremes in an Ensemble of Transient Climate Simulation with a Coupled Atmosphere-Ocean GCM. *Journal of Climate*, 13, 3760-3788.

Kiefer, C.J. and Chu, H.H., 1957. Synthetic storm pattern for drainage design. *Journal of the Hydraulics Division, ASCE*, Vol.83, no.HY4 1332-1 - 1332-25.

Koutsoyannis, D., 2006. Nonstationarity versus scaling in hydrology. *Journal of Hydrology* 324 (1-4): 239-254.

Mailhot, A., Deschenes, S., Talbot, G., 2007. Assessment of future change in intensity-duration-frequency (IDF) curves for Southern Quebec using the Canadian Regional Climate Model (CRCM). *Journal of Hydrology* 347(1), 197 - 210.

Mann, H.B., 1945. Non-parametric tests against trend. *Econometrica*

Marsalek, J. and Watt, W.E., 1984. Design storms for urban drainage design. Proceedings of 6th Hydrotechnical Conference, Canadian Society for Civil Engineering, Ottawa, Ontario 2, 574-584.

Palynchuk, B.A. and Guo, Y., 2008. Threshold analysis of rainstorm depth and duration statistics at Toronto, Canada. *Journal of Hydrology* 348, 535-545.

Palynchuk, B.A., and Guo, Y., 2011. A probabilistic description of rain storms incorporating peak intensities. *Journal of Hydrology* 409, 71 - 80.

Restrepo-Posada, P.J., Eagleson, P.S., 1982. Identification of Independent Rainstorms. *Journal of Hydrology* 55, 303-319.

Rosenberg, E., Keys, P., Booth, D., Hartley, D., Burkey, J., Steinemann, A., Lettermaier, D., 2010. Precipitation extremes and the impacts of climate change on storm water infrastructure in Washington State. *Climate Change*, 1 - 31.

Trenberth, K.E., Dai, A., Rasmussen, R.M., Parsons, D.B., 2003. The changing character of precipitation, *Bull. Am. Meteorol. Soc.* (84) 1205 - 1217.

Wark, K., 1988. Generalized Thermodynamic Relationships. *Thermodynamics* 5th ed. McGraw-Hill, Inc., New York.

Yang, Y.J, Goodrich, J.A., 2008. Timing and prediction of climate change and hydrological impacts: periodicity in natural variations. *Environmental Geology*, (57)

1065-1078.

Zwiers, F.W., and G.C. Hegerl, 2008: Climate change: attributing cause and effect, *Nature*, 453, 296-297.

Chapter 5

Kiefer, C.J. and Chu, H.H., 1957. Synthetic storm pattern for drainage design. *Journal of the Hydraulics Division, ASCE*, Vol.83, no.HY4 1332-1 - 1332-25.

Wenzel, H.G., 1982. Rainfall for urban stormwater design, Chapter 2, *Urban Stormwater Hydrology*, Kibler, D.F., Editor, American Geophysical Union, Washington, D.C.

Yen, B.C., Chow, V.T., 1980. Design Hyetographs for Small Drainage Structures. *Journal of the Hydraulics Division, Proceedings of the American Society of Civil Engineers* 106 (HY6), 1055 - 1076.

Chapter 6

Dunkerley, D., 2008. Identifying individual rain events from pluviograph records; a review with analysis of data from an Australian dryland site. *Hydrological Processes*.

Jobin, E., Nestor, I, Jobin, D., Lodewyk, S., 2010. Towards a New Rainfall Storm Classification Method, Presentation to City of Edmonton, University of Ottawa.